Vibrations of Thickness-and-width Tapered Laminated Composite Beams with Rigid and Elastic Supports

Pooya Salajegheh

A thesis

In the Department

Of

Mechanical and Industrial Engineering

Presented in Partial Fulfillment of the Requirements

For the Degree of

Master of Applied Science (Mechanical Engineering) at

Concordia University

Montreal, Quebec, Canada

March 2013

CONCORDIA UNIVERSITY

SCHOOL OF GRADUATE STUDIES

This is to certify that the Thesis prepared,

By: **Pooya Salajegheh**

Entitled: **"Vibrations of Thickness-and-width Tapered Laminated Composite Beams with Rigid and Elastic Supports"**

and submitted in partial fulfillment of the requirements for the Degree of

Master of Applied Science (Mechanical Engineering)

complies with the regulations of this University and meets the accepted standards with respect to originality and quality.

Signed by the final Examining Committee:

_____ Chair
Dr. O. Kuzgunkaya

_____ Examiner
Dr. M. Hojjati

_____ Examiner (external)
Dr. A. Amer

_____ Supervisor
Dr. R. Ganesan

Approved by: _____
Dr. S. Narayanswamy, MASc Program Director
Department of Mechanical and Industrial Engineering

_____
Dean Dr. Robin Drew
Faculty of Engineering & Computer Science

Date: _____

ABSTRACT

Vibrations of Thickness-and-width Tapered Laminated Composite Beams with Rigid and Elastic Supports

Pooya Salajegheh

Variable-width variable-thickness laminated composite beams provide stiffness-tailoring and mass-tailoring design capabilities. They are increasingly and widely being used in engineering applications including robotic manipulators, aircraft wings, space structures, helicopter blades and yokes, turbine blades, and civil infrastructure. These structures are subjected to time-varying loadings. In the present work, the free and the forced vibration response of symmetric linear-thickness-and-width-tapered laminated composite beams are considered. Considering a variety of tapered configurations according to different types of plies drop-off configurations, both conventional and advanced finite element formulations are developed based on the Kirchhoff and cylindrical laminated beam bending theories. Natural frequencies, mode shapes and forced vibration response of different types of internally-tapered composite beams are determined. Rigid and elastic supports are considered for the free vibration response of the beams. Rigid supports are considered for the forced vibration response of the beams. Comparison of the finite element solution with the Rayleigh-Ritz solution is performed. A parametric study is conducted to investigate the effects of taper configurations, thickness-tapering angle, width-ratios, damping and boundary conditions on the free and forced vibration response of the variable-thickness variable-width laminated composite beams.

ACKNOWLEDGEMENT

It is a great pleasure to thank many people who made this thesis possible.

First and foremost, I would like to thank my dear parents Mr. Ali Salajegheh and Mrs. Maliheh Karegary for all their love, encouragement and support. I am thankful to my brothers, Mr. Sina Salajegheh and Dr. Nima Salajegheh for their support and encouragement during my master's study.

Then, I offer my sincerest gratitude to my supervisor, Dr. Rajamohan Ganesan, who has supported me, throughout my thesis research with his enthusiasm, inspiration, patience and immense knowledge. Throughout my thesis-writing period, he provided encouragement, sound advice, good teaching, and lots of good ideas.

I am thankful to all my friends at graduate research office EV 13.167 and my dear friend Mr. Kian Gorji who supported me by sharing ideas and discussion during my research studies.

I gratefully acknowledge the funding sources for my Masters Thesis provided by the NSERC and Concordia University.

Thank You.

Table of Contents

List of Figures

List of Tables

Nomenclature

H	Height of the laminate
H_L	Height of the beam at the left section
t_k	Ply thickness
t_k'	Specific ply thickness in the z direction
L	Length of the beam
l	Length of the element
B	Uniform width of the beam
B_l, B_r	Width at the left section and the right section of the beam
$b(x)$	Width of the beam at coordinate x
b_e	Width of the element at the mid-point of the element
r_b	Width ratio
x	Longitudinal direction of the laminated beam
y	Transverse direction of the laminated beam
z	Thickness direction of the laminated beam
z_k	Distance of the k'th ply interface from the center line of the beam
c	Intercept of the centre line of each ply
t	Time
$w(x,t)$	The transverse displacement of the beam
E_1	Longitudinal modulus
E_2	Transverse modulus
G_{12}	In-plane shear modulus

G_{23}	Out-of-plane shear modulus
ρ_k	Density of ply
ρ_s	Mass per unit length per unit width
ν_{12}	Major Poisson's ratio
ν_{21}	Minor Poisson's ratio
D_{11}	The first coefficient of bending stiffness matrix
B_{11}, B_{16}	Coefficients of coupling stiffness matrix
[A], [B], [D]	Laminate stiffness matrices
$\bar{Q}_{ij}$	Coefficient of the transformed reduced stiffness matrix
$\widetilde{M}_x$	Bending moment per unit width about the y-axis
M	Bending moment
k	Curvature
$\widetilde{N}_x^i$	Axial force per unit width along the x-axis
N_i, N_j	Shape functions of the beam
$\tilde{q}(x)$	Distributed transverse load per unit width
n	Number of plies
Ψ	Rotations about the y-axis
k_{ij}^e	Coefficient of the element stiffness matrix
$[k]$	Element Stiffness matrix
$[K]$	Global stiffness matrix
m_{ij}^e	Coefficient of the element mass matrix
$[m]$	Element mass matrix
$[M]$	Global mass matrix

[C]	Damping matrix
λ	Square of the natural frequency of the beam
$\{w\}$	Eigenvector
$\{y\}$	Vector of displacements in the transformed coordinates
$\{F\}$	Force vector
ω	Natural frequency
FEM	Finite Element Method
CFEM	Conventional Finite Element Method
AFEM	Advanced Finite Element Method
R-R	Rayleigh-Ritz method
φ	Thickness-tapering angle
$[\tilde{S}]$	Orthonormal eigenvector matrix
α	Mass proportional Rayleigh damping constant
β	Stiffness proportional Rayleigh damping constant
TS	Translational spring
RS	Rotational spring

Chapter-1

Introduction, literature survey and scope of the thesis

1.1. Vibration analysis in mechanical design

Mechanical vibration is a time-dependent phenomenon which deals with the repetitive motion of an object relative to a stationary frame of reference or nominal position. More often, vibration is undesirable, not only because of the waste of energy and the reduction in the performance and the resulting unpleasant motions but also because of creating unwanted sound and noise. Vibration may also lead to fatigue and unpredictable failure of the structure or machine due to the created dynamic stresses in the structure. Noise is generally considered to be undesirable sound. The study of noise or sound (pressure waves) and vibration are closely related since noise is generally produced by the vibration of structures. Hence in order to reduce the unwanted noise often the problem of controlling the vibration of the structure is encountered.

The vibration of a system may occur due to an excitation generated by initial displacement and/or initial velocity of the mass (free vibration) or may occur due to an excitation created by harmonically excited force (forced vibration). In the first case (free vibration), mechanical system will vibrate at one or more of its natural frequencies. In this case, damping or friction from material itself or surrounding medium will cause the vibration to stop. In the second case (forced vibration), the system is forced to vibrate at the same frequency as that of the excited harmonic force. In this case if the frequency of exciting force gets close to the natural frequencies of the system, the structure will

undergo a vibration resonance in which the system will respond at greater amplitude than it does at other frequencies. There are many examples of structures failing or not meeting objectives or heavily reduced lifetime due to vibration resonances, fatigue or high noise levels in the system which can be avoided by proper vibration analysis.

1.2. Composite materials and structures

Composite material refers to material that is created by the synthetic assembly of two or more organic or inorganic materials in order to obtain specific material properties such as high strength and high modulus to weight ratio, corrosion resistance, thermal properties, fatigue life and wear resistance and increased tolerance to damage [1]. Carbon fiber is one of the most important high-performance fibers for military and aerospace applications. High-strength carbon fiber came out of the development laboratories in Japan, England, and the United States in the late 1960s. The initial fibers were very expensive (more than 400 to 500 dollars per pound) which limited their applications to high-value military aerospace and space systems. The results of early military composite development programs can be seen today in systems fielded by each of the military services. For example, more than 350 parts of the F-22 Raptor, accounting for 25 percent of the structural weight, are carbon-epoxy composites. But in the early 1970s, continuous processes were developed and the cost declined steadily over the next decade. The Air Force Materials Laboratory took the lead in U.S. government-sponsored material development and hardware demonstration. By the late 1970s, composite materials were used in the production of primary structures for military aircraft and missiles. These applications were followed by selective use in commercial aircraft. For 20 years, between 1969 and 1989, the carbon fiber industry had phenomenal technological success and

double-digit annual growth in aerospace and defense industries, with additional use in sports equipment and some limited use in automotive and industrial applications. This growth attracted many large international companies into the industry. The vision was that continued growth in military and commercial aircraft use would be followed by a very large industrial market by the year 2000 [2].

Development and design of polymer composite materials and structures is the fastest growing segment of lightweight (durable and sustainable) construction and product engineering (in general 'moving and moved beings'). Since fifteen years for each five years period the world market volume of advanced polymer composites was doubled (100 percent growth per quinquennial). For the first decade of this millennium a growth of at least 700 percent was foreseen (350 percent growth per quinquennial). The majority of structural parts in novel aircraft and space platform designs will be materialized in polymer composite materials. In case of fireproof interiors including floors and supporting structures (beams and brackets) the applied volume of composites are reaching the maximum of almost 100 percent and for the high performance and durable exterior shell structures almost 80 percent by volume is within the reach.

The same trends and developments are true for inshore and offshore wind turbine blade designs (wing structures possessing a radius equal to the total span of a Boeing 747) and the development of the latest fast transport systems varying from trains, cars, ferries, trucks to ships and yachts, shows similar tendencies [3].

In Some specific applications of composite structures such as helicopter yoke, robot arms, turbine blades and satellite antenna, the laminates need to be stiff at one location and flexible at another location. For example in a helicopter yoke, a progressive

variation in the thickness of the yoke is required to provide high stiffness at the hub and flexibility at the middle of yoke length to accommodate for flapping. This type of structure is created by terminating or dropping off selected plies at specific locations to reduce the stiffness of that structure which is called as the tapered composite structure [4].

1.3. Finite element method

Finite element method is a numerical technique derived from variational method for finding approximate solutions to problems. This method overcomes the disadvantage of the traditional variational methods by providing a systematic procedure for the derivation of the approximation functions over subregions of the domain. The method is endowed with three basic features that account for its superiority over other competing methods. First, a geometrically complex domain of the problem is represented as a collection of geometrically simple subdomains, called finite elements. Second, over each finite element, the approximation functions are derived using the basic idea that any continuous function can be represented by a linear combination of algebraic polynomials. Third, algebraic relations among undetermined coefficients (i.e., nodal values) are obtained by satisfying the governing equations, often in a weighted-integral sense, over each element. Thus, the finite element method can be viewed, in particular, as an element-wise application of the Rayleigh-Ritz or weighted-residual methods. The finite element method is one of the most powerful numerical techniques ever devised for solving differential (and integral) equations of initial and boundary-value problems in geometrically complicated regions [5]. The greatest advantage of the finite element method is its flexibility to analyse structures with arbitrary geometry, boundary

conditions as well as arbitrary shape of non-homogeneous structures that are made up of numerous different material regions. Consequently, it is one of the most accurate and powerful tools used to predict the behaviour of complex mechanical structures such as the vibration of tapered laminated composite beams.

The convergence and accuracy of the results determined using finite element formulation depend strongly on the selected type of element. Two types of element are considered for the finite element formulation in this study. Four degrees of freedom per node (deflection w, rotation $-\frac{dw}{dx}$, curvature $-\frac{d^2w}{dx^2}$ and the gradient of curvature $\frac{d^3w}{dx^3}$) and two nodes per element are considered for the advanced finite element formulation and two degrees of freedom per node (deflection w and rotation $-\frac{dw}{dx}$) and two nodes per element are considered for the conventional finite element formulation. It can be predicted that in order to obtain accurate results using conventional finite element method compared to advanced finite element method, large number of elements are required.

1.4. Literature survey

In this section, a comprehensive and up-to-date literature survey on the important works done on the free and forced vibration response of uniform, uniform-thickness width-tapered and thickness-tapered width-tapered laminated composite beams is presented. There is a wealth of literature available for the vibration analysis of laminated plates and shells. Study on the vibration analysis and especially the forced vibration analysis of laminated beams on the other hand, has been very limited despite their applicability in the industry.

Abarcar and Cunniff [6] obtained experimental results for natural frequencies and mode shapes of uniform clamped-free laminated composite beams made of graphite-epoxy and boron-epoxy composite material without considering the effects of shear deformation and rotary inertia. Miller and Adams [7] have studied the vibration characteristic of orthotropic clamped-free uniform beams using classical laminated beam theory without considering the effect of shear deformation. Chen and Yang [8] have studied the static and dynamic response of symmetrically laminated composite beams. Chandrashekhara et al. [9] have studied the free vibrations and obtained the natural frequencies of advanced composite beams. They have considered the effect of rotary inertia and shear deformation in the free vibration analysis of the beams. Hodges et al. [10] conducted the free vibration analysis of composite beams using exact integration method. Krishnaswamy et al. [11] obtained analytical solutions to the free vibration of generally laminated composite beams including the effect of transverse shear and rotary inertia in the energy formulation. Reddy and Khdeir [12] have studied the free vibration of laminated composite beams with arbitrary boundary conditions. Vinson and Sierakowski [13]obtained the exact solutions for the natural frequencies of a simply supported uniform laminated composite beam based on classical laminated beam theory. Abramovich [14] obtained exact solutions for the free vibrations of composite beams including the effect of rotary inertia and shear deformation. Reddy [15], Berthelot [16], Whitney [17] and Jones [18] have found the exact solutions for the free vibrations of uniform laminated composite beams. Abramovich and Livshits [19] established analytical solution of free vibration and obtained the mode shapes and the natural frequencies of non-symmetrical cross-ply laminated beams. Matsunaga [20] have studied the vibration

of multi-layer composite beams based on higher-order deformation theories. Rao and Ganesan [21] investigated the harmonic response of uniform-width thickness-tapered composite beams with general boundary conditions using finite element method. Farghaly and Gadelrab [22] have studied the free vibration of stepped uniform-width thickness-tapered Timoshenko composite beams using finite element method. He et al. [23] presented a complete review of different configurations of tapered composite structures. Singh and Abdelnassar [24] examined the forced vibration response of composite beams considering a third order shear deformation theory. Chandrashekhara and Bangera [25] studied the free vibration characteristics of laminated composite beams using a third order shear deformation theory. Asghar et al. [26] conducted the forced vibration analysis developed by the modal superposition technique and the layer wise theory of Reddy to study the low velocity impact response of laminated plates. Kadivar et al. [27] studied the forced vibration of an unsymmetrical laminated composite beam subjected to moving loads. They studied a one-dimensional element with 24 degrees of freedom, which included the effects of transverse shear deformation, rotary and higher order inertia to get the response. Faruk [28] analyzed the free and the forced vibrations of non-uniform composite beams in the Laplace domain. He adopted Timoshenko beam theory in the derivation of governing equation. Hassan and Sabuncu [29] have conducted the stability analysis of a cantilever composite beam resting on elastic supports. Karnovsky and Lebed [30] have studied the free vibrations of uniform beams having elastic supports. Marur and Kant [31] conducted the free vibration analysis of uniform laminated composite beams using finite element formulation. They have proposed three higher order refined displacement models (one model with five degrees of freedom per

node and two models with four degrees of freedom per node) for the free vibration analysis of composite beam fabrications. Shi and Lam [32] have studied the free vibration of laminated composite beams using third order shear deformation theory and finite element method. Ganapathi et al. [33] used a three node beam element in the finite element formulation based on Hermite cubic functions for deflection and quadratic functions for rotations and linear functions for axial displacements to obtain the natural frequencies of uniform laminated composite beams. The two end nodes have four degrees of freedom (axial displacement, deflection, slope and rotation) each, whereas the center node has one degree of freedom (rotation). Abd El-Maksoud [34] presented a dynamic analysis of uniform and uniform-width variable-thickness composite beams using conventional and advanced finite element formulations. Zienkiewicz [35], Cook [36], Reddy [5] have used finite element method to analyze the vibration of beams. They have used two nodes per element and two degrees of freedom per node (deflection and rotation) in the formulations. To [37] have considered four degrees of freedom per node (deflection, rotation, curvature and gradient of curvature) and two nodes per element in the finite element formulations in order to obtain stiffness and mass matrices for linearly tapered beams based on Euler-Bernoulli beam theory. Gupta and Rao [38] have used two nodes per element and two degrees of freedom per node in the finite element formulation to obtain the stiffness and mass matrices of linearly tapered and twisted beams. Heyliger and Reddy [39] established a higher order beam finite element for bending and vibration problems. Zabihollah [40] analyzed the free vibration and buckling of uniform-width thickness-tapered composite beams using both conventional and advanced finite element formulations. He has used two nodes per element and four degrees of freedom per node

(deflection, slope, curvature, derivative of curvature) in the advanced finite element formulations. Uniform-width thickness-tapered laminated composite beams have been studied for their dynamic response in the works of Ganesan and Zabihollah [41] and [42] using an advanced finite element formulation and parametric study. Two nodes per element and four degrees of freedom per node (deflection, slope, curvature, derivative of curvature) were considered in the advanced finite element formulations. Nabi and Ganesan [43] developed a general finite element formulation based on a first-order shear deformation theory with 16 degrees of freedom per element to study the free vibration characteristics of laminated composite beams. They also conducted a parametric study on the influence of beam geometry and boundary conditions on the natural frequencies of the beam. Eftakher [4] conducted free and forced vibration analysis of uniform-width thickness-tapered laminated composite beams using Rayleigh-Ritz method and conventional and advanced finite element formulations. He has used two nodes per element and four degrees of freedom (deflection, slope, curvature and gradient of curvature) per node in the advanced finite element formulation. Chen [44] has studied the free vibration response of tapered composite beams using hierarchical finite element method and Rayleigh-Ritz method. Vijay [45] conducted the free and forced vibration analysis of thickness-tapered width-tapered laminated composite beams using Rayleigh-Ritz method.

1.5. Objectives of the thesis

The dynamic response of variable-thickness variable-width laminated composite beams is concerned within the present thesis. The objectives of the work are: 1) To investigate the free vibration response of uniform-thickness width-tapered, uniform-width

thickness-tapered and thickness-tapered width-tapered laminated composite beams using conventional and advanced finite element formulations and to conduct a detailed parametric study on the effects of width ratio, thickness-tapering angle, taper configuration, laminate configurations and boundary conditions on the free vibrations of the beams; The convergence and accuracy of the results obtained using advanced and conventional finite element formulations are illustrated; 2) To investigate the forced vibration response of undamped and damped variable-thickness variable-width laminated composite beams using conventional and advanced finite element formulations and to conduct a detailed parametric study on the effects of damping, width ratio, thickness-tapering angle, taper configuration and boundary conditions on the forced vibrations of the beams (the amplitude of deflection). Similar variable-thickness variable-width laminated composite beams to those that were considered for the free vibration analysis are considered for the forced vibration analysis; 3) To compare the free and forced vibration response of tapered laminated composite beams obtained using conventional and advanced finite element formulations with the results obtained using Rayleigh-Ritz method [45]; 4) To investigate the free vibration response of variable-thickness variable-width laminated composite beams with rigid and elastic supports modeled using translational and rotational springs attached to the beams and to study the effects of different combinations of translational and rotational springs with different stiffnesses on the natural frequencies of these beams.

The dynamic response of variable-thickness variable-width laminated composite beams is determined based on classical laminated beam theory using conventional and advanced finite element formulations.

1.6. Layout of the thesis

The present chapter provides a brief introduction and literature survey on free and forced vibrations of variable-thickness and variable-width laminated composite beams using conventional and advanced finite element formulations.

In chapter 2, free vibration analysis of variable-thickness variable-width laminated composite beams is carried out using conventional finite element formulation based on Kirchhoff and cylindrical laminated beam bending theories. Free vibration of beams with different boundary conditions, width ratios, thickness-tapering angles, laminate configurations and thickness taper configurations is studied. Determined natural frequencies are compared and validated with the existing results obtained using Rayleigh-Ritz method.

In chapter 3, free vibration analysis of variable-thickness variable-width laminated composite beams is carried out using advanced finite element formulations. Advantages of using advanced finite element formulation compared to the conventional finite element formulation in the convergence of the natural frequencies and the accuracy of the results are demonstrated in this chapter.

In chapter 4, forced vibration response of undamped and damped variable-thickness variable-width laminated composite beams is studied using modal analysis and conventional and advanced finite element formulations. Numerous plots of amplitude of deflection of the response point versus frequency of vibration are presented in order to show the effects of damping, boundary conditions and thickness taper configuration on the amplitude of deflection of the beams. Determined results are compared and validated with the existing results obtained using Rayleigh-Ritz method.

In chapter 5, free vibration analysis of variable-thickness variable-width laminated composite beams with elastic supports is carried out using conventional and advanced finite element formulations. Elastic supports are modeled using translational and rotational springs with arbitrary stiffness values. Determined results are compared and validated with the existing results. The effect of the spring stiffness on the free vibration response of the beams is illustrated.

The thesis ends with chapter 6, which provides the overall conclusions of the present work.

Chapter-2

Conventional finite element formulation for free vibration analysis of composite beams

2.1. Introduction

Laminated composite beams are increasingly and widely being used in engineering applications including robotic manipulators, aircraft wings, space structures, helicopter blades and yokes, turbine blades and civil infrastructure due to their enhanced stiffness-to-weight and strength-to-weight ratios. These structures are subjected to time-varying loadings. In this chapter free vibration analysis of uniform, uniform-thickness width-tapered and width-tapered thickness-tapered laminated composite beams is conducted using conventional finite element formulation. Simply supported, clamped-free and clamped-clamped boundary conditions are considered in this study. Finite element method is one of the most accurate and powerful tools used to predict the behaviour of complex mechanical structures such as the vibration of tapered laminated composite beams. Two degrees of freedom (deflection w, rotation $-\frac{dw}{dx}$) per node and two nodes per element are considered in the conventional finite element formulation. The material chosen in this study is NCT-301 graphite-epoxy prepreg [46] which is available in the laboratory of Concordia Centre for Composites (CONCOM). The mechanical properties of the ply and the resin are given in the Tables 2.1 and 2.2. Symmetric laminate is considered in all problems.

Table 2.1: Mechanical properties of unidirectional NCT-301 graphite-epoxy prepreg

Longitudinal modulus (E_1)	113.9 GPa
Transverse modulus (E_2)	7.985 GPa
$E_3=E_2$	7.985 GPa
In-plane shear modulus (G_{12})	3.137 GPa
Out-of-plane shear modulus (G_{23})	2.852 GPa
Density of ply (ρ_k)	1480 kg/m^3
Major Poisson's ratio (ν_{12})	0.288
Minor Poisson's ratio (ν_{21})	0.018

Table 2.2: Mechanical properties of resin material

Elastic modulus (E)	3.93 GPa
Shear modulus (G)	1.034 GPa
Density of resin (ρ_r)	1000 kg/m^3
Poisson's ratio (ν)	0.37

2.2. Uniform and uniform-thickness width-tapered beams

When the cross-section area of a beam is constant through the length of the beam, it is considered a uniform beam as shown in Figures 2.1 and 2.3. In the case of a uniform beam, the properties of the beam are constant through the length of the beam. Laminated composite beams which are considered in this section have uniform thickness, consequently the D_{11} (the first coefficient of bending stiffness matrix) is constant through the length of these beams, while the width of the beams varies linearly through the length

of the beam with respect to x. Width-tapering is achieved by cutting the beam on the surfaces perpendicular to the mid-plane of the beam as shown in Figures 2.2 and 2.3.

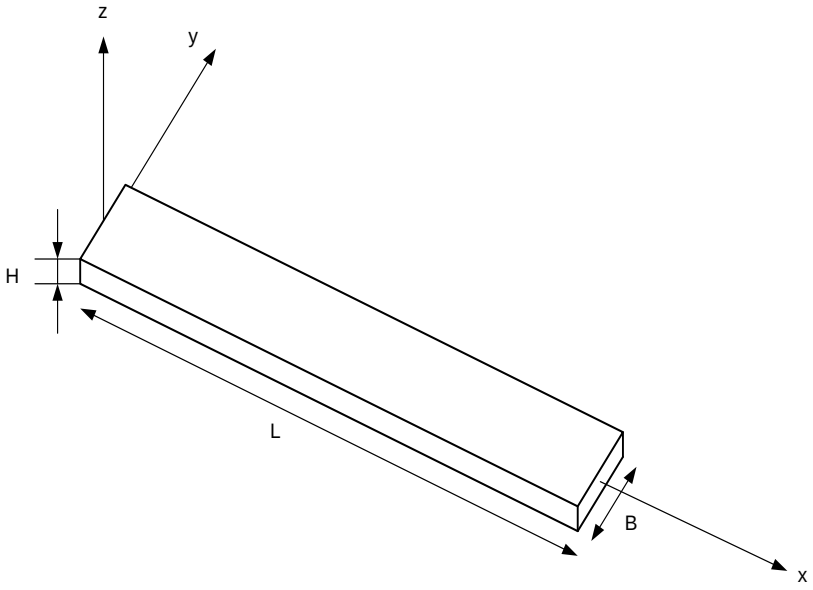

Figure 2.1: A uniform beam

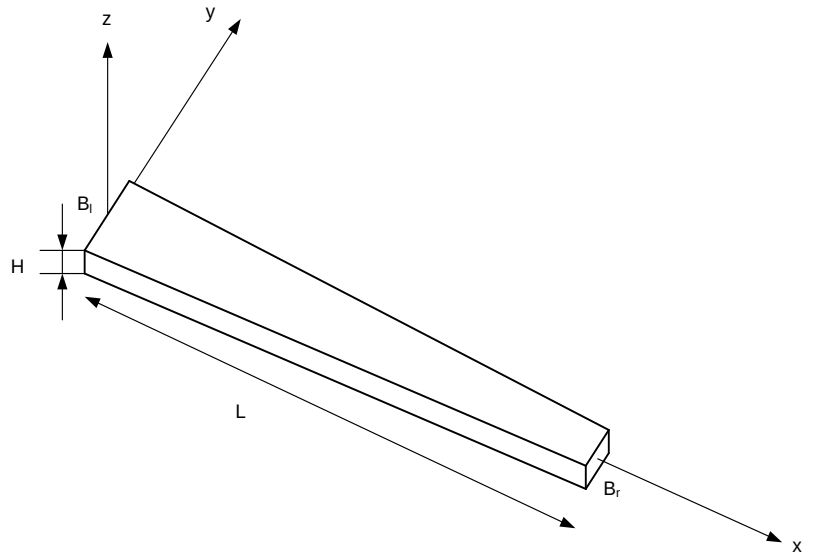

Figure 2.2: A uniform-thickness width-tapered beam

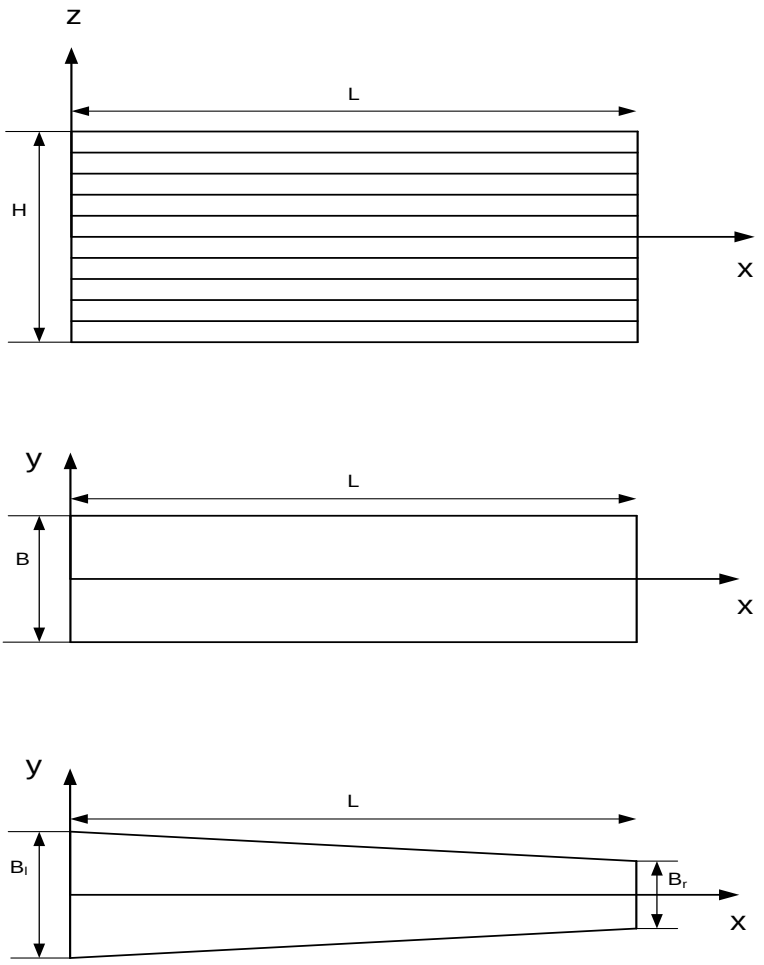

Figure 2.3: Uniform and uniform-thickness width-tapered laminated beams

In Figures 2.2 and 2.3, B_l denotes the width at the left section and B_r denotes the width at the right section of the beam.

2.2.1. Conventional finite element formulation

The equation of motion based on classical laminated beam theory is given as [16]:

$$\frac{\partial^2(b(x)\widetilde{M}_x)}{\partial x^2} + b(x)\widetilde{N}_x^i \frac{\partial^2 w}{\partial x^2} + q(x) = b(x)\rho_s \frac{\partial^2 w}{\partial t^2} \tag{2.1}$$

in which $b(x)$ denotes the width of the beam. For a linearly width-tapered beam:

$$b(x) = B_l - \frac{(B_l - B_r)}{l} x \tag{2.2}$$

$\widetilde{M}_x$ denotes the bending moment per unit width about the y-axis, $\widetilde{N}_x^i$ is the axial force per unit width along the x-axis, w is the deflection in the thickness direction, $q(x)$ is the distributed transverse load per unit length, ρ_s is mass per unit length per unit width and t represents time.

In the present study width-tapering is described by the width ratio (r_b) as:

$$r_b = \frac{B_r}{B_l} \tag{2.3}$$

One can write the bending moment for a symmetric laminated composite beam using two different approaches [16]: (a) cylindrical bending theory and (b) one-dimensional laminated beam theory.

2.2.1.1. Cylindrical bending theory (plane strain)

In this approach the bending moment is given as:

$$M_x = b(x)(B_{11}\frac{\partial u_0}{\partial x} + B_{16}\frac{\partial v_0}{\partial x} - D_{11}\frac{\partial^2 w}{\partial x^2}) \tag{2.4}$$

in which B_{11} and B_{16} denote coefficients of coupling stiffness, which are equal to zero for symmetric beams according to [16]:

$$B_{ij} = \frac{1}{2}\sum_{k=1}^{n} \bar{Q}_{ij}{}^{k} ({z_k}^2 - {z_{k-1}}^2) \tag{2.5}$$

D_{11} is the coefficient of bending stiffness which is given as:

$$D_{ij} = \frac{1}{3}\sum_{k=1}^{n} \bar{Q}_{ij}{}^{k} ({z_k}^3 - {z_{k-1}}^3) \tag{2.6}$$

in which n denotes the number of plies, $\bar{Q}_{ij}{}^{k}$ represents the coefficient of the transformed reduced stiffness matrix of k-th ply and z_k is the distance of the k-th ply interface from the center line of the beam.

Consequently for a symmetric laminated composite beam, the bending moment based on cylindrical bending theory is given as:

$$M_x = -b(x)D_{11}(x)\frac{\partial^2 w}{\partial x^2} \tag{2.7}$$

2.2.1.2. One-dimensional laminated beam theory (plane stress)

Using one dimensional laminated beam theory assumption, one can find the relation between moments and curvatures as [16]:

$$\begin{bmatrix} M_x \\ M_y \\ M_{xy} \end{bmatrix} = \begin{bmatrix} D_{11} & D_{12} & D_{16} \\ D_{12} & D_{22} & D_{26} \\ D_{16} & D_{26} & D_{66} \end{bmatrix} \begin{bmatrix} k_x \\ k_y \\ k_{xy} \end{bmatrix} \tag{2.8}$$

$$\begin{bmatrix} k_x \\ k_y \\ k_{xy} \end{bmatrix} = \begin{bmatrix} D_{11}{}^{*} & D_{12}{}^{*} & D_{16}{}^{*} \\ D_{12}{}^{*} & D_{22}{}^{*} & D_{26}{}^{*} \\ D_{16}{}^{*} & D_{26}{}^{*} & D_{66}{}^{*} \end{bmatrix} \begin{bmatrix} M_x \\ M_y \\ M_{xy} \end{bmatrix} \tag{2.9}$$

$$M_x = -b\frac{1}{D_{11}^{*}}\frac{\partial^2 w}{\partial x^2} \tag{2.10}$$

$$D_{11}^{*} = \frac{1}{\Delta}(D_{22}D_{66} - D_{26}^2) \tag{2.11}$$

$$\Delta = D_{11}D_{22}D_{66} + 2D_{12}D_{16}D_{26} - D_{11}D_{26}^2 - D_{22}D_{16}^2 - D_{66}D_{12}^2 \tag{2.12}$$

2.2.1.3. Coefficients of element stiffness and mass matrices

In this chapter, conventional finite element method is used to analyze the free vibration of symmetric laminated composite beams. Two degrees of freedom per node

(deflection w and rotation $-\frac{\partial w}{\partial x}$) and two nodes per element are used in the formulation as shown in Figure 2.4.

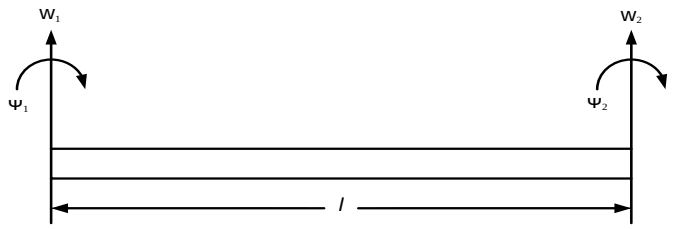

Figure 2.4: Element degrees of freedom

In Figure 2.4, w_1 and w_2 represent the deflections in the thickness direction at the first and the second node respectively and Ψ_1 and Ψ_2 denote the rotations about the y-axis at the first and the second node respectively.

Coefficients of element's stiffness and mass matrices are given as [40] and [4]:

$$k_{ij}^{e} = \int_0^l b(x) D_{11} \frac{d^2 N_i}{dx^2} \frac{d^2 N_j}{dx^2} dx \tag{2.13}$$

$$k_{ij}^{e} = \int_0^l b(x) \frac{1}{D_{11}^{*}} \frac{d^2 N_i}{dx^2} \frac{d^2 N_j}{dx^2} dx \tag{2.14}$$

$$m_{ij}^{e} = \int_0^l b(x) \rho_s N_i N_j dx \tag{2.15}$$

In the equation (2.13), k_{ij}^{e} represents the coefficient of the element stiffness matrix using cylindrical bending theory, while in the equation (2.14), it denotes the coefficient of the element stiffness matrix using one-dimensional laminated beam theory. In the equation (2.15), m_{ij}^{e} represents the coefficient of the element mass matrix. In equations (2.13), (2.14) and (2.15), N_i and N_j represent the shape functions of the beam.

2.2.1.4. Derivation of shape functions

Having two degrees of freedom per node and four degrees of freedom per element, a third-order polynomial is required for the expression of deflection to satisfy the boundary conditions as below:

$$w^e(x,t) = c_1^e + c_2^e x + c_3^e x^2 + c_4^e x^3 \tag{2.16a}$$

$$\varphi^e(x,t) = -\frac{\partial w(x)}{\partial x} = -(c_2^e + 2c_3^e x + 3c_4^e x^2) \tag{2.16b}$$

Applying the boundary conditions considering the first node at x=0 and the second node at x=l, one will have:

$$w^e(0,t) = w_1^e \tag{2.17a}$$

$$\varphi^e(0,t) = w_2^e \tag{2.17b}$$

$$w^e(l,t) = w_3^e \tag{2.17c}$$

$$\varphi^e(l,t) = w_4^e \tag{2.17d}$$

Having the equations (2.16) and (2.17) in the matrix form one has:

$$\begin{Bmatrix} w_1^e \\ w_2^e \\ w_3^e \\ w_4^e \end{Bmatrix} = \begin{bmatrix} 1 & 0 & 0 & 0 \\ 0 & -1 & 0 & 0 \\ 1 & l & l^2 & l^3 \\ 0 & -1 & -2l & -3l^2 \end{bmatrix} \begin{Bmatrix} c_1^e \\ c_2^e \\ c_3^e \\ c_4^e \end{Bmatrix} \tag{2.18}$$

Having two nodes and two degrees of freedom per node the interpolation functions are derived as [40]:

$$N_1^e = 1 - \frac{3x^2}{l^2} + \frac{2x^3}{l^3} \tag{2.19a}$$

$$N_2^e = -x + \frac{2x^2}{l} - \frac{x^3}{l^2} \tag{2.19b}$$

$$N_3^e = \frac{3x^2}{l^2} - \frac{2x^3}{l^3} \tag{2.19c}$$

$$N_4^e = \frac{x^2}{l} - \frac{x^3}{l^2} \tag{2.19d}$$

2.2.1.5. Stiffness and mass matrices

Using MATLAB® software and solving equations (2.13), (2.14) and (2.15) the stiffness and mass matrices for an element of a uniform or a uniform-thickness width-tapered beam are derived as:

$$[k]_{CBT} = \frac{2b_e D_{11}}{l^3}\begin{bmatrix} 6 & -3l & -6 & -3l \\ -3l & 2l^2 & 3l & l^2 \\ -6 & 3l & 6 & 3l \\ -3l & l^2 & 3l & 2l^2 \end{bmatrix} \tag{2.20a}$$

$$[k]_{1-D\ LBT} = \frac{2b_e}{l^3 D_{11}^*}\begin{bmatrix} 6 & -3l & -6 & -3l \\ -3l & 2l^2 & 3l & l^2 \\ -6 & 3l & 6 & 3l \\ -3l & l^2 & 3l & 2l^2 \end{bmatrix} \tag{2.20b}$$

$$[m] = \frac{b_e \rho_s}{420}\begin{bmatrix} 156 & -22l & 54 & 13l \\ -22l & 4l^2 & -13l & -3l^2 \\ 54 & -13l & 156 & 22l \\ 13l & -3l^2 & 22l & 4l^2 \end{bmatrix} \tag{2.20c}$$

in which b_e denotes the average width of the element and l is the length of the element. In the equation $(2.20a)$, $[k]_{CBT}$ represents the element stiffness matrix using cylindrical bending theory, while in the equation $(2.20b)$, $[k]_{1-D\ LBT}$ denotes the element stiffness matrix using one-dimensional laminated beam theory. In the equation $(2.20c)$, $[m]$ represents the element mass matrix.

Having the stiffness and mass matrices determined using conventional finite element formulation, one can analyze the free vibration of a beam element as:

$$[m]\{\ddot{w}\} + [k]\{w\} = \{0\} \tag{2.21}$$

Knowing the stiffness and mass matrices for each element based on the conventional finite element formulation, the global stiffness matrix $[K]$ and the global

mass matrix $[M]$ can be established for the beam. The free vibration of the beam can be analyzed solving the below eigenvalue problem.

$$([K] - \lambda[M])\{w\} = \{0\} \tag{2.22}$$

in which λ denotes the square of the natural frequency of the beam and $\{w\}$ denotes the eigenvector (mode shape) corresponding to each specific natural frequency. Solving equation (2.22) using MATLAB® software, the natural frequencies and the mode shapes of uniform and uniform-thickness width-tapered laminated composite beams can be determined.

Since the determined results using both cylindrical bending theory and one-dimensional laminated beam theory are very close for the considered beams in this study, only the results determined using cylindrical bending theory are presented.

2.2.2. Exact natural frequencies of uniform laminated composite beams

The exact natural frequencies of a uniform beam for the three boundary conditions considered in this study (simply supported, clamped-free and clamped-clamped) can be determined as explained in Refs. [13] and [16] .

Exact natural frequencies of a simply supported uniform beam are given in [13] and [16] as:

$$\omega_n = \frac{n^2\pi^2}{l^2}\sqrt{\frac{D_{11}}{\rho H}} \tag{2.23a}$$

in which n represents the mode number of the natural frequency considered, H denotes the thickness of the beam, ρ is the density and l is the length of the beam.

Exact natural frequencies of a clamped-free uniform beam are given in [13] and [16] as:

$$\omega_n = \frac{\xi_n}{l^2}\sqrt{\frac{D_{11}}{\rho H}} \qquad (2.23b)$$

in which $\xi_1 = 6.516$, $\xi_2 = 22.034$ and $\xi_3 = 61.701$.

Exact natural frequencies of clamped-clamped uniform beam are given in [13] and [16] as:

$$\omega_n = \left(\frac{\xi_n}{l}\right)^2\sqrt{\frac{D_{11}}{\rho H}} \qquad (2.23c)$$

in which $\xi_1 = 4.73004$, $\xi_2 = 7.853$ and $\xi_3 = 10.996$.

2.2.3. Validation

In order to validate the results obtained using the conventional finite element formulation and to understand how many elements should be considered for the convergence of the natural frequencies, the results have been compared with the exact natural frequencies and existing results obtained using finite element formulation [40] and Rayleigh-Ritz method [45].

Uniform beams are considered with a) simply supported, b) clamped-free and c) clamped-clamped boundary conditions, as shown in Figure 2.5. These beams are made of 36 plies of NCT 301 graphite-epoxy prepreg with 25 cm length and 2 cm width. The laminate configuration is $[0/90]_{9s}$.

The first three natural frequencies and mode shapes of the beams are considered.

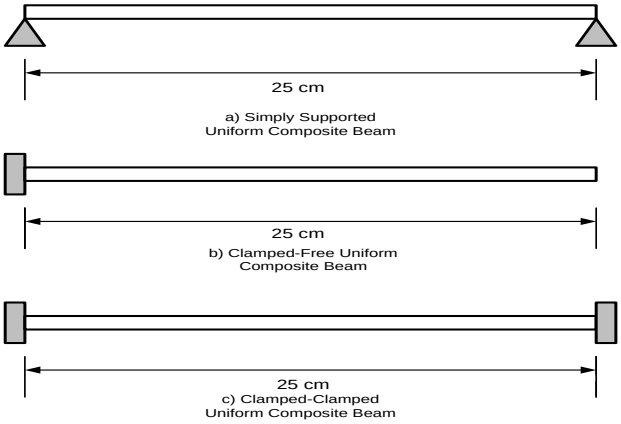

Figure 2.5: Uniform beam with simply supported, clamped-free and clamped-clamped boundary conditions

The natural frequencies have been determined, validated and compared with the exact natural frequencies as shown in Tables 2.3, 2.4 and 2.5. As it can be understood, as the number of elements increases the results become more accurate. The convergence of the calculated natural frequencies is shown in Figure 2.6 for the three considered boundary conditions. In Figure 2.6, the solid lines represents the exact natural frequencies and the dotted lines indicate the results obtained using conventional finite element formulation.

Table 2.3: Exact and approximate lowest three natural frequencies for simply supported uniform beam (rad/s)

First, second and third natural frequencies ($x10^3$ rad/s) for simply supported uniform beam						
Mode	Exact NF	1 E	2 E	3 E	4 E	10 E
1^{st}	1.37	1.52	1.37	1.37	1.37	1.37
2^{nd}	5.47	6.95	6.07	5.53	5.49	5.47
3^{rd}	12.3	_	15.25	13.65	12.52	12.31

in which E denotes the number of elements and NF denotes Natural Frequency.

Table 2.4: Exact and approximate lowest three natural frequencies for clamped-free uniform beam (rad/s)

First, second and third natural frequencies ($x10^3$ rad/s) for clamped-free uniform beam						
Mode	Exact NF	1 E	2 E	3 E	4 E	10 E
1^{st}	0.49	0.49	0.49	0.49	0.49	0.49
2^{nd}	3.05	4.82	3.08	3.06	3.05	3.05
3^{rd}	8.54	_	10.41	8.65	8.61	8.55

Table 2.5: Exact and approximate lowest three natural frequencies for clamped-clamped uniform beam (rad/s)

First, second and third natural frequencies ($x10^3$ rad/s) for clamped-clamped Uniform Beam						
Mode	Exact NF	1 E	2 E	3 E	4 E	10 E
1^{st}	3.1	_	3.15	3.11	3.1	3.1
2^{nd}	8.54	_	11.35	8.71	8.62	8.54
3^{rd}	16.74	_	_	20.26	17.1	16.76

As it can be understood from the above tables, when applying the conventional finite element method and using only one element for the analysis, only the first and second natural frequencies of the simply supported and clamped-free beams and none of the natural frequencies of the clamped-clamped beam can be derived. In these tables the blank units indicate the results which cannot be derived using that specific number of elements for the corresponding boundary condition.

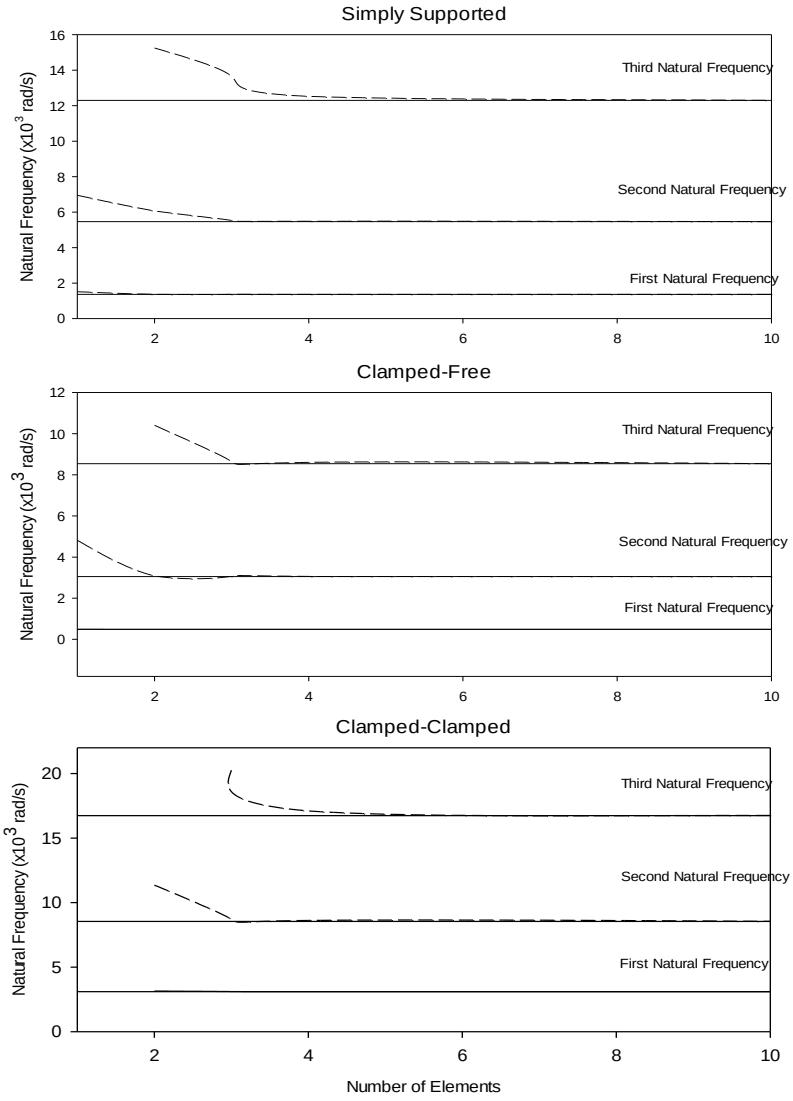

Figure 2.6: Convergence of the natural frequencies obtained using conventional finite element formulation of uniform a) simply supported, b) clamped-free and c) clamped-clamped laminated composite beams, when the number of elements increases from 1 to 10

Having the eigenvectors obtained from equation 2.22 for these uniform beams, one can have the mode shapes of these uniform laminated composite beams. First three mode shapes of uniform laminated composite beams with simply supported, clamped-free and clamped-clamped boundary conditions are shown in Figure 2.7. In Figure 2.7, the dotted lines, the dashed lines and the dashed dotted lines represent the first, the second and the third mode shapes of the beams respectively.

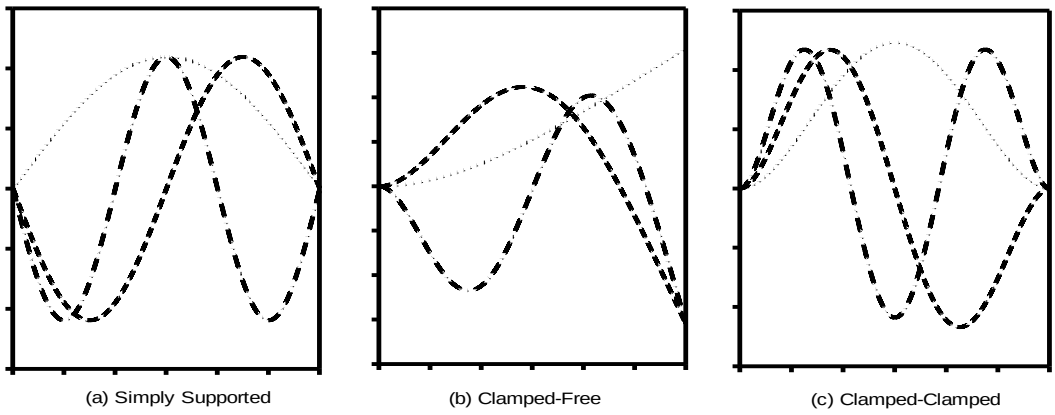

Figure 2.7: First three mode shapes of uniform laminated composite beams with different boundary conditions; dotted line represents the 1st mode, dashed line represents the 2nd mode and dashed dotted line represents the 3rd mode

Uniform beams are considered with a) simply supported, b) clamped-free and c) clamped-clamped boundary conditions. These beams are made of 36 plies of NCT 301 graphite-epoxy prepreg and have 25 cm length and 2 cm width. Five different laminate configurations ($[0/90]_{9s}$, $[90]_{18s}$, $[0]_{18s}$, $[0/45/-45]_{6s}$ and $[45/-45/0]_{6s}$) are considered. The effect of ply orientation on the free vibration of these uniform laminated composite beams is considered. The first three natural frequencies of the beams are to be determined.

Table 2.6: First three natural frequencies of simply supported uniform laminated composite beams with different ply orientations

Natural Frequencies of a Uniform Laminated Simply Supported Beam with 36 Plies (rad/s)					
Fiber Orientations	$[90]_{18s}$	$[0/45/-45]_{6s}$	$[0/90]_{9s}$	$[45/-45/0]_{6s}$	$[0]_{18s}$
1st	478	1273	1367	1368	1804
2nd	1911	5093	5467	5474	7218
3rd	4302	11464	12307	12323	16247

Table 2.7: First three natural frequencies of clamped-free uniform laminated composite beams with different ply orientations

Natural Frequencies of a Uniform Laminated Clamped-Free Beam with 36 Plies (rad/s)					
Fiber Orientations	$[90]_{18s}$	$[0/45/-45]_{6s}$	$[0/90]_{9s}$	$[45/-45/0]_{6s}$	$[0]_{18s}$
1st	170	454	487	488	643
2nd	1067	2842	3051	3055	4028
3rd	2987	7961	8546	8557	11281

Table 2.8: First three natural frequencies of clamped-clamped uniform laminated composite beams with different ply orientations

Natural Frequencies of a Uniform Laminated Clamped-Clamped Beam with 36 Plies (rad/s)					
Fiber Orientations	$[90]_{18s}$	$[0/45/-45]_{6s}$	$[0/90]_{9s}$	$[45/-45/0]_{6s}$	$[0]_{18s}$
1st	1083	2886	3098	3102	4090
2nd	2986	7958	8542	8553	11277
3rd	5858	15611	16759	16780	22124

It can be understood from the natural frequencies that the closer the orientation of plies are to zero degree with respect to the x axis, the stiffer the beams will become, and the least stiff beams are the beams with plies only oriented at 90 degrees. These results are shown in Figure 2.8.

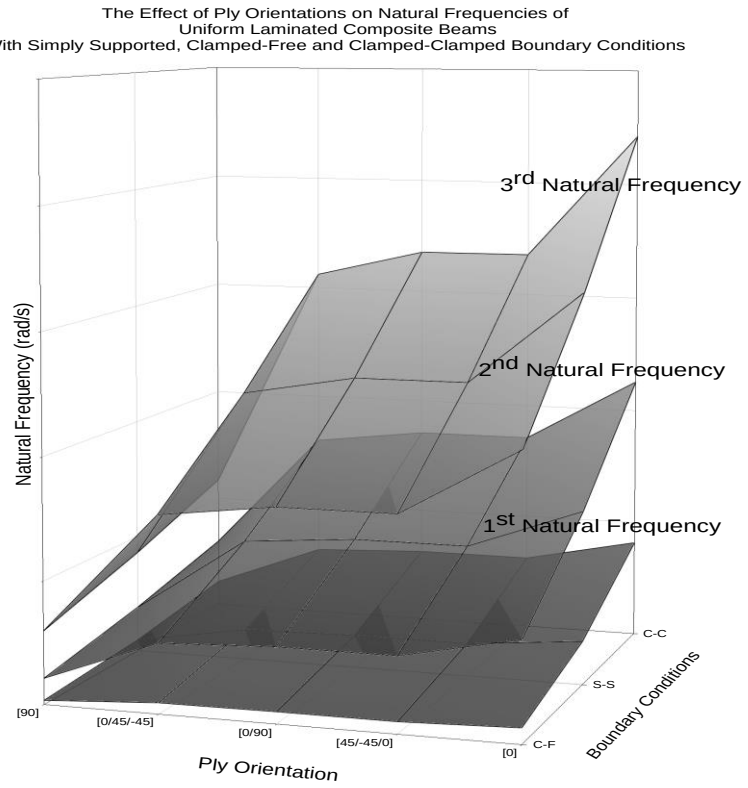

Figure 2.8: The effect of ply orientations on free vibration of uniform laminated composite beams with simply supported, clamped-free and clamped-clamped boundary conditions

Uniform-thickness width-tapered beams are considered with a) simply supported, b) clamped-free, c) clamped-clamped and d) free-clamped boundary conditions. Beams are made of 36 plies of NCT 301 graphite-epoxy prepreg and are 25 cm long. Width of the beams at the left section is 1.66 cm. The laminate configuration is $[0/90]_{9s}$. Nine width ratios (the ratio of the width of the beam at the right section to that of the beam at the left section) (0.01, 0.02, 0.05, 0.1, 0.2, 0.4, 0.6, 0.8 and 1) are considered for these beams.

The first three natural frequencies of the beams are considered. Comparison is made with the existing results [45] obtained using Rayleigh-Ritz method and shown in Table 2.9.

Table 2.9: Comparison of the natural frequencies determined using finite element formulation and the existing results obtained using Rayleigh-Ritz Method for uniform-thickness width-tapered laminated composite beams

Width Ratio		0.01			0.02			0.05		
		R-R	FEM	Difference (%)	R-R	FEM	Difference (%)	R-R	FEM	Difference (%)
S-S	ω_1 (rad/s)	1199	1199	**0.07**	1203	1204	**0.1**	1214	1216	**0.13**
	ω_2 (rad/s)	5056	5055	**0**	5063	5065	**0.05**	5077	5083	**0.11**
	ω_3 (rad/s)	11438	11428	**0.09**	11446	11446	**0**	11460	11470	**0.08**
C-C	ω_1 (rad/s)	2475	2439	**1.45**	2511	2495	**0.65**	2591	2591	**0.01**
	ω_2 (rad/s)	7264	7159	**1.45**	7328	7273	**0.75**	7470	7462	**0.11**
	ω_3 (rad/s)	14657	14505	**1.04**	14754	14679	**0.51**	14971	14958	**0.08**
C-F	ω_1 (rad/s)	902	904	**0.14**	886	887	**0.14**	841	842	**0.14**
	ω_2 (rad/s)	3917	3922	**0.13**	3851	3855	**0.13**	3692	3696	**0.13**
	ω_3 (rad/s)	9531	9542	**0.12**	9385	9396	**0.12**	9068	9079	**0.12**
F-C	ω_1 (rad/s)	151	150	**0.66**	167	167	**0.04**	199	199	**0.19**
	ω_2 (rad/s)	2019	2015	**0.22**	2075	2076	**0.07**	2186	2190	**0.17**
	ω_3 (rad/s)	6879	6868	**0.16**	6981	6985	**0.07**	7173	7184	**0.16**
Width Ratio		0.1			0.2			0.4		
		R-R	FEM	Difference (%)	R-R	FEM	Difference (%)	R-R	FEM	Difference (%)
S-S	ω_1 (rad/s)	1227	1229	**0.14**	1244	1246	**0.14**	1260	1261	**0.12**
	ω_2 (rad/s)	5088	5094	**0.13**	5091	5098	**0.13**	5086	5092	**0.12**
	ω_3 (rad/s)	11464	11478	**0.12**	11456	11471	**0.13**	11439	11453	**0.12**
C-C	ω_1 (rad/s)	2674	2677	**0.13**	2761	2765	**0.14**	2836	2839	**0.12**
	ω_2 (rad/s)	7614	7621	**0.08**	7759	7770	**0.14**	7874	7883	**0.12**
	ω_3 (rad/s)	15188	15178	**0.07**	15383	15370	**0.14**	15485	15504	**0.13**
C-F	ω_1 (rad/s)	781	782	**0.14**	694	695	**0.13**	590	591	**0.12**
	ω_2 (rad/s)	3511	3515	**0.13**	3300	3304	**0.13**	3090	3093	**0.12**
	ω_3 (rad/s)	8760	8771	**0.13**	8456	8467	**0.13**	8200	8210	**0.12**
F-C	ω_1 (rad/s)	233	233	**0.16**	279	280	**0.15**	341	342	**0.13**
	ω_2 (rad/s)	2300	2303	**0.16**	2438	2442	**0.14**	2599	2603	**0.12**
	ω_3 (rad/s)	7348	7359	**0.16**	7531	7542	**0.14**	7709	7719	**0.13**

Width Ratio		0.6			0.8			1		
		R-R	FEM	Difference (%)	R-R	FEM	Difference (%)	R-R	FEM	Difference (%)
S-S	ω_1(rad/s)	1267	1268	**0.11**	1269	1270	**0.1**	1270	1271	**0.08**
	ω_2(rad/s)	5082	5087	**0.11**	5080	5085	**0.1**	5080	5084	**0.08**
	ω_3(rad/s)	11432	11444	**0.11**	11429	11440	**0.1**	11430	11440	**0.08**
C-C	ω_1(rad/s)	2865	2868	**0.11**	2876	2879	**0.1**	2879	2881	**0.08**
	ω_2(rad/s)	7915	7924	**0.11**	7931	7939	**0.1**	7936	7943	**0.08**
	ω_3(rad/s)	15533	15550	**0.11**	15552	15567	**0.09**	15558	15571	**0.08**
C-F	ω_1(rad/s)	527	528	**0.11**	484	485	**0.1**	452	453	**0.08**
	ω_2(rad/s)	2974	2977	**0.11**	2895	2898	**0.1**	2835	2838	**0.08**
	ω_3(rad/s)	8076	8085	**0.11**	7997	8004	**0.1**	7939	7946	**0.08**
F-C	ω_1(rad/s)	386	387	**0.11**	422	423	**0.1**	452	453	**0.08**
	ω_2(rad/s)	2701	2704	**0.11**	2776	2779	**0.1**	2835	2838	**0.08**
	ω_3(rad/s)	7810	7818	**0.11**	7882	7889	**0.1**	7939	7946	**0.08**

In Table 2.9, R-R denotes Rayleigh-Ritz method and FEM represents Finite Element Method. In Table 2.9, the comparison of the natural frequencies obtained using conventional finite element formulation and Rayleigh-Ritz method is done with respect to the results obtained using Rayleigh-Ritz method.

2.3. Uniform-width thickness-tapered beams

Generally, there are three types of thickness-tapered beams: externally tapered, mid-plane tapered and internally-tapered beams. Thickness-tapering is achieved by terminating selected plies at specific locations through the length of the beam. In the present study, four types of internally thickness-tapered configurations corresponding to four different types of plies drop-offs are considered, as shown in Figure 2.9. The width of beams is constant through the length of the beams. Conventional finite element method

is used to analyze the free vibration response of these symmetric beams. Two nodes per element and two degrees of freedom (deflection and rotation) per node are considered in this method.

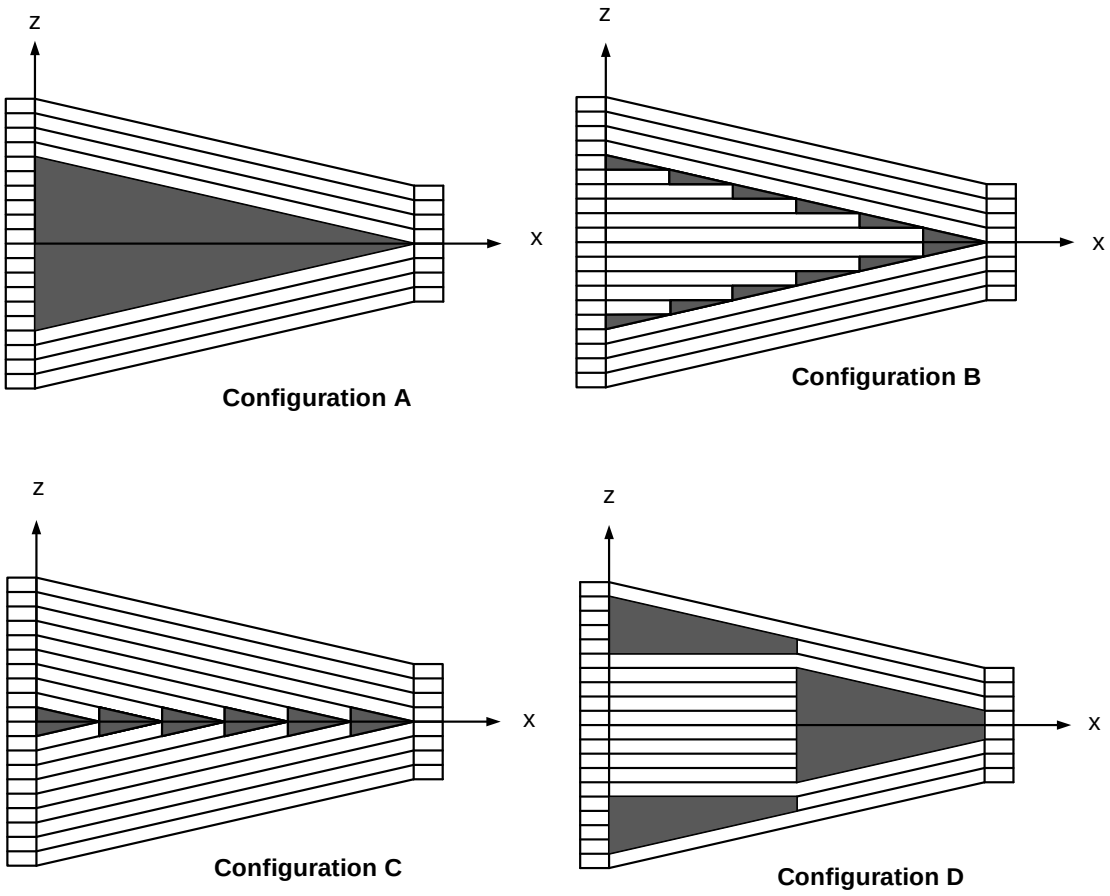

Figure 2.9: Four different configurations of internally thickness-tapered beams

2.3.1. Conventional finite element formulation

In a thickness-tapered beam, the properties of the beam vary through the length of the beam. As a result, the stiffness matrix and the mass matrix are different for each element.

2.3.1.1. Derivation of coefficients of stiffness and mass matrices

For a thickness-tapered beam using cylindrical bending theory the bending moment is given as [40]:

$$M_x = -bD_{11}(x)\cos^4(\varphi)\frac{\partial^2 w}{\partial x^2} \tag{2.24}$$

in which φ denotes the thickness-tapering angle which is shown in Figure 2.10 and $D_{11}(x)$ for a thickness-tapered beam is given as below [16]:

$$D_{11}(x) = \sum_{k=1}^{n} \frac{1}{3}\left({h'_k}^3 - {h'_{k-1}}^3\right)\bar{Q}_{11} \tag{2.25}$$

in which $\bar{Q}_{11}$ is the first coefficient of the transformed reduced ply stiffness matrix. h'_k and h'_{k-1} denote distances to the top and to the bottom interfaces of each ply from the centerline of the beam respectively and are shown in Figure 2.10.

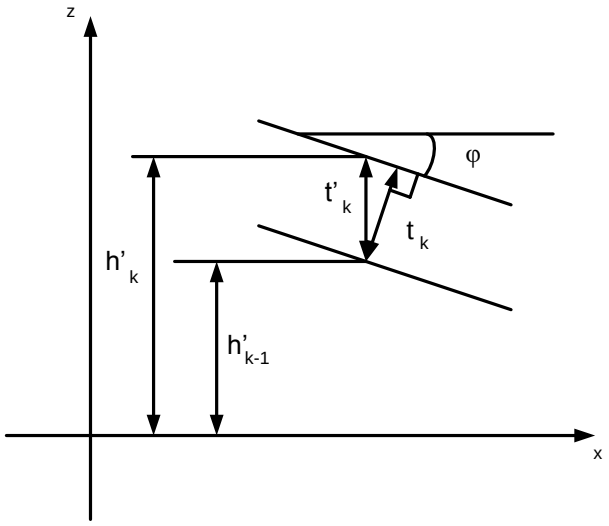

Figure 2.10: Arbitrary ply in the thickness-tapered composite beam

Inserting equation (2.24) into equation (2.1), one can derive the equation of motion for uniform-width thickness-tapered beams as:

$$\frac{\partial^2}{\partial x^2}\left(bD_{11}(x)\cos^4(\varphi)\frac{\partial^2 w}{\partial x^2}\right) - b\tilde{N}_x^i\frac{\partial^2 w}{\partial x^2} - b\tilde{q}(x) + b\rho_s\frac{\partial^2 w}{\partial t^2} = 0 \qquad (2.26)$$

Coefficients of element's stiffness and mass matrices of a uniform-width thickness-tapered beam are given as [40]:

$$k_{ij}^e = \int_0^l b(x)D_{11}(x)\cos^4(\varphi)\frac{d^2N_i}{dx^2}\frac{d^2N_j}{dx^2}dx \qquad (2.27a)$$

$$m_{ij}^e = \int_0^l b(x)\rho_s N_i N_j dx \qquad (2.27b)$$

It is important to mention that for an element of a thickness-tapered beam which might have both composite plies and resin pockets, ρ_s is given as:

$$\rho_s = \sum_{k=1}^{n}\rho_k(h_k' - h_{k-1}') \qquad (2.28)$$

in which n denotes the number of plies and ρ_k is the density of each ply.

In the equations $(2.27a)$ and $(2.27b)$, k_{ij}^e and m_{ij}^e denote the coefficients of the element stiffness and mass matrices of a symmetric, thickness-tapered uniform-width laminated composite beam respectively.

2.3.1.2. Stiffness and mass matrices

Integrating equations (2.27a) and (2.27b) using MATLAB® software, one can find the coefficients of the stiffness and the mass matrices for an element. Equations $(2.30a)$ and $(2.30b)$ provide the first and the last coefficients of the stiffness matrix, and all the other coefficients are listed in the Appendix A.

$$[k^e] = \cos^3(\varphi)\begin{bmatrix} k_{11}^e & k_{12}^e & k_{13}^e & k_{14}^e \\ k_{12}^e & k_{22}^e & k_{23}^e & k_{24}^e \\ k_{13}^e & k_{23}^e & k_{33}^e & k_{34}^e \\ k_{14}^e & k_{24}^e & k_{34}^e & k_{44}^e \end{bmatrix} \tag{2.29}$$

$$k_{11}^e = \sum_{k=1}^{n} b(\bar{Q}_{11})_k t_k \frac{24m^2l^2 + 60clm + 60c^2 + {t_k'}^2}{5l^3} \tag{2.30a}$$

$$k_{44}^e = \sum_{k=1}^{n} b(\bar{Q}_{11})_k t_k \frac{38m^2l^2 + 90clm + 60c^2 + 5{t_k'}^2}{15l} \tag{2.30b}$$

In the equation (2.30), l represents the length of the element, m is the slope of an arbitrary ply and c denotes the intercept of the centre line of each ply with respect to the x axis.

In the derivation of the element mass matrix of a thickness-tapered beam, it should be noted that the cross-section area varies through the length of the beam and each element may have both composite plies and resin pockets, consequently, ρ_s should be found using equation (2.28). Using equation (2.20c) and having ρ_s for an element, one can derive the element mass matrix for a thickness-tapered beam.

Knowing the stiffness and mass matrices for each element based on the conventional finite element formulation, the global stiffness matrix $[K]$ and the global mass matrix $[M]$ can be established for the beam. The free vibration of uniform-width thickness-tapered beams can be analyzed solving the similar eigenvalue problem to that considered in equation (2.22) using MATLAB® software.

2.3.2. Validation

Validation of results is performed for two cases as follows: (i) Natural frequency of a thickness-tapered beam for each mode should be between the exact natural frequency

of that mode of uniform beams with number of plies equal to the number of plies at the thick section and at the thin section of the thickness-tapered beam. Uniform beams considered here should have the similar material properties, length, width and ply orientations as those of the thickness-tapered beam. Note that there exists an exception for clamped-free boundary condition in which the decrease in the weight at the free end of the beam will cause it to have higher natural frequencies than a uniform beam with number of plies equal to the number of plies at the thick section of the thickness-tapered beam. (ii) Comparing the present results with the existing results [4].

Uniform-width thickness-tapered beams are considered with a) simply supported, b) clamped-free and c) clamped-clamped boundary conditions. These beams are made of 20 plies at the thick section and 16 plies at the thin section and are made of NCT-301 graphite-epoxy prepreg as shown in Figure 2.11. Length of these beams is equal to 25 cm, their width is equal to 2 cm and the laminate configuration at the thick section is $[0/90]_{5s}$.

First three natural frequencies of the beams are considered. Obtained natural frequencies for each boundary condition of these uniform-width thickness-tapered beams should lie between the exact natural frequencies of a uniform beam with 20 plies and a uniform beam with 16 plies with the same boundary condition as that of the considered uniform-width thickness-tapered beam. These results are derived and shown in Table 2.10.

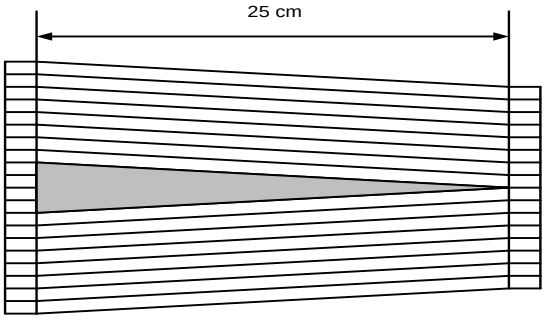

Figure 2.11: Uniform-width thickness-tapered beam, 20-16 plies

Table 2.10: Comparison of the results for thickness-tapered beams with that of uniform beams

Natural Frequency (rad/s)									
	Simply Supported Beam			Clamped-Free Beam			Clamped-Clamped Beam		
	Mode 1	Mode 2	Mode 3	Mode 1	Mode 2	Mode 3	Mode 1	Mode 2	Mode 3
Exact NF, Uniform 20 Plies	684	2735	6154	244	1526	4274	1550	4272	8376
20-16 Thickness-Tapered	619	2477	5572	251	1439	3925	1403	3868	7581
Exact NF, Uniform 16 Plies	537	2147	4830	191	1198	3355	1217	3353	6574

In the Table 2.10, NF denotes Natural Frequency.

As illustrated and expected, except the first natural frequency of the clamped-free beam, all the natural frequencies of the thickness-tapered beam lie between the exact natural frequencies of uniform beams with 16 plies and 20 plies.

Uniform-width thickness-tapered beams are considered with a) simply supported, b) clamped-free and c) clamped-clamped boundary conditions. These beams are made of configurations A, B, C and D as shown in Figure 2.12. These beams are made of 36 plies at the thick section and 12 plies at the thin section and are made of NCT-301 graphite-

epoxy prepreg. The laminate configuration at the thick section is $[0/90]_{9s}$. Beams are 3.45 cm long and their width is equal to 0.5 cm**.**

First three natural frequencies of the beams are considered. Natural frequencies determined using conventional finite element formulation are validated using the existing results [4] and are shown in Table 2.11.

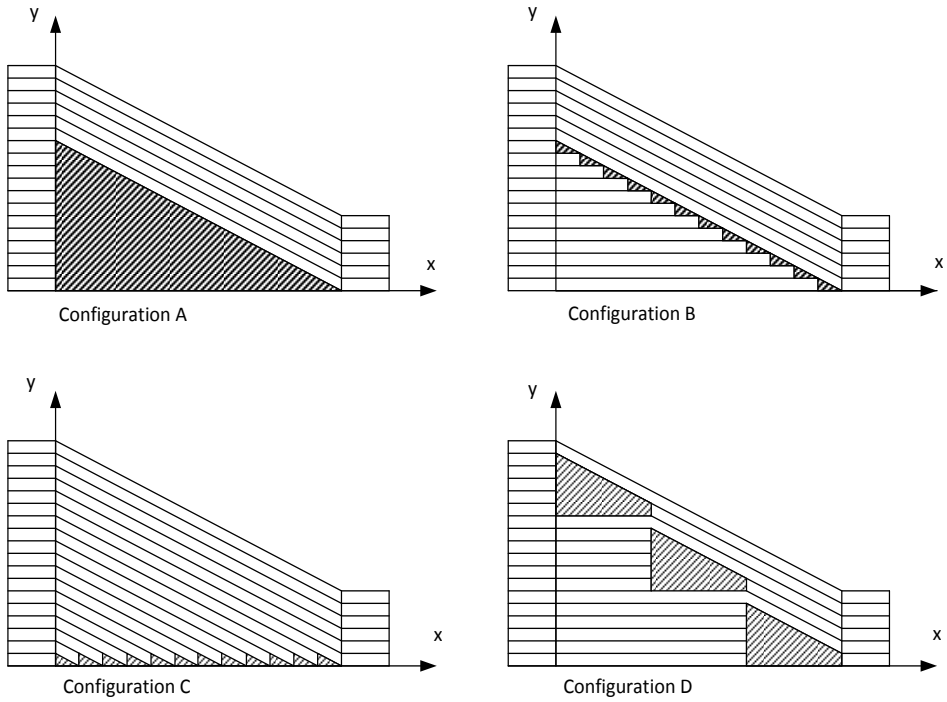

Figure 2.12: Side-view of the upper half of the thickness-tapered beams made of configurations A, B, C and D with 36-12 plies

As it is shown in Figure 2.12, these configurations have different patterns of ply dropping-off, the size and the location of the resin pockets, and also, the way the resin pockets are separated is different for each configuration. In this study it will be shown that configuration D is the stiffest configuration considered. That is because in configuration D, large resin pockets are separated with a bent continuous composite ply

which increases the stiffness of this configuration whereas in the other configurations composite plies are dropped somehow that there does not exist any continuous ply between the resin pockets. It is shown that in the configuration A, there exist one large resin pocket which reduces its stiffness and in configurations B and C, small resin pockets are connected which decreases the stiffness of the structure.

Table 2.11: Comparison of the natural frequencies of thickness-tapered beams determined using conventional finite element formulation with existing results [4]

Natural Frequencies ($\times 10^4$ rad/sec)											
			Mode-1	Mode-2	Mode-3	**Average Percentage Error**		Mode-1	Mode-2	Mode-3	**Average Percentage Error**
Configuration A	S-S	Existing Results [4]	4.268	17.502	39.183	**3.940**	Configuration B	4.540	18.776	43.886	**3.992**
		CFEM Results	4.121	16.788	37.500			4.407	18.315	40.999	
		Percentage Error	**3.446**	**4.079**	**4.295**			**2.943**	**2.455**	**6.578**	
	C-F	Existing Results [4]	2.635	11.613	29.028	**3.545**		2.839	12.057	30.451	**1.048**
		CFEM Results	2.553	11.196	27.884			2.872	12.284	30.486	
		Percentage Error	**3.098**	**3.595**	**3.940**			**-1.145**	**-1.884**	**-0.115**	
	C-C	Existing Results [4]	9.697	26.855	52.777	**4.041**		10.175	28.682	59.052	**2.951**
		CFEM Results	9.336	25.755	50.506			10.230	28.168	55.201	
		Percentage Error	**3.725**	**4.096**	**4.303**			**-0.539**	**1.793**	**6.521**	
Configuration C	S-S	Existing Results [4]	4.520	19.279	45.114	**3.679**	Configuration D	5.132	21.635	50.139	**4.280**
		CFEM Results	4.492	18.683	41.812			5.165	20.821	45.911	
		Percentage Error	**0.630**	**3.089**	**7.320**			**-0.647**	**3.761**	**8.432**	
	C-F	Existing Results [4]	2.955	12.541	31.605	**0.900**		2.824	13.241	34.908	**1.075**
		CFEM Results	2.983	12.602	31.204			2.811	13.321	34.147	
		Percentage Error	**-0.949**	**-0.483**	**1.268**			**0.438**	**-0.606**	**2.181**	
	C-C	Existing Results [4]	10.555	29.823	60.967	**3.873**		11.463	33.027	67.663	**5.571**
		CFEM Results	10.469	28.812	56.443			11.109	31.540	61.489	
		Percentage Error	**0.807**	**3.391**	**7.421**			**3.086**	**4.503**	**9.125**	

In the Table 2.11, CFEM denotes Conventional Finite Element Method.

In Table 2.11, the natural frequencies of the uniform-width thickness-tapered laminated composite beams with simply supported, clamped-free and clamped-clamped

boundary conditions and four thickness-tapering configurations (configurations A, B, C and D) are obtained using conventional finite element formulation. A comparison is performed with respect to the existing results [4], and excellent agreement has been observed. These results are also shown in Figure 2.13.

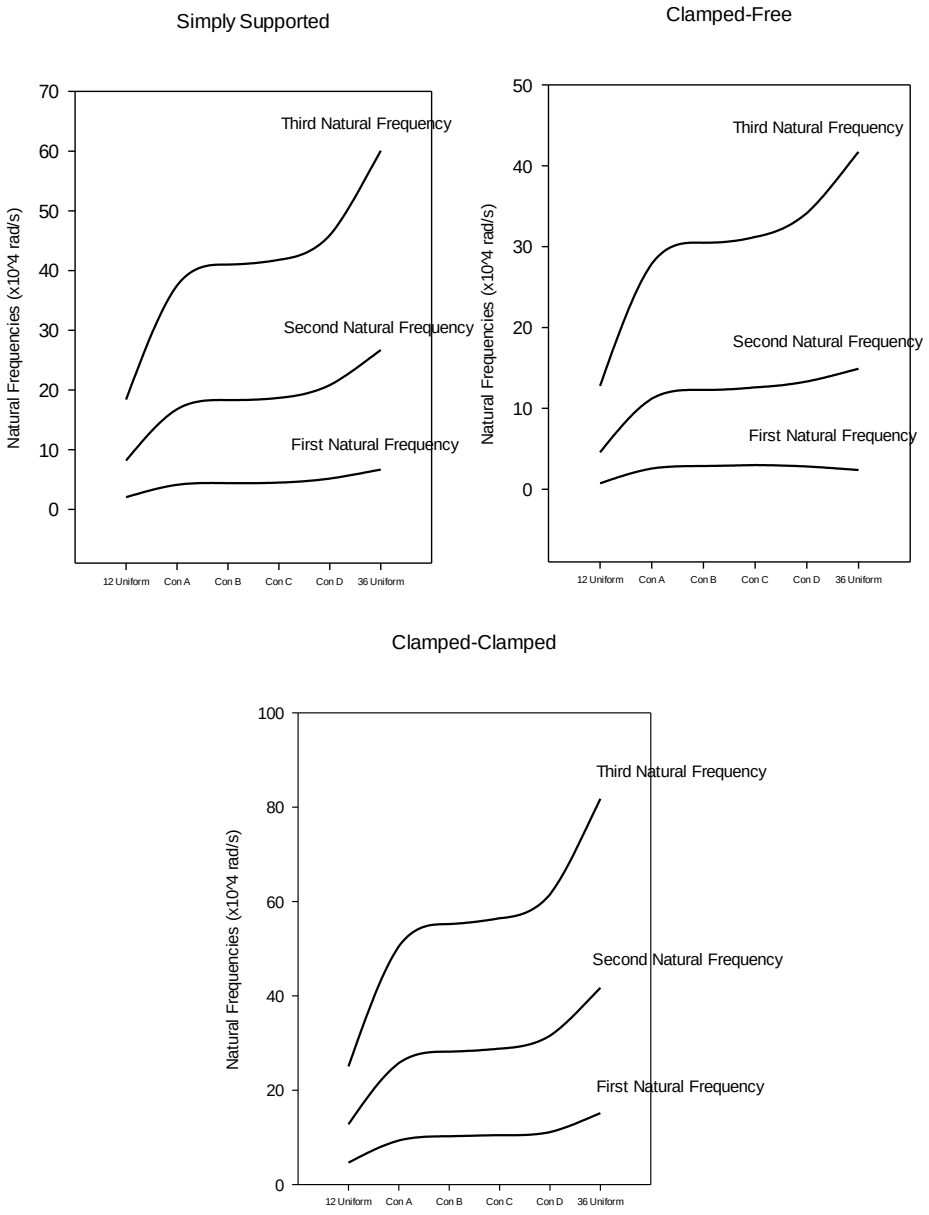

Figure 2.13: First three finite element natural frequencies for uniform-width thickness-tapered beams (configurations A, B, C and D) and exact natural frequencies of uniform beams with 12 and 36 plies

In the Figure 2.13, Con A, Con B, Con C and Con D denote configurations A, B, C and D respectively.

2.4. Width-tapered thickness-tapered beams

As explained previously, thickness-tapering is achieved by terminating selected plies at specific locations through the length of the beam. Similarly, width-tapering is done by linearly cutting the beam on the surfaces perpendicular to the mid-plane of the beam. In this chapter, we consider four types of internally-thickness-tapered configurations corresponding to four different types of plies drop-offs, as shown in Figure 2.14.

The beam's width varies linearly along its length from B_l at x = 0 to B_r at x = L, as shown in Figure 2.14.

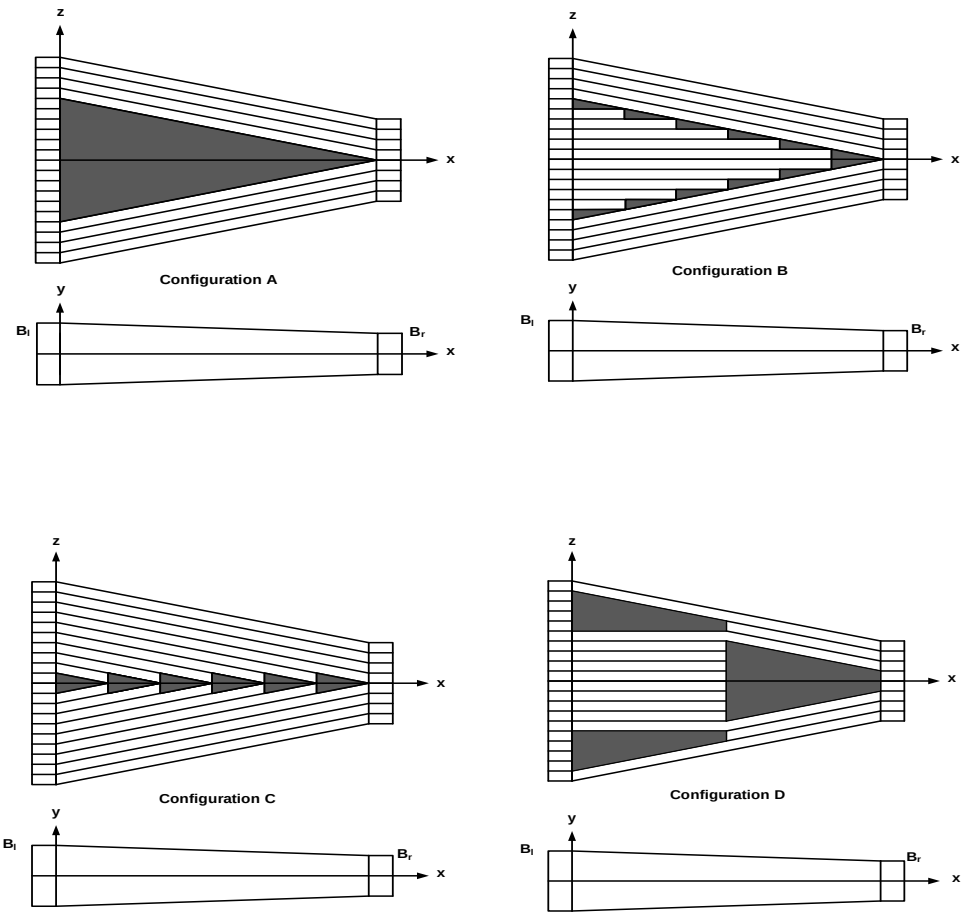

Figure 2.14: Width-tapered thickness-tapered beams

2.4.1. Conventional finite element formulation

Free vibration analysis has been done on these symmetric variable-width variable-thickness laminated composite beams using conventional finite element formulation. Similar steps to those that were performed in the previous sections are followed in this section in order to derive stiffness and mass matrices for the beams.

Integrating the equation of motion based on classical laminated beam theory for a variable-width variable-thickness laminated composite beam through the length of the

beam, one can derive the similar coefficients of stiffness and mass matrices to those represented in equation (2.27). The only difference is that the width of each element is different and needs to be considered in the formulation. For this reason, width at the mid-point of each element is considered in the formulations of the element stiffness and mass matrices.

Knowing the stiffness and mass matrices of each element based on the conventional finite element formulation, the global stiffness matrix $[K]$ and the global mass matrix $[M]$ can be established for the beam. The free vibration of thickness-tapered width-tapered beams can be analyzed solving the similar eigenvalue problem to that considered in the equation (2.22) using MATLAB® software.

In the present study width-tapering angle is described by the width ratio (the ratio of the width of the beam at the right section to that of the beam at the left section) as shown in the equation (2.3).

2.4.2. Validation

Validation of results is performed using the existing results obtained using Rayleigh-Ritz method [45]. Obtained results have been validated using two cases: i) beams with constant thickness-tapering angle and different width ratios, and ii) beams with constant width ratio and different thickness-tapering angles.

Thickness-tapered width-tapered beams are considered with a) simply supported, b) clamped-free and c) clamped-clamped boundary conditions. Five width ratio values are considered for these beams (0.2, 0.4, 0.6, 0.8 and 1). The beams are made of configurations A, B, C and D as shown in Figure 2.12. These beams are made of 36 plies at the thick section and 12 plies at the thin section and are made of NCT-301 graphite-

epoxy prepreg. These beams are 15 cm long and their width is equal to 1.5 cm at the left end**.** Laminate configuration is $[0/90]_{9s}$ at the thick section.

First three natural frequencies of these beams are considered. Comparison is done with existing results obtained using Rayleigh-Ritz method [45] and is shown in Table 2.12.

Table 2.12: Comparison of the natural frequencies obtained using conventional finite element and Rayleigh-Ritz methods for laminated composite beams with constant thickness-tapering angle and varying width-ratio

	Configuration A-SS					Configuration B-SS				
width ratio ($\frac{B_r}{B_l}$)	0.2	0.4	0.6	0.8	1	0.2	0.4	0.6	0.8	1
ω_1 (R-R)	1943	2022	2047	2075	2091	2188	2256	2293	2317	2333
ω_1 (FEM)	2003	2087	2129	2160	2178	2200	2294	2350	2383	2405
% difference	**3.09**	**3.19**	**4.03**	**4.10**	**4.20**	**0.56**	**1.67**	**2.47**	**2.86**	**3.12**
ω_2 (R-R)	9016	9005	8996	8992	8991	10142	10088	9954	9931	9915
ω_2 (FEM)	9034	8972	8928	8900	8880	10486	10400	10346	10308	10281
% difference	**0.20**	**0.37**	**0.76**	**1.02**	**1.23**	**3.40**	**3.09**	**3.93**	**3.80**	**3.69**
ω_3 (R-R)	20286	20254	20238	20232	20230	22683	22577	22515	22478	22454
ω_3 (FEM)	20096	19979	19910	19866	19836	23379	23235	23150	23093	23054
% difference	**0.94**	**1.36**	**1.62**	**1.81**	**1.95**	**3.07**	**2.92**	**2.82**	**2.73**	**2.67**
	Configuration A-CC					Configuration B-CC				
width ratio ($\frac{B_r}{B_l}$)	0.2	0.4	0.6	0.8	1	0.2	0.4	0.6	0.8	1
ω_1 (R-R)	4890	5021	5071	5091	5096	5837	5850	5809	5765	5713
ω_1 (FEM)	5006	5032	5009	4975	4938	6071	6072	6027	5972	5916
% difference	**2.38**	**0.22**	**1.22**	**2.27**	**3.09**	**4.01**	**3.80**	**3.76**	**3.60**	**3.55**
ω_2 (R-R)	13740	13941	14013	14040	14046	15653	15754	15602	15573	15536
ω_2 (FEM)	13722	13755	13721	13674	13623	16218	16238	16186	16117	16047
% difference	**0.13**	**1.33**	**2.08**	**2.61**	**3.01**	**3.61**	**3.07**	**3.74**	**3.49**	**3.29**
ω_3 (R-R)	27179	27418	27499	27529	27535	30398	30517	30516	30486	30444
ω_3 (FEM)	26826	26863	26824	26771	26715	31447	31477	31419	31345	31270
% difference	**1.30**	**2.02**	**2.45**	**2.75**	**2.98**	**3.45**	**3.15**	**2.96**	**2.82**	**2.71**

	Configuration A-CF					Configuration B-CF				
width ratio ($\frac{B_r}{B_l}$)	0.2	0.4	0.6	0.8	1	0.2	0.4	0.6	0.8	1
ω_1 (R-R)	1929	1671	1499	1386	1293	2464	2115	1926	1777	1667
ω_1 (FEM)	1999	1726	1557	1438	1347	2551	2193	1999	1848	1740
% difference	**3.59**	**3.28**	**3.90**	**3.77**	**4.19**	**3.52**	**3.68**	**3.78**	**4.00**	**4.40**
ω_2 (R-R)	6758	6268	6032	5871	5749	7941	7421	7137	6954	6812
ω_2 (FEM)	6905	6454	6211	6047	5924	8227	7689	7397	7197	7046
% difference	**2.17**	**2.97**	**2.96**	**2.99**	**3.05**	**3.60**	**3.61**	**3.65**	**3.49**	**3.44**
ω_3 (R-R)	15411	14799	14574	14291	14186	17993	17413	17122	16929	16786
ω_3 (FEM)	15851	15326	15060	14883	14752	18641	18014	17691	17474	17310
% difference	**2.85**	**3.56**	**3.34**	**4.14**	**3.99**	**3.60**	**3.45**	**3.32**	**3.22**	**3.12**
	Configuration C-SS					Configuration D-SS				
width ratio ($\frac{B_r}{B_l}$)	0.2	0.4	0.6	0.8	1	0.2	0.4	0.6	0.8	1
ω_1 (R-R)	2110	2182	2222	2248	2265	2843	2931	2980	3010	3030
ω_1 (FEM)	2184	2269	2322	2357	2378	2691	2792	2854	2894	2923
% difference	**3.51**	**4.00**	**4.48**	**4.88**	**5.01**	**5.34**	**4.73**	**4.22**	**3.86**	**3.53**
ω_2 (R-R)	9791	9722	9677	9649	9630	12460	12390	12343	12313	12293
ω_2 (FEM)	10073	10000	9948	9915	9892	12816	12750	12703	12673	12657
% difference	**2.88**	**2.86**	**2.80**	**2.76**	**2.73**	**2.86**	**2.91**	**2.92**	**2.92**	**2.96**
ω_3 (R-R)	21687	21570	21504	21462	21434	27857	27720	27644	27596	27565
ω_3 (FEM)	22436	22303	22224	22173	22137	29009	28817	28697	28615	28557
% difference	**3.45**	**3.40**	**3.35**	**3.31**	**3.28**	**4.13**	**3.96**	**3.81**	**3.69**	**3.60**
	Configuration C-CC					Configuration D-CC				
width ratio ($\frac{B_r}{B_l}$)	0.2	0.4	0.6	0.8	1	0.2	0.4	0.6	0.8	1
ω_1 (R-R)	5364	5413	5404	5378	5347	6920	6999	6998	6972	6938
ω_1 (FEM)	5629	5653	5625	5586	5542	7172	7166	7108	7038	6967
% difference	**4.95**	**4.43**	**4.09**	**3.86**	**3.65**	**3.64**	**2.39**	**1.57**	**0.94**	**0.41**
ω_2 (R-R)	14596	14672	14660	14624	14581	19051	19170	19168	19132	19086
ω_2 (FEM)	15367	15404	15366	15312	15254	18957	19053	19041	19000	18952
% difference	**5.28**	**4.99**	**4.82**	**4.70**	**4.62**	**0.49**	**0.61**	**0.66**	**0.69**	**0.70**
ω_3 (R-R)	28449	28543	28531	28492	28446	37330	37472	37470	37431	37380
ω_3 (FEM)	30003	30048	30005	29946	29883	38051	38138	38103	38042	37975
% difference	**5.46**	**5.27**	**5.17**	**5.10**	**5.05**	**1.93**	**1.78**	**1.69**	**1.63**	**1.59**

	Configuration C-CF					Configuration D-CF				
width ratio ($\frac{B_r}{B_l}$)	0.2	0.4	0.6	0.8	1	0.2	0.4	0.6	0.8	1
ω_1 (R-R)	2238	1931	1738	1621	1524	2858	2455	2205	2054	1931
ω_1 (FEM)	2319	1997	1806	1684	1579	2958	2548	2300	2143	2012
% difference	**3.64**	**3.39**	**3.94**	**3.90**	**3.59**	**3.50**	**3.80**	**4.30**	**4.31**	**4.20**
ω_2 (R-R)	7599	7108	6841	6659	6522	9249	8649	8325	8105	7939
ω_2 (FEM)	7788	7276	7000	6813	6672	9582	8954	8603	8364	8179
% difference	**2.49**	**2.36**	**2.32**	**2.31**	**2.30**	**3.60**	**3.53**	**3.34**	**3.20**	**3.03**
ω_3 (R-R)	17217	16661	16377	16033	15892	21492	20798	20447	20217	20045
ω_3 (FEM)	17779	17180	16874	16672	16521	21987	21263	20906	20675	20506
% difference	**3.26**	**3.11**	**3.03**	**3.99**	**3.96**	**2.30**	**2.24**	**2.25**	**2.27**	**2.30**

In the Table 2.12, R-R denotes Rayleigh-Ritz method.

In the Table 2.12, the comparison of the natural frequencies obtained using conventional finite element and Rayleigh-Ritz methods is done with respect to the results obtained using Rayleigh-Ritz method. Excellent agreement has been observed.

Fundamental natural frequencies of these beams are shown in Figure 2.15 to demonstrate the effect of width ratio on the natural frequencies of width-tapered thickness-tapered beams.

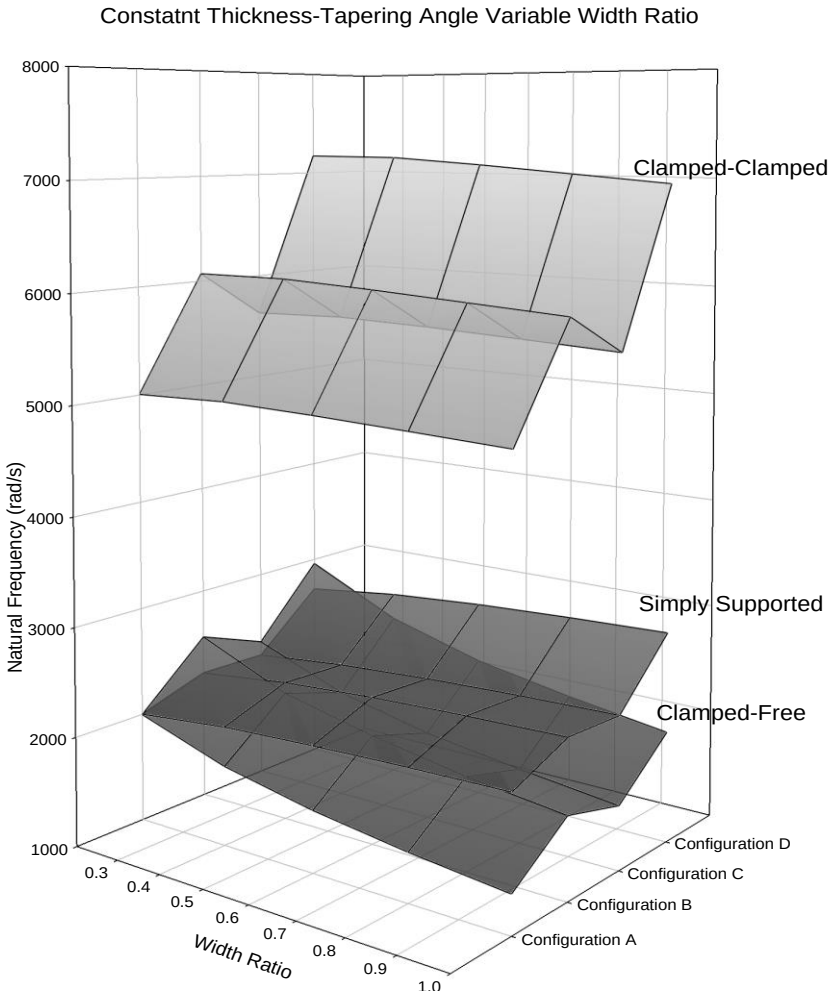

Figure 2.15: Fundamental natural frequencies obtained using conventional finite element formulation for constant thickness-tapering angle varying width-ratio of simply supported, clamped-free and clamped-clamped beams

Thickness-tapered width-tapered beams are considered with a) simply supported, b) clamped-free and c) clamped-clamped boundary conditions. Width ratio of these beams is constant and is equal to 0.5. The beams are made of configurations A, B, C and D. These beams are made of 36 plies at the thick section and 12 plies at the thin section and are made of NCT-301 graphite-epoxy prepreg as shown in Figure 2.12. Different thickness-tapering angles are considered for these beams. Thickness-tapering angle varies

with the change in the length of the beams from 0.344 degrees to 0.86 degrees. The laminate configuration at the thick section is $[0/90]_{9s}$. Width is equal to 1.5 cm at the left end and 0.75 cm at the right end**.**

First three natural frequencies of the beams are considered. Natural frequencies determined using conventional finite element formulation are validated using the existing results obtained using Rayleigh-Ritz method [45] and are represented in Table 2.13.

Table 2.13: Comparison of finite element natural frequencies of constant width-tapering angle variable thickness-tapering angle beams with Rayleigh-Ritz solution

	Configuration A-SS				**Configuration B-SS**			
Thickness-Tapering Angle (deg)	0.344	0.43	0.573	0.86	0.344	0.43	0.573	0.86
L (m)	0.25	0.2	0.15	0.1	0.25	0.2	0.15	0.1
$\frac{L}{H_l}$	56	44	33	22	56	44	33	22
$\frac{L}{B_l}$	17	13	10	7	17	13	10	7
ω_1 (R-R)	781	1219	2165	4868	820	1282	2277	5115
ω_1 (FEM)	760	1188	2110	4745	838	1307	2322	5230
% difference	**2.61**	**2.57**	**2.55**	**2.53**	**2.14**	**2.02**	**1.98**	**2.25**
ω_2 (R-R)	3244	5069	9000	20219	3655	5696	10121	22741
ω_2 (FEM)	3221	5033	8949	20134	3733	5833	10369	23327
% difference	**0.70**	**0.71**	**0.57**	**0.42**	**2.15**	**2.41**	**2.45**	**2.58**
ω_3 (R-R)	7298	11402	20245	45482	8126	12681	22541	50549
ω_3 (FEM)	7179	11217	19940	44867	8348	13043	23187	52167
% difference	**1.63**	**1.63**	**1.50**	**1.35**	**2.73**	**2.86**	**2.87**	**3.20**

	Configuration A-CC				Configuration B-CC			
ω_1 (R-R)	1821	2845	5052	11349	2136	3322	5898	13225
ω_1 (FEM)	1808	2826	5024	11302	2179	3404	6051	13619
% difference	**0.71**	**0.69**	**0.55**	**0.41**	**2.02**	**2.47**	**2.60**	**2.98**
ω_2 (R-R)	5041	7877	13985	31420	5716	8910	15810	35548
ω_2 (FEM)	4947	7730	13742	30918	5838	9121	16215	36483
% difference	**1.87**	**1.86**	**1.74**	**1.60**	**2.13**	**2.37**	**2.56**	**2.63**
ω_3 (R-R)	9902	15470	27468	61711	11092	17283	30643	68897
ω_3 (FEM)	9665	15101	26847	60405	11323	17692	31452	70762
% difference	**2.39**	**2.38**	**2.26**	**2.12**	**2.08**	**2.37**	**2.64**	**2.71**
	Configuration A-CF				**Configuration B-CF**			
ω_1 (R-R)	563	878	1552	3520	733	1139	2025	4541
ω_1 (FEM)	583	913	1617	3682	752	1170	2081	4694
% difference	**3.53**	**4.01**	**4.20**	**4.60**	**2.54**	**2.71**	**2.78**	**3.36**
ω_2 (R-R)	2213	3457	6137	13919	2644	4130	7337	16477
ω_2 (FEM)	2274	3554	6317	14218	2710	4234	7526	16939
% difference	**2.79**	**2.79**	**2.93**	**2.15**	**2.51**	**2.52**	**2.58**	**2.80**
ω_3 (R-R)	5238	8184	14531	32646	6276	9804	17418	39123
ω_3 (FEM)	5463	8536	15176	34147	6420	10031	17833	40122
% difference	**4.29**	**4.30**	**4.44**	**4.60**	**2.29**	**2.32**	**2.38**	**2.55**
	Configuration C-SS				**Configuration D-SS**			
ω_1 (R-R)	810	1268	2247	5054	1066	1665	2959	6647
ω_1 (FEM)	827	1296	2299	5175	1020	1591	2826	6366
% difference	**2.16**	**2.21**	**2.35**	**2.41**	**4.31**	**4.44**	**4.48**	**4.23**
ω_2 (R-R)	3494	5457	9700	21821	4454	6958	12364	27776
ω_2 (FEM)	3590	5609	9971	22433	4581	7158	12725	28629
% difference	**2.75**	**2.79**	**2.79**	**2.80**	**2.84**	**2.87**	**2.92**	**3.07**
ω_3 (R-R)	7841	12238	21740	48911	9972	15577	27677	62179
ω_3 (FEM)	8013	12521	22259	50081	10351	16173	28750	64684
% difference	**2.20**	**2.32**	**2.39**	**2.39**	**3.81**	**3.82**	**3.88**	**4.03**

	Configuration C-CC				Configuration D-CC			
ω_1 (R-R)	1950	3046	5412	12154	2523	3941	7003	15733
ω_1 (FEM)	2031	3174	5642	12693	2570	4016	7141	16067
% difference	**4.15**	**4.19**	**4.24**	**4.44**	**1.87**	**1.89**	**1.96**	**2.12**
ω_2 (R-R)	5287	8258	14671	32946	6909	10792	19176	43080
ω_2 (FEM)	5540	8657	15389	34624	6860	10717	19052	42865
% difference	**4.80**	**4.83**	**4.89**	**5.09**	**0.71**	**0.69**	**0.64**	**0.50**
ω_3 (R-R)	10525	16456	29242	65697	13503	21093	37478	84198
ω_3 (FEM)	10812	16893	30031	67566	13726	21447	38126	85779
% difference	**2.72**	**2.65**	**2.70**	**2.85**	**1.65**	**1.68**	**1.73**	**1.88**
	Configuration C-CF				**Configuration D-CF**			
ω_1 (R-R)	651	1026	1807	4093	850	1326	2355	5295
ω_1 (FEM)	681	1070	1891	4269	869	1357	2412	5425
% difference	**4.57**	**4.29**	**4.66**	**4.31**	**2.22**	**2.33**	**2.39**	**2.47**
ω_2 (R-R)	2437	3806	6761	15182	3089	4826	8568	19262
ω_2 (FEM)	2564	4007	7123	16026	3154	4928	8761	19712
% difference	**5.24**	**5.28**	**5.35**	**5.56**	**2.13**	**2.11**	**2.26**	**2.34**
ω_3 (R-R)	5834	9112	16343	36699	7422	11594	20601	46280
ω_3 (FEM)	6123	9567	17008	38265	7583	11848	21062	47386
% difference	**4.96**	**4.99**	**4.07**	**4.27**	**2.16**	**2.19**	**2.24**	**2.39**

In Table 2.13, H_l denotes the height of the beam at the left section. In this table, the comparison of the natural frequencies determined using conventional finite element formulation is done with respect to the results obtained using Rayleigh-Ritz method. Excellent agreement has been observed.

Fundamental natural frequencies of these beams are used in Figure 2.16 to show the effect of thickness-tapering angle on the natural frequencies of width-tapered thickness-tapered beams.

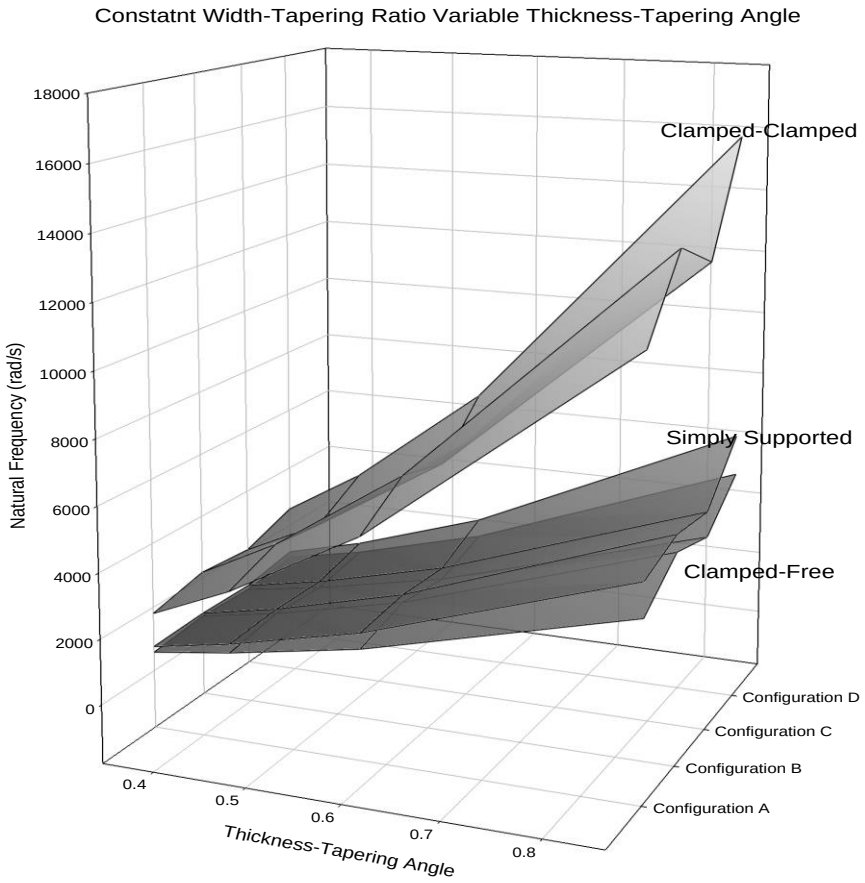

Figure 2.16: Fundamental natural frequencies obtained using conventional finite element formulation of constant width ratio (0.5) varying thickness-tapering angle beams with simply supported, clamped-free and clamped-clamped boundary conditions

Thickness-tapered width-tapered laminated composite beams are considered with configurations A, B, C and D. Simply supported, clamped-free and clamped-clamped boundary conditions are considered for these beams. Width ratio of these beams is constant and equal to 0.5, the length of the beams is also constant and equal to 25 cm. Five different laminate configurations ($[0/90]_{9s}$, $[90/0]_{9s}$, $[90]_{18s}$, $[0]_{18s}$, $[0/45/-45]_{6s}$ and $[45/-45/0]_{6s}$) are considered at the thick section of the beams. The effect of ply orientations on the free vibrations of thickness-tapered width-tapered laminated

composite beams is considered. These beams are made of 36 plies at the thick section and 12 plies at the thin section and are made of NCT-301 graphite-epoxy prepreg as shown in Figure 2.12. Width is equal to 1.5 cm at the left end and 0.75 cm at the right end of the beam**.** First three natural frequencies of these beams are derived and represented in Table 2.14.

Table 2.14: Natural frequencies of thickness-tapered width-tapered laminated composite beams (configurations A, B, C and D) having different ply orientations

NFs of Simply Supported Configuration A (rad/s)							**NFs of Simply Supported Configuration C (rad/s)**						
Fiber Orientations	[90]	[0/90]	[0/45/-45]	[90/0]	[45/-45/0]	[0]	Fiber Orientations	[90]	[0/90]	[0/45/-45]	[90/0]	[45/-45/0]	[0]
1st NF	278	705	708	798	799	1029	1st NF	262	672	674	770	772	988
2nd NF	1192	3000	3010	3375	3382	4359	2nd NF	1142	2942	2953	3349	3357	4311
3rd NF	2657	6683	6704	7530	7546	9718	3rd NF	2546	6554	6580	7473	7492	9614
NFs of Clamped-Free Configuration A (rad/s)							**NFs of Clamped-Free Configuration C (rad/s)**						
1st NF	222	556	557	600	601	788	1st NF	223	587	588	645	646	843
2nd NF	844	2129	2134	2360	2364	3065	2nd NF	822	2132	2139	2398	2403	3103
3rd NF	2018	5081	5096	5692	5703	7363	3rd NF	1946	5025	5044	5701	5714	7350
NFs of Clamped-Clamped Configuration A (rad/s)							**NFs of Clamped-Clamped Configuration C (rad/s)**						
1st NF	676	1688	1694	1896	1900	2449	1st NF	648	1672	1679	1899	1904	2448
2nd NF	1841	4613	4629	5193	5205	6704	2nd NF	1764	4542	4561	5174	5188	6660
3rd NF	3591	9012	9043	10157	10180	13106	3rd NF	3439	8851	8888	10096	10122	12987
NFs of Simply Supported Configuration B (rad/s)							**NFs of Simply Supported Configuration D (rad/s)**						
Fiber Orientations	[90]	[0/90]	[0/45/-45]	[90/0]	[45/-45/0]	[0]	Fiber Orientations	[90]	[0/90]	[0/45/-45]	[45/-45/0]	[90/0]	[0]
1st NF	271	701	702	787	789	1019	1st NF	281	343	594	964	964	1015
2nd NF	1223	3181	3189	3532	3539	4599	2nd NF	1302	1801	2766	4340	4341	4657
3rd NF	2731	7095	7122	7894	7906	10270	3rd NF	3027	4061	6652	9871	9875	10972
NFs of Clamped-Free Configuration B (rad/s)							**NFs of Clamped-Free Configuration D (rad/s)**						
1st NF	257	684	685	724	725	963	1st NF	285	493	643	847	848	998
2nd NF	899	2360	2364	2576	2580	3379	2nd NF	961	1462	2168	3027	3029	3442
3rd NF	2106	5493	5502	6067	6077	7918	3rd NF	2172	3288	4687	7174	7176	7755
NFs of Clamped-Clamped Configuration B (rad/s)							**NFs of Clamped-Clamped Configuration D (rad/s)**						
1st NF	720	1880	1885	2070	2075	2706	1st NF	789	1249	1800	2464	2465	2838
2nd NF	1919	4993	5006	5533	5544	7213	2nd NF	1993	3138	4339	6508	6510	7094
3rd NF	3715	9656	9702	10728	10734	13967	3rd NF	3988	5420	8669	13068	13073	14360

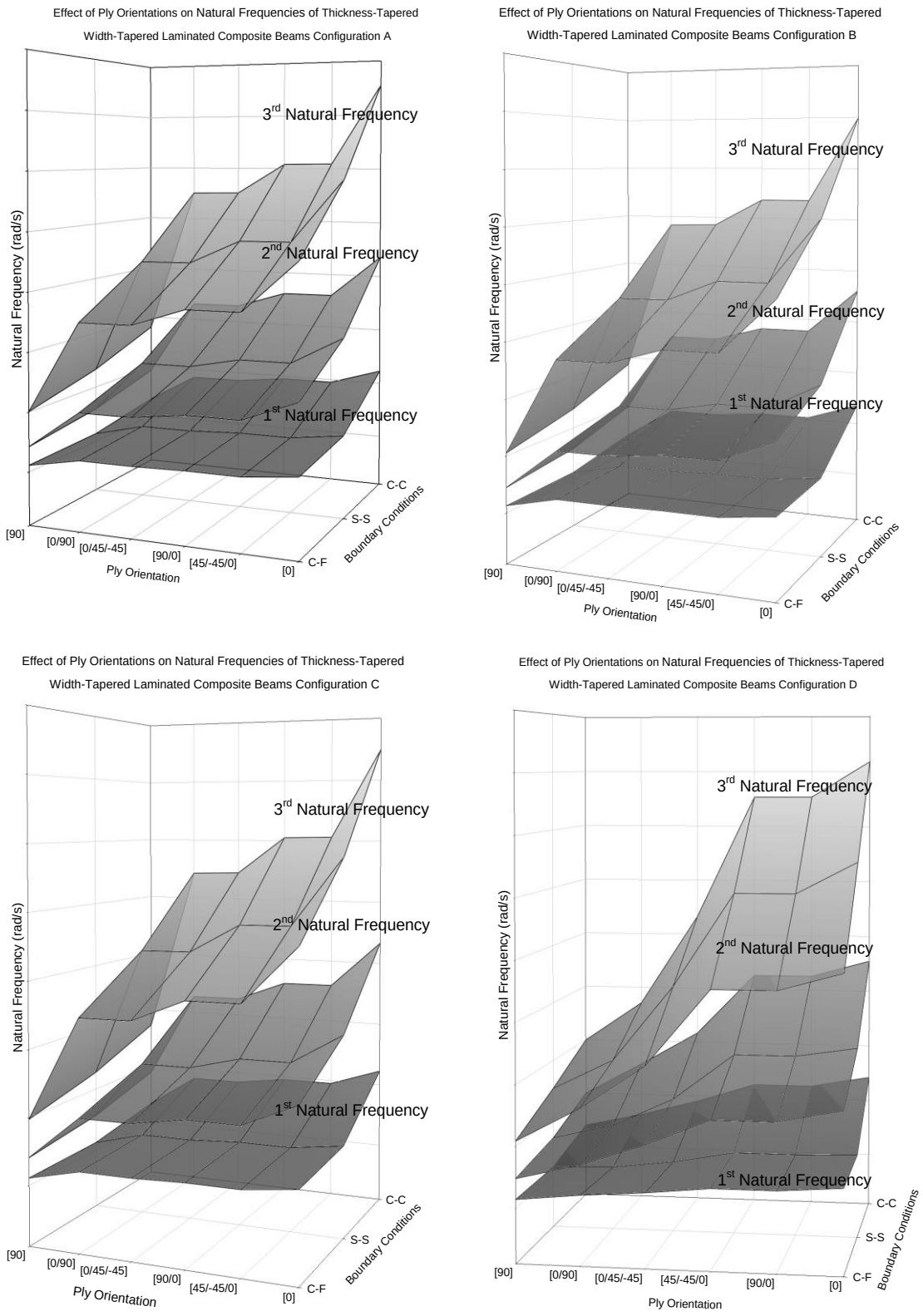

Figure 2.17: Natural frequencies of thickness-tapered width-tapered laminated composite beams with different ply orientations

It can be understood from the natural frequencies represented in Table 2.14 and Figure 2.17 that the closer the orientation of plies are to zero degree with respect to the x axis, the stiffer the beams will become, and the least stiff beams are the beams with plies only oriented at 90 degrees. This is a common observation for all the configurations.

2.5. Discussion and conclusion

In this chapter, the conventional finite element formulation has been developed for the free vibration analysis of uniform and variable-thickness variable-width laminated composite beams based on classical laminate theory. Stiffness and mass matrices have been derived for the beams. A set of examples were provided in order to validate the obtained results. The first three natural frequencies of the beams were obtained and validated with the existing results and they were presented in variety of graphs and tables.

The effects of boundary condition, thickness-tapering configuration, width ratio and orientation of plies on the free vibration of laminated composite beams were studied. As illustrated, among the boundary conditions considered in this study (clamped-free, simply supported and clamped-clamped), beams with clamped-clamped boundary conditions have the highest natural frequencies, whilst clamped-free beams have the lowest natural frequencies. It also can be observed that the closer the ply orientations are to zero degree with respect to the x axis, the stiffer the beam will become. Based on the results obtained, configuration D has the highest natural frequencies, configuration C and configuration B have the second highest and the third highest natural frequencies respectively. Configuration A has the lowest natural frequencies among all the considered configurations. It can also be concluded that the natural frequencies of the clamped-clamped and the simply supported thickness-tapered beams, lie between the natural

frequencies of the same mode of uniform-thickness beams with the number of plies equal to the number of plies at the thick section and at the thin section of the thickness-tapered beams which have the same length, width, material properties and orientation of plies. In the case of a clamped-free thickness-tapered beam, on the other hand, since the weight at the free end of the beam is reduced, its natural frequencies might be higher than the natural frequencies of a uniform beam with the number of plies equal to the number of plies at the thick section of the thickness-tapered beam which has the same length, width, material properties and orientation of plies.

Chapter-3

Advanced finite element formulation for free vibration analysis of composite beams

3.1. Introduction

In order to have the results with acceptable accuracy in vibration analysis and calculation of natural frequencies of the beams using conventional finite element method, the beam needs to be divided into many elements. Moreover, use of low degree polynomial displacement functions in conventional finite element method yields crude curvature distributions and discontinuous bending moments across element interfaces. Using advanced finite element method of analysis, on the other hand, acceptable results can be obtained using reasonable number of elements by increasing the number of degrees of freedom in each element. In this study, four degrees of freedom per node (deflection w, rotation $-\frac{dw}{dx}$, curvature $-\frac{d^2w}{dx^2}$ and the gradient of curvature $\frac{d^3w}{dx^3}$) and two nodes per element are considered for the advanced finite element analysis of variable-thickness variable-width laminated composite beams. The material chosen in this study is NCT-301 graphite-epoxy prepreg [46] which is available in the laboratory of Concordia Centre for Composites (CONCOM). The mechanical properties of the ply and the resin were given in the Tables 2.1 and 2.2. Symmetric laminate is considered in all problems.

3.2. Uniform and uniform-thickness width-tapered beams

3.2.1. Advanced finite element formulation

Having four degrees of freedom per node and eight degrees of freedom per element, a seventh-order polynomial for the expression of deflection is required to satisfy the boundary conditions [4]:

$$w^e(x,t) = c_1^e + c_2^e x + c_3^e x^2 + c_4^e x^3 + c_5^e x^4 + c_6^e x^5 + c_7^e x^6 + c_8^e x^7 \qquad (3.1a)$$

$$\varphi^e(x,t) = -\frac{\partial w(x)}{\partial x} = -(c_2^e + 2c_3^e x + 3c_4^e x^2 + 4c_5^e x^3 + 5c_6^e x^4 + 6c_7^e x^5 + 7c_8^e x^6) \qquad (3.1b)$$

$$K^e(x,t) = -\frac{\partial^2 w(x)}{\partial x^2} = -(2c_3^e + 6c_4^e x + 12c_5^e x^2 + 20c_6^e x^3 + 30c_7^e x^4 + 42c_8^e x^5) \qquad (3.1c)$$

$$GK^e(x,t) = \frac{\partial^3 w(x)}{\partial x^3} = 6c_4^e + 24c_5^e x + 60c_6^e x^2 + 120c_7^e x^3 + 210c_8^e x^4 \qquad (3.1d)$$

3.2.1.1. Derivation of shape functions

Applying the boundary conditions considering the first node at x=0 and the second node at x=l,

$$w^e(0,t) = w_1^e \qquad (3.2a)$$

$$\varphi^e(0,t) = w_2^e \qquad (3.2b)$$

$$K^e(0,t) = w_3^e \qquad (3.2c)$$

$$GK^e(0,t) = w_4^e \qquad (3.2d)$$

$$w^e(l,t) = w_5^e \qquad (3.2e)$$

$$\varphi^e(l,t) = w_6^e \qquad (3.2f)$$

$$K^e(l,t) = w_7^e \tag{3.2g}$$

$$GK^e(l,t) = w_8^e \tag{3.2h}$$

Having the equations (3.1) and (3.2) in the matrix form one has:

$$\begin{Bmatrix} w_1^e \\ w_2^e \\ w_3^e \\ w_4^e \\ w_5^e \\ w_6^e \\ w_7^e \\ w_8^e \end{Bmatrix} = \begin{bmatrix} 1 & 0 & 0 & 0 & 0 & 0 & 0 & 0 \\ 0 & -1 & 0 & 0 & 0 & 0 & 0 & 0 \\ 0 & 0 & 0 & 6 & 0 & 0 & 0 & 0 \\ 0 & 0 & -2 & 0 & 0 & 0 & 0 & 0 \\ 1 & l & l^2 & l^3 & l^4 & l^5 & l^6 & l^7 \\ 0 & -1 & -2l & -3l^2 & -4l^3 & -5l^4 & -6l^5 & -7l^6 \\ 0 & 0 & 0 & 6 & 24l & 60l^2 & 120l^3 & 210l^4 \\ 0 & 0 & -2 & -6l & -12l^2 & -20l^3 & -30l^4 & -42l^5 \end{bmatrix} \begin{Bmatrix} c_1^e \\ c_2^e \\ c_3^e \\ c_4^e \\ c_5^e \\ c_6^e \\ c_7^e \\ c_8^e \end{Bmatrix} \tag{3.3}$$

Having two nodes and four degrees of freedom per node the interpolation functions are derived as [4]:

$$N_1^e = 1 - \frac{35x^4}{l^4} + \frac{84x^5}{l^5} - \frac{70x^6}{l^6} + \frac{20x^7}{l^7} \tag{3.4a}$$

$$N_2^e = -x + \frac{20x^4}{l^3} - \frac{45x^5}{l^4} + \frac{36x^6}{l^5} - \frac{10x^7}{l^6} \tag{3.4b}$$

$$N_3^e = \frac{x^3}{6} - \frac{2x^4}{3l} + \frac{x^5}{l^2} - \frac{2x^6}{3l^3} + \frac{x^7}{6l^4} \tag{3.4c}$$

$$N_4^e = -\frac{x^2}{2} + \frac{5x^4}{l^2} - \frac{10x^5}{l^3} + \frac{15x^6}{2l^4} - \frac{2x^7}{l^5} \tag{3.4d}$$

$$N_5^e = \frac{35x^4}{l^4} - \frac{84x^5}{l^5} + \frac{70x^6}{l^6} - \frac{20x^7}{l^7} \tag{3.4e}$$

$$N_6^e = \frac{15x^4}{l^3} - \frac{39x^5}{l^4} + \frac{34x^6}{l^5} - \frac{10x^7}{l^6} \tag{3.4f}$$

$$N_7^e = -\frac{x^4}{6l} + \frac{x^5}{2l^2} - \frac{x^6}{2l^3} + \frac{x^7}{6l^4} \tag{3.4g}$$

$$N_8^e = -\frac{5x^4}{2l^2} + \frac{7x^5}{l^3} - \frac{13x^6}{2l^4} + \frac{2x^7}{l^5} \tag{3.4h}$$

3.2.1.2. Stiffness and mass matrices

Using MATLAB® program and solving equations (2.13) and (2.15) and having interpolation functions, the stiffness and mass matrices for an element of a uniform beam or a uniform-thickness width-tapered beam using advanced finite element method with eight degrees of freedom per element are determined as:

$$[k]=\begin{bmatrix}
\frac{280b_eD_{11}}{11l^3} & \frac{-140b_eD_{11}}{11l^2} & \frac{1}{22} & \frac{-40}{33l} & \frac{-280b_eD_{11}}{11l^3} & \frac{-140b_eD_{11}}{11l^2} & \frac{1}{22} & \frac{40}{33l} \\
\frac{-140b_eD_{11}}{11l^2} & \frac{600b_eD_{11}}{77l} & \frac{-8l}{231} & \frac{379}{462} & \frac{140b_eD_{11}}{11l^2} & \frac{380b_eD_{11}}{77l} & \frac{-5l}{462} & \frac{-181}{462} \\
\frac{1}{22} & \frac{-8l}{231} & \frac{2l^3}{3465b_eD_{11}} & \frac{-l^2}{99b_eD_{11}} & \frac{-1}{22} & \frac{-5l}{462} & \frac{-l^3}{4620b_eD_{11}} & \frac{-5l^2}{2772b_eD_{11}} \\
\frac{-40}{33l} & \frac{379}{462} & \frac{-l^2}{99b_eD_{11}} & \frac{50l}{231b_eD_{11}} & \frac{40}{33l} & \frac{181}{462} & \frac{5l^2}{2772b_eD_{11}} & \frac{-l}{462b_eD_{11}} \\
\frac{-280b_eD_{11}}{11l^3} & \frac{140b_eD_{11}}{11l^2} & \frac{-1}{22} & \frac{40}{33l} & \frac{280b_eD_{11}}{11l^3} & \frac{140b_eD_{11}}{11l^2} & \frac{-1}{22} & \frac{-40}{33l} \\
\frac{-140b_eD_{11}}{11l^2} & \frac{380b_eD_{11}}{77l} & \frac{-5l}{462} & \frac{181}{462} & \frac{140b_eD_{11}}{11l^2} & \frac{600b_eD_{11}}{77l} & \frac{-8l}{231} & \frac{-379}{462} \\
\frac{1}{22} & \frac{-5l}{462} & \frac{-l^3}{4620b_eD_{11}} & \frac{5l^2}{2772b_eD_{11}} & \frac{-1}{22} & \frac{-8l}{231} & \frac{2l^3}{3465b_eD_{11}} & \frac{l^2}{99b_eD_{11}} \\
\frac{40}{33l} & \frac{-181}{462} & \frac{-5l^2}{2772b_eD_{11}} & \frac{-l}{462b_eD_{11}} & \frac{-40}{33l} & \frac{-379}{462} & \frac{l^2}{99b_eD_{11}} & \frac{50l}{231b_eD_{11}}
\end{bmatrix} \tag{3.5a}$$

in which b_e denotes the width of the element at the midpoint of the element and l represents the length of the element.

$$[m]=\begin{bmatrix}
\frac{521lb_e\rho}{1287} & \frac{-151l^2b_e\rho}{2002} & \frac{383l^4\rho}{1081080D_{11}} & \frac{137l^3\rho}{18018D_{11}} & \frac{245lb_e\rho}{2574} & \frac{127l^2b_e\rho}{4004} & \frac{521l^4\rho}{2162160D_{11}} & \frac{-155l^3\rho}{36036D_{11}} \\
\frac{-151l^2b_e\rho}{2002} & \frac{5l^3b_e\rho}{273} & \frac{-l^5\rho}{10010D_{11}} & \frac{7l^4\rho}{3432D_{11}} & \frac{-127l^2b_e\rho}{4004} & \frac{-373l^3b_e\rho}{36036} & \frac{l^5\rho}{13104D_{11}} & \frac{199l^4\rho}{144144D_{11}} \\
\frac{383l^4\rho}{1081080D_{11}} & \frac{-l^5\rho}{10010D_{11}} & \frac{l^7\rho}{1621620{D_{11}}^2b_e} & \frac{-l^6\rho}{83160{D_{11}}^2b_e} & \frac{521l^4\rho}{2162160D_{11}} & \frac{l^5\rho}{13104D_{11}} & \frac{-l^7\rho}{1853280{D_{11}}^2b_e} & \frac{-43l^6\rho}{4324320{D_{11}}^2b_e} \\
\frac{137l^3\rho}{18018D_{11}} & \frac{7l^4\rho}{3432D_{11}} & \frac{-l^6\rho}{83160{D_{11}}^2b_e} & \frac{43l^5\rho}{180180{D_{11}}^2b_e} & \frac{-155l^3\rho}{36036D_{11}} & \frac{-199l^4\rho}{144144D_{11}} & \frac{43l^6\rho}{4324320{D_{11}}^2b_e} & \frac{131l^5\rho}{720720{D_{11}}^2b_e} \\
\frac{245lb_e\rho}{2574} & \frac{-127l^2b_e\rho}{4004} & \frac{521l^4\rho}{2162160D_{11}} & \frac{-155l^3\rho}{36036D_{11}} & \frac{521l\rho b_e}{1287} & \frac{151l^2\rho b_e}{2002} & \frac{-383l^4\rho}{1081080D_{11}} & \frac{-137l^3\rho}{18018D_{11}} \\
\frac{127l^2b_e\rho}{4004} & \frac{-373l^3b_e\rho}{36036} & \frac{l^5\rho}{13104D_{11}} & \frac{-199l^4\rho}{144144D_{11}} & \frac{151l^2\rho b_e}{2002} & \frac{5l^3\rho b_e}{273} & \frac{-l^5\rho}{10010D_{11}} & \frac{-7l^4\rho}{3432D_{11}} \\
\frac{521l^4\rho}{2162160D_{11}} & \frac{l^5\rho}{13104D_{11}} & \frac{-l^7\rho}{1853280{D_{11}}^2b_e} & \frac{43l^6\rho}{4324320{D_{11}}^2b_e} & \frac{-383l^4\rho}{1081080D_{11}} & \frac{-l^5\rho}{10010D_{11}} & \frac{l^7\rho}{1621620{D_{11}}^2b_e} & \frac{l^6\rho}{83160{D_{11}}^2b_e} \\
\frac{-155l^3\rho}{36036D_{11}} & \frac{199l^4\rho}{144144D_{11}} & \frac{-43l^6\rho}{4324320{D_{11}}^2b_e} & \frac{131l^5\rho}{720720{D_{11}}^2b_e} & \frac{-137l^3\rho}{18018D_{11}} & \frac{-7l^4\rho}{3432D_{11}} & \frac{l^6\rho}{83160{D_{11}}^2b_e} & \frac{43l^5\rho}{180180{D_{11}}^2b_e}
\end{bmatrix} \tag{3.5b}$$

Knowing the stiffness and mass matrices for each element based on the advanced finite element formulation, the global stiffness matrix $[K]$ and mass matrix $[M]$ can be

established for the beam. The free vibration of uniform and uniform-thickness width-tapered beams can be analyzed solving the similar eigenvalue problem to that considered in equation (2.22) using MATLAB® software. Obviously as the number of elements increases in the analysis the results become more accurate.

3.2.2. Validation

Similar beams to those considered in the second chapter are investigated to validate the formulation. Natural frequencies have been obtained for each beam using different number of elements and have been compared with the exact natural frequencies of the beam. This comparison shows the convergence of the results. Results obtained using conventional and advanced finite element methods have been used in this comparison. This comparison indicates better accuracy of the results obtained using advanced finite element method compared to those obtained using conventional finite element method, especially when the number of elements is less.

Uniform beams are considered with a) simply supported, b) clamped-free and c) clamped-clamped boundary conditions, as shown in Figure 2.4. Beams are made of 36 plies of NCT-301 graphite-epoxy prepreg and have 25 cm length and 2 cm width. The laminate configuration is $[0/90]_{9s}$.

The first three natural frequencies of the beams are considered. Comparison needs to be made with existing results obtained using conventional finite element method and the exact natural frequencies. Accuracy of the results obtained using advanced finite element method compared to the results obtained using conventional finite element method is shown in Tables 3.1, 3.2 and 3.3.

Table 3.1: Comparison of exact and finite element natural frequencies for a simply supported uniform beam

The Lowest Three Natural Frequencies (x10^3 rad/s) for Simply Supported Uniform Beam								
Mode	Exact NF			1 E	2 E	3 E	4 E	10 E
1	1.3667	CFEM	Natural Frequency	1.5169	1.3721	1.3678	1.367	1.3667
			Percentage Error	**10.99**	**0.39**	**0.08**	**0.03**	**0**
		AFEM	Natural Frequency	1.3667	1.3667	1.3667	1.3667	1.3667
			Percentage Error	**0**	**0**	**0**	**0**	**0**
2	5.4667	CFEM	Natural Frequency	6.9514	6.0676	5.5314	5.4883	5.4673
			Percentage Error	**27.16**	**10.99**	**1.18**	**0.39**	**0.01**
		AFEM	Natural Frequency	5.4669	5.4668	5.4667	5.4667	5.4667
			Percentage Error	**0**	**0**	**0**	**0**	**0**
3	12.3002	CFEM	Natural Frequency	-	15.2515	13.6522	12.5249	12.3068
			Percentage Error	-	**23.99**	**10.99**	**1.83**	**0.05**
		AFEM	Natural Frequency	12.6444	12.3004	12.3002	12.3002	12.3002
			Percentage Error	**2.8**	**0**	**0**	**0**	**0**

Table 3.2: Comparison of exact and finite element natural frequencies for a clamped-free uniform beam

The Lowest Three Natural Frequencies (x10^3 rad/s) for Clamped-Free Uniform Beam								
Mode	Exact NF			1 E	2 E	3 E	4 E	10 E
1	0.4869	CFEM	Natural Frequency	0.4892	0.4871	0.4869	0.4869	0.4869
			Percentage Error	**0.48**	**0.05**	**0.01**	**0**	**0**
		AFEM	Natural Frequency	0.4869	0.4869	0.4869	0.4869	0.4869
			Percentage Error	**0**	**0**	**0**	**0**	**0**
2	3.0511	CFEM	Natural Frequency	4.8199	3.0771	3.0612	3.0548	3.0513
			Percentage Error	**57.97**	**0.85**	**0.33**	**0.12**	**0.01**
		AFEM	Natural Frequency	3.0513	3.0512	3.0512	3.0512	3.0512
			Percentage Error	**0.01**	**0**	**0**	**0**	**0**
3	8.544	CFEM	Natural Frequency	-	10.4073	8.6499	8.6096	8.5457
			Percentage Error	-	**21.81**	**1.24**	**0.77**	**0.02**
		AFEM	Natural Frequency	8.5532	8.5435	8.5435	8.5435	8.5435
			Percentage Error	**0.11**	**-0.01**	**-0.01**	**-0.01**	**-0.01**

Table 3.3: Comparison of exact and finite element natural frequencies for a clamped-clamped uniform beam

The Lowest Three Natural Frequencies ($x10^3$ rad/s) for Clamped-Clamped Uniform Beam								
Mode	Exact NF			1 E	2 E	3 E	4 E	10 E
1	3.0981	CFEM	Natural Frequency	-	3.1483	3.1108	3.1022	3.0982
			Percentage Error	-	**1.62**	**0.41**	**0.13**	**0**
		AFEM	Natural Frequency	3.0982	3.0981	3.0981	3.0981	3.0981
			Percentage Error	**0**	**0**	**0**	**0**	**0**
2	8.5397	CFEM	Natural Frequency	-	11.3515	8.7106	8.6191	8.5423
			Percentage Error	-	**32.93**	**2**	**0.93**	**0.03**
		AFEM	Natural Frequency	8.5429	8.5401	8.5401	8.5401	8.5401
			Percentage Error	**0.04**	**0.01**	**0.01**	**0.01**	**0.01**
3	16.7432	CFEM	Natural Frequency	-	-	20.2594	17.0996	16.7585
			Percentage Error	-	-	**21**	**2.13**	**0.09**
		AFEM	Natural Frequency	17.6737	16.7447	16.742	16.742	16.742
			Percentage Error	**5.56**	**0.01**	**-0.01**	**-0.01**	**-0.01**

In Tables 3.1, 3.2 and 3.3, NF denotes Natural Frequency and E represents the number of elements used.

As it can be understood from the above tables, when applying the conventional finite element method and using only one element for the analysis, only the first and second natural frequencies of the simply supported and clamped-free beams and none of the natural frequencies of the clamped-clamped beam can be derived. Whereas when applying the advanced finite element method, all the first three natural frequencies of the simply supported and clamped-free beams as well as the first two natural frequencies of the clamped-clamped beam can be obtained. In these tables the blank units indicate the

results which cannot be derived using that specific number of elements for the corresponding boundary condition and the method used.

Uniform-thickness width-tapered laminated composite beams are considered with a) simply supported, b) clamped-free and c) clamped-clamped boundary conditions. Beams are made of 36 plies of NCT-301 graphite-epoxy prepreg. Length of the beams is equal to 25 cm, and they have 1.5 cm width at the left end, width ratio is 0.5 (the ratio of the width of the beam at the right section to that of the beam at the left section) and the laminate configuration is $[0/90]_{9s}$.

The first three natural frequencies of these beams are to be determined. Different numbers of elements are employed to derive the results using I) advanced and II) conventional finite element methods. Convergence of the natural frequencies obtained using advanced finite element method and conventional finite element method when the considered number of elements for the analysis increases is represented in Figure 3.1.

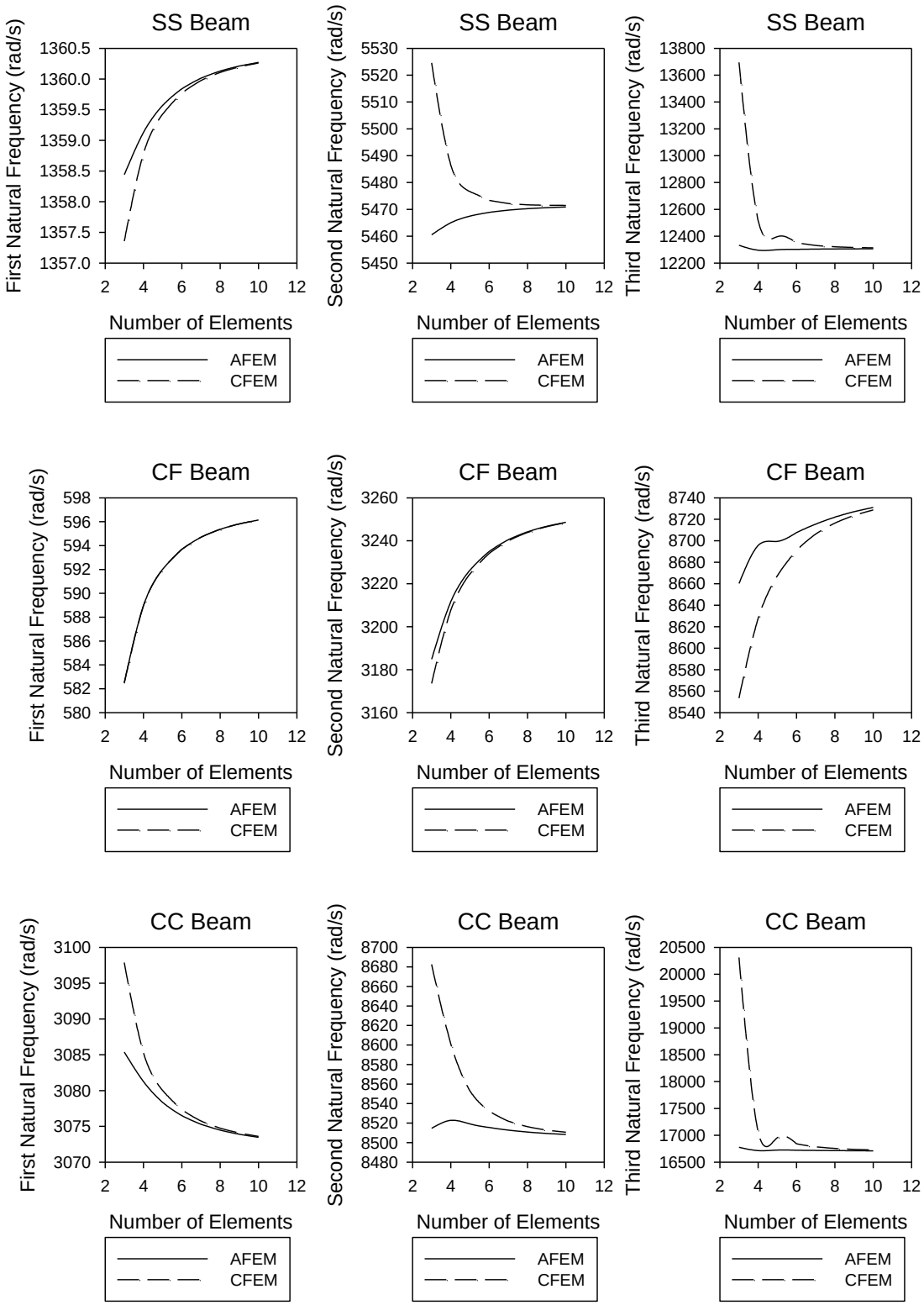

Figure 3.1: First three natural frequencies of uniform-thickness width-tapered laminated composite beams obtained using Conventional Finite Element Method (CFEM) and Advanced Finite Element Method (AFEM)

In Figure 3.1 SS, CF and CC respectively denote simply supported, clamped-free and clamped-clamped boundary conditions. AFEM and CFEM denote advanced and conventional finite element methods respectively.

3.3. Width-tapered thickness-tapered beams

3.3.1. Advanced finite element formulation

Similar thickness-tapered width-tapered beams to that studied in the second chapter using conventional finite element method are considered in this chapter to be analyzed using advanced finite element method. These beams are shown in Figure 2.11.

Two nodes per element and four degrees of freedom per node (deflection w, rotation $-\frac{dw}{dx}$, curvature $-\frac{d^2w}{dx^2}$ and the gradient of curvature $\frac{d^3w}{dx^3}$) are assumed in the advanced finite element formulation for the free vibration analysis of thickness-tapered width-tapered laminated composite beams.

3.3.1.1. Derivation of coefficients of stiffness and mass matrices

Having the equations for the coefficients of the stiffness and mass matrices as in equations $(2.27a)$ and $(2.27b)$ for an element, and inserting the interpolation functions as in equations $(3.4a-h)$, one can find the coefficients of the stiffness and mass matrices for the advanced finite element method.

Equations $(3.6a)$ and $(3.6b)$ provide the first and the last coefficients of the stiffness matrix, and all the other coefficients are listed in the Appendix A.

$$k_{11}=\sum_{k=1}^{n}70Hb_e(\bar{Q}_{11})_k t'_k\frac{48H^2m^2l^2+156H^2mcl+156H^2c^2+13{t'_k}^2}{429l^3} \quad (3.6a)$$

$$k_{88} = \sum_{k=1}^{n} Hl(\bar{Q}_{11})_k t_k' \frac{2134H^2m^2l^2 + 5460H^2mcl + 3900H^2c^2 + 325{t_k'}^2}{18018b_e{(D_{11})_2}^2} \qquad (3.6b)$$

in which k_{ij} represents the coefficient of the element stiffness matrix in advanced finite element formulation for the thickness-tapered width-tapered laminated composite beam, n represents the number of plies in the element, H denotes element thickness, l is the element length, $\bar{Q}_{11}$ is the first coefficient of the reduced stiffness matrix of the ply, t_k' denotes the specific ply thickness in the z direction as shown in Figure 2.8., m is the slope of the ply in the thickness-tapered laminate, c is the intercept of the centre line of each ply with x axis, b_e is the width of the element and $(D_{11})_1$ is the first coefficient of bending stiffness matrix at the left end of the element and $(D_{11})_2$ is the first coefficient of bending stiffness matrix at the right end of the element.

Equations $(3.7a)$ and $(3.7b)$ provide the first and the last coefficients of the mass matrix, and all the other coefficients are listed in the Appendix A.

$$m_{11} = \frac{lb_e\rho(1042c + 235ml)}{2574} \qquad (3.7a)$$

$$m_{88} = \frac{l^5\rho(86c + 51ml)}{360360b_e{(D_{11})_2}^2} \qquad (3.7b)$$

in which m_{ij} represents the coefficient of element mass matrix in advanced finite element formulation for the thickness-tapered width-tapered laminated composite beam and ρ denotes density of the ply material.

Having equations (3.6) and (3.7), one can find the element stiffness [k] and mass [m] matrices of a thickness-tapered width-tapered laminated composite beam using advanced finite element method. Knowing the stiffness and mass matrices for each element based on the advanced finite element formulation, the global stiffness matrix $[K]$

and mass matrix $[M]$ can be established for the beam. The free vibration of thickness-tapered width-tapered beams can be analyzed solving the similar eigenvalue problem to that considered in equation (2.22) using MATLAB® software.

3.3.2. Validation

Validation of results is performed using the existing results obtained using conventional finite element and Rayleigh-Ritz methods. Similar beams to those considered in the previous chapter are chosen to be analyzed.

Thickness-tapered width-tapered beams are considered with a) simply supported, b) clamped-free and c) clamped-clamped boundary conditions. Five width ratio values are considered for these beams (0.2, 0.4, 0.6, 0.8 and 1). The beams are made of configurations A, B, C and D as shown in Figure 2.11. These beams are made of 36 plies at the thick section and 12 plies at the thin section and are made of NCT-301 graphite-epoxy prepreg. Beams are 15 cm long and their width is equal to 1.5 cm at the left end**.** Laminate configuration is $[0/90]_{9s}$ at the thick section.

First three natural frequencies of these beams are considered. Natural frequencies obtained using advanced finite element method are validated using the existing results obtained using conventional finite element method. The results are presented in Table 3.4.

Table 3.4: Comparison of the natural frequencies obtained using advanced and conventional finite element methods for laminated composite beams with constant thickness-tapering angle and varying width ratio

	Configuration A-SS					**Configuration B-SS**				
width ratio ($\frac{b_R}{b_L}$)	0.2	0.4	0.6	0.8	1	0.2	0.4	0.6	0.8	1
ω_1 (AFEM)	2246	2332	2380	2411	2432	2133	2222	2273	2306	2329
ω_1 (CFEM)	2253	2337	2386	2413	2436	2145	2232	2298	2318	2340
% differ	**0.35**	**0.22**	**0.23**	**0.1**	**0.18**	**0.54**	**0.42**	**1.08**	**0.53**	**0.48**
ω_2 (AFEM)	10027	9976	9938	9912	9895	9826	9769	9727	9698	9678
ω_2 (CFEM)	10068	10005	9961	9932	9913	9876	9808	9765	9728	9705
% differ	**0.41**	**0.29**	**0.23**	**0.2**	**0.19**	**0.51**	**0.4**	**0.39**	**0.3**	**0.27**
ω_3 (AFEM)	22342	22252	22194	22155	22129	21894	21799	21736	21695	21666
ω_3 (CFEM)	22438	22319	22248	22202	22172	22010	21887	21814	21762	21727
% differ	**0.43**	**0.3**	**0.24**	**0.21**	**0.2**	**0.52**	**0.4**	**0.36**	**0.31**	**0.28**
	Configuration A-CC					**Configuration B-CC**				
width ratio ($\frac{b_R}{b_L}$)	0.2	0.4	0.6	0.8	1	0.2	0.4	0.6	0.8	1
ω_1 (AFEM)	5604	5633	5614	5581	5545	5534	5550	5523	5485	5445
ω_1 (CFEM)	5563	5604	5587	5555	5519	5492	5520	5497	5467	5417
% differ	**0.73**	**0.52**	**0.49**	**0.48**	**0.47**	**0.77**	**0.53**	**0.46**	**0.33**	**0.51**
ω_2 (AFEM)	15403	15435	15405	15359	15309	15113	15131	15092	15040	14987
ω_2 (CFEM)	15301	15359	15332	15288	15238	15025	15058	15032	14979	14922
% differ	**0.67**	**0.5**	**0.47**	**0.46**	**0.47**	**0.58**	**0.48**	**0.4**	**0.41**	**0.44**
ω_3 (AFEM)	30148	30171	30132	30081	30028	29512	29524	29478	29421	29364
ω_3 (CFEM)	29963	30029	29999	29949	29894	29354	29401	29365	29306	29250
% differ	**0.62**	**0.47**	**0.44**	**0.44**	**0.45**	**0.54**	**0.42**	**0.38**	**0.39**	**0.39**

	Configuration A-CF					**Configuration B-CF**				
width ratio ($\frac{b_R}{b_L}$)	0.2	0.4	0.6	0.8	1	0.2	0.4	0.6	0.8	1
ω_1 (AFEM)	2135	1837	1657	1534	1443	2233	1928	1743	1617	1523
ω_1 (CFEM)	2149	1842	1661	1547	1455	2284	1865	1759	1649	1459
% differ	**0.64**	**0.32**	**0.21**	**0.84**	**0.79**	**2.23**	**3.33**	**0.88**	**1.91**	**4.41**
ω_2 (AFEM)	7515	7049	6795	6621	6490	7508	7040	6783	6609	6477
ω_2 (CFEM)	7601	7105	6836	6657	6521	7603	7100	6837	6646	6508
% differ	**1.13**	**0.79**	**0.61**	**0.54**	**0.47**	**1.25**	**0.85**	**0.78**	**0.57**	**0.48**
ω_3 (AFEM)	17383	16882	16620	16445	16312	17150	16645	16380	16201	16067
ω_3 (CFEM)	17610	17028	16733	16539	16395	17379	16801	16500	16302	16154
% differ	**1.29**	**0.86**	**0.67**	**0.57**	**0.5**	**1.32**	**0.93**	**0.73**	**0.62**	**0.54**
	Configuration C-SS					**Configuration D-SS**				
width ratio ($\frac{b_R}{b_L}$)	0.2	0.4	0.6	0.8	1	0.2	0.4	0.6	0.8	1
ω_1 (AFEM)	2172	2264	2316	2351	2374	2535	2625	2675	2707	2729
ω_1 (CFEM)	2184	2272	2322	2355	2378	2550	2649	2680	2721	2739
% differ	**0.55**	**0.34**	**0.24**	**0.18**	**0.15**	**0.57**	**0.9**	**0.18**	**0.53**	**0.36**
ω_2 (AFEM)	10028	9968	9924	9894	9873	11104	11072	11041	11019	11002
ω_2 (CFEM)	10074	9998	9949	9915	9893	11158	11112	11071	11050	11032
% differ	**0.45**	**0.3**	**0.25**	**0.21**	**0.2**	**0.49**	**0.36**	**0.27**	**0.28**	**0.27**
ω_3 (AFEM)	22334	22233	22168	22125	22094	24502	24409	24345	24303	24273
ω_3 (CFEM)	22436	22303	22224	22172	22137	24608	24483	24404	24360	24326
% differ	**0.46**	**0.31**	**0.25**	**0.22**	**0.19**	**0.43**	**0.3**	**0.24**	**0.24**	**0.22**

	Configuration C-CC					**Configuration D-CC**				
width ratio ($\frac{b_R}{b_L}$)	0.2	0.4	0.6	0.8	1	0.2	0.4	0.6	0.8	1
ω_1 (AFEM)	5665	5679	5650	5610	5568	5908	5964	5962	5942	5914
ω_1 (CFEM)	5630	5653	5624	5586	5544	5870	5927	5934	5909	5883
% differ	**0.62**	**0.47**	**0.46**	**0.43**	**0.43**	**0.65**	**0.62**	**0.48**	**0.56**	**0.52**
ω_2 (AFEM)	15458	15473	15430	15375	15319	16778	16854	16848	16818	16779
ω_2 (CFEM)	15368	15404	15366	15312	15255	16681	16783	16777	16745	16709
% differ	**0.59**	**0.44**	**0.42**	**0.41**	**0.42**	**0.58**	**0.43**	**0.42**	**0.43**	**0.42**
ω_3 (AFEM)	30167	30173	30123	30063	30003	32765	32833	32816	32780	32737
ω_3 (CFEM)	30004	30049	30005	29946	29883	32553	32667	32657	32621	32576
% differ	**0.54**	**0.41**	**0.39**	**0.39**	**0.4**	**0.65**	**0.51**	**0.49**	**0.49**	**0.49**
	Configuration C-CF					**Configuration D-CF**				
width ratio ($\frac{b_R}{b_L}$)	0.2	0.4	0.6	0.8	1	0.2	0.4	0.6	0.8	1
ω_1 (AFEM)	2301	1986	1797	1667	1570	2211	1910	1724	1595	1499
ω_1 (CFEM)	2322	1996	1806	1672	1577	2253	1898	1719	1555	1537
% differ	**0.92**	**0.49**	**0.5**	**0.3**	**0.43**	**1.85**	**0.63**	**0.31**	**2.6**	**2.51**
ω_2 (AFEM)	7695	7216	6954	6775	6640	8158	7639	7358	7169	7027
ω_2 (CFEM)	7787	7277	7001	6814	6673	8245	7713	7397	7207	7055
% differ	**1.18**	**0.83**	**0.67**	**0.57**	**0.49**	**1.06**	**0.95**	**0.52**	**0.53**	**0.39**
ω_3 (AFEM)	17540	17024	16753	16570	16433	19161	18607	18325	18138	17999
ω_3 (CFEM)	17778	17179	16874	16672	16521	19408	18778	18450	18244	18092
% differ	**1.34**	**0.9**	**0.72**	**0.61**	**0.53**	**1.27**	**0.91**	**0.68**	**0.58**	**0.51**

In Table 3.4, the comparison of the natural frequencies obtained using advanced and conventional finite element methods is done with respect to the results obtained using conventional finite element method.

Thickness-tapered width-tapered beams are considered with a) simply supported, b) clamped-free and c) clamped-clamped boundary conditions. Width ratio of these beams is constant and is equal to 0.5. The beams are made of configurations A, B, C and D. These beams are made of 36 plies at the thick section and 12 plies at the thin section and are made of NCT-301 graphite-epoxy prepreg. Different thickness-tapering angles are considered for these beams. Thickness-tapering angle varies with the change in the length of the beams from 0.344 degrees to 0.86 degrees. The laminate configuration at the thick section is $[0/90]_{9s}$. Width is equal to 1.5 cm at the left end and 0.75 cm at the right end**.**

First three natural frequencies of these beams are considered. Natural frequencies obtained using advanced finite element method are validated using the existing results obtained using conventional finite element method. The results are presented in Table 3.5.

Table 3.5: Comparison of the natural frequencies obtained using advanced and conventional finite element methods for laminated composite beams with varying thickness-tapering angle and constant width ratio

	Configuration A-SS				Configuration B-SS			
Thickness-Tapering Angle (deg)	0.344	0.43	0.573	0.86	0.344	0.43	0.573	0.86
L (m)	0.25	0.2	0.15	0.1	0.25	0.2	0.15	0.1
$\frac{L}{H_L}$	56	44	33	22	56	44	33	22
$\frac{L}{b_L}$	17	13	10	7	17	13	10	7
ω_1 (AFEM)	758	1184	2104	4734	810	1266	2251	5063
ω_1 (CFEM)	760	1188	2110	4745	816	1270	2260	5055
% differ	**0.36**	**0.34**	**0.27**	**0.22**	**0.71**	**0.34**	**0.42**	**0.16**
ω_2 (AFEM)	3211	5017	8920	20068	3509	5482	9746	21927
ω_2 (CFEM)	3221	5033	8949	20134	3520	5500	9771	21997
% differ	**0.32**	**0.3**	**0.32**	**0.33**	**0.33**	**0.32**	**0.25**	**0.32**
ω_3 (AFEM)	7156	11180	19876	44718	7835	12243	21764	48965
ω_3 (CFEM)	7179	11217	19940	44867	7863	12284	21839	49136
% differ	**0.32**	**0.32**	**0.32**	**0.33**	**0.35**	**0.33**	**0.34**	**0.35**
	Configuration A-CC				Configuration B-CC			
ω_1 (AFEM)	1820	2843	5054	11371	1994	3116	5539	12461
ω_1 (CFEM)	1808	2826	5024	11302	1984	3105	5511	12403
% differ	**0.62**	**0.61**	**0.6**	**0.61**	**0.49**	**0.34**	**0.5**	**0.47**
ω_2 (AFEM)	4977	7776	13824	31102	5441	8502	15114	34005
ω_2 (CFEM)	4947	7730	13742	30918	5418	8467	15053	33854
% differ	**0.6**	**0.6**	**0.6**	**0.6**	**0.44**	**0.42**	**0.41**	**0.44**
ω_3 (AFEM)	9720	15187	26998	60742	10622	16596	29503	66377
ω_3 (CFEM)	9665	15101	26847	60405	10581	16531	29389	66113
% differ	**0.57**	**0.57**	**0.56**	**0.56**	**0.39**	**0.39**	**0.39**	**0.4**

	Configuration A-CF				Configuration B-CF			
ω_1 (AFEM)	581	908	1614	3632	657	1027	1826	4108
ω_1 (CFEM)	583	913	1617	3682	677	1053	1856	4300
% differ	**0.31**	**0.59**	**0.19**	**1.38**	**2.96**	**2.46**	**1.65**	**4.47**
ω_2 (AFEM)	2258	3527	6271	14109	2483	3880	6897	15517
ω_2 (CFEM)	2274	3554	6317	14218	2506	3906	6952	15672
% differ	**0.74**	**0.73**	**0.73**	**0.77**	**0.92**	**0.68**	**0.78**	**0.99**
ω_3 (AFEM)	5419	8467	15052	33866	5939	9280	16497	37114
ω_3 (CFEM)	5463	8536	15176	34147	5987	9352	16633	37415
% differ	**0.81**	**0.81**	**0.82**	**0.82**	**0.81**	**0.77**	**0.82**	**0.81**
	Configuration C-SS				Configuration D-SS			
ω_1 (AFEM)	826	1290	2293	5160	955	1493	2653	5969
ω_1 (CFEM)	827	1296	2299	5175	959	1502	2654	6035
% differ	**0.21**	**0.47**	**0.26**	**0.3**	**0.41**	**0.65**	**0.03**	**1.08**
ω_2 (AFEM)	3580	5594	9944	22372	3980	6219	11056	24873
ω_2 (CFEM)	3590	5609	9971	22433	3992	6240	11093	24953
% differ	**0.27**	**0.28**	**0.27**	**0.27**	**0.29**	**0.34**	**0.33**	**0.32**
ω_3 (AFEM)	7991	12486	22197	49940	8775	13711	24374	54836
ω_3 (CFEM)	8013	12521	22259	50081	8800	13750	24446	54989
% differ	**0.27**	**0.28**	**0.28**	**0.28**	**0.28**	**0.28**	**0.29**	**0.28**
	Configuration C-CC				Configuration D-CC			
ω_1 (AFEM)	2040	3188	5667	12750	2148	3357	5967	13424
ω_1 (CFEM)	2031	3174	5642	12693	2137	3343	5940	13358
% differ	**0.44**	**0.43**	**0.45**	**0.45**	**0.51**	**0.4**	**0.46**	**0.5**
ω_2 (AFEM)	5564	8693	15454	34769	6069	9482	16856	37922
ω_2 (CFEM)	5540	8657	15389	34624	6044	9443	16790	37773
% differ	**0.42**	**0.42**	**0.42**	**0.42**	**0.4**	**0.41**	**0.39**	**0.39**
ω_3 (AFEM)	10855	16960	30151	67834	11819	18467	32829	73857
ω_3 (CFEM)	10812	16893	30031	67566	11761	18376	32671	73503
% differ	**0.4**	**0.4**	**0.4**	**0.4**	**0.5**	**0.5**	**0.48**	**0.48**

	Configuration C-CF				Configuration D-CF			
ω_1 (AFEM)	677	1058	1882	4233	651	1017	1808	4066
ω_1 (CFEM)	681	1070	1891	4269	674	998	1780	3931
% differ	**0.5**	**1.07**	**0.48**	**0.84**	**3.41**	**1.88**	**1.55**	**3.46**
ω_2 (AFEM)	2545	3977	7070	15906	2694	4209	7482	16833
ω_2 (CFEM)	2564	4007	7123	16026	2713	4235	7527	16911
% differ	**0.74**	**0.75**	**0.75**	**0.75**	**0.71**	**0.61**	**0.6**	**0.46**
ω_3 (AFEM)	6074	9491	16873	37961	6642	10378	18448	41505
ω_3 (CFEM)	6123	9567	17008	38265	6692	10455	18591	41826
% differ	**0.79**	**0.79**	**0.8**	**0.8**	**0.75**	**0.74**	**0.77**	**0.77**

In Table 3.5, H_L denotes the height of the beam at the left section. In this table, the comparison of the natural frequencies obtained using advanced and conventional finite element methods is done with respect to the results obtained using conventional finite element method.

3.4. Discussion and conclusion

In this chapter, the advanced finite element formulation has been developed for the free vibration analysis of uniform and variable-thickness variable-width laminated composite beams based on classical laminate theory. In the case of uniform laminated composite beams, natural frequencies obtained using advanced finite element method have been compared with the exact natural frequencies and with those obtained using conventional finite element method.

It has been indicated that use of advanced finite element method in free vibration analysis of the beams results in better accuracy of the obtained natural frequencies compared to those obtained using conventional finite element method, especially when

using low number of elements in the analysis. The advantages of using the advanced finite element method for the analysis of the laminated composite beams can be further explained in the stress analysis of the beams.

The advanced finite element method of analysis has also been applied for the free vibration analysis of variable-thickness variable-width laminated composite beams. Four configurations (configurations A, B, C and D) and three boundary conditions (clamped-clamped, simply supported and clamped-free) have been considered for these beams. The obtained natural frequencies have been validated using the existing results obtained using conventional finite element method.

Based on the results obtained, configuration D has the highest natural frequencies, and then configurations C and B respectively have the second highest and the third highest natural frequencies. The configuration A has the lowest natural frequencies among all configurations.

Chapter-4

Forced vibration analysis of laminated composite beams using conventional and advanced finite element formulations

4.1. Introduction

In this chapter, forced vibration analysis of laminated composite beams is carried out using modal analysis. Deflection of an arbitrary point through the length of a beam is to be derived when a sinusoidal force is applied at a point through the length of the beam. Advanced and conventional finite element formulations are used in order to derive systems matrices.

Obtained results have been compared with existing results obtained using Rayleigh-Ritz method [45]. The material chosen in this study is NCT-301 graphite-epoxy prepreg [46] which is available in the laboratory of Concordia Centre for Composites (CONCOM). The mechanical properties of the ply and the resin are given in the Tables 2.1 and 2.2. Symmetric laminated beams are considered in all problems.

4.2. Undamped forced vibration analysis

The equation of motion of an undamped linear system is given as:

$$[M]\{\ddot{w}\} + [K]\{w\} = \{F\} \tag{4.1}$$

in which $[M]$ denotes the mass matrix, $[K]$ is the stiffness matrix, $\{w\}$ represents the displacement vector and $\{F\}$ is the force vector of the beam. Stiffness and mass matrices for the beam can be obtained using advanced and conventional finite element

formulations as it has been explained in previous chapters. The forced vibration of the composite laminated beams is determined using mode superposition method.

Having the stiffness and the mass matrices for a laminated composite beam and solving a similar eigenvalue problem as in equation (2.26) using MATLAB® software, one can find the eigenvalues and the orthonormal eigenvector matrix $[\tilde{S}]$ of the beam. Eigenvalues are equal to the square of natural frequencies and the orthonormal eigenvector matrix $[\tilde{S}]$ can be used to decouple the equations of motion.

One can decouple the equations of motion by transforming the coordinates using eigenvector matrix as:

$$\{w\} = [\tilde{S}]\{y\} \tag{4.2}$$

Substituting equation (4.2) into equation (4.1) and pre-multiplying by $[\tilde{S}]^T$ leads to:

$$[\tilde{S}]^T[M][\tilde{S}]\{\ddot{y}\} + [\tilde{S}]^T[K][\tilde{S}]\{y\} = [\tilde{S}]^T\{F\} \tag{4.3}$$

in the equation (4.3), $[M]$ and $[K]$ respectively denote mass and stiffness matrices of the beam which can be derived based on formulations explained in the previous chapters using advanced or conventional finite element methods. $\{y\}$ is the vector of displacements in the transformed coordinates. $\{F\}$ is the force vector applied to the beam which represents the nodal forces applied to the beam. In the equation (4.3), $[\tilde{S}]^T[M][\tilde{S}]$ is an identity matrix and $[\tilde{S}]^T[K][\tilde{S}]$ is a diagonal matrix in which its diagonal coefficients represent the square of natural frequencies of the beam. These two facts can be used to check the system matrices prior to the forced vibration analysis of the beam. Equation (4.3) contains n (number of beam's degrees of freedom) decoupled equations,

which can be solved for $\{y\}$, using MATLAB® software. In order to find the displacements in the original coordinate, the orthonormal eigenvector matrix should be used again as was used in equation (4.2).

4.2.1. Flowchart

The chart in the Figure 4.1 explains all the steps that need to be carried out in order to derive the forced vibration response of an undamped beam at any point through its length.

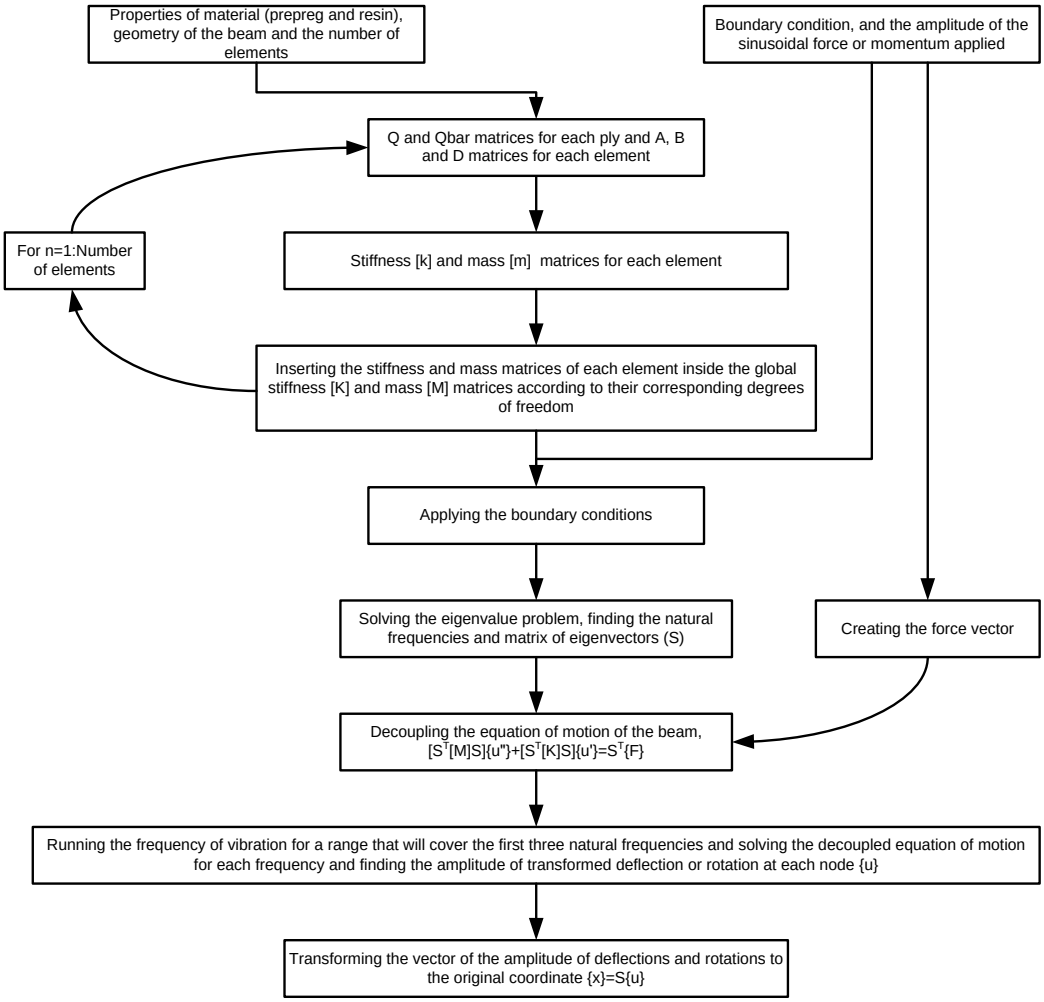

Figure 4.1: Modal analysis procedure for composite beams using finite element method

In this chapter forced vibration analysis of undamped and damped, variable-width variable-thickness laminated composite beams is carried out using advanced and conventional finite element methods. Magnitude of the deflection of an arbitrary point through the length of the beam versus frequency of vibration is desired when applying sinusoidal force to the beam. The obtained results are validated and compared with the existing results obtained using Rayleigh-Ritz method. The results will be shown in graphs which represent amplitude of deflection in meters versus frequency of vibration in radians per second. The frequency range of the forced vibration that each beam undergoes is chosen such that at least the first three natural frequencies of that beam will lie in that frequency range.

4.2.2. Validation

The results obtained using advanced and conventional finite element methods are compared with the existing results obtained using Rayleigh-Ritz method [45] for three cases (uniform beam, uniform-thickness width-tapered beam and width-tapered thickness-tapered beam) of the undamped laminated composite beams.

In the first case, uniform beams are considered with a) simply supported, b) clamped-free and c) clamped-clamped boundary conditions, as shown in Figure 2.4. Beams are made of 36 plies of NCT-301 graphite-epoxy prepreg. These beams are 25 cm long and have 2 cm width. The laminate configuration considered is $[0/90]_{9s}$. The natural frequencies and the deflection of the response point versus frequency of vibration is to be determined using conventional and advanced finite element methods. These results are compared with the existing results obtained using Rayleigh-Ritz method [45].

Sinusoidal force with the magnitude of 2 N is applied to the beams. The point where the force is applied to is chosen based on the beam's boundary conditions, as explained in Figure 4.2. In order to avoid applying the force to the nodal points of the second mode shape of the uniform beams, the force is not applied exactly at the middle of the clamped-clamped and simply supported beams as is shown in Figure 4.2. Considering ten elements and 11 nodes for each beam, the location of the point where the force is applied to and the corresponding point of response are shown in Figure 4.2 for all the boundary conditions considered in this study.

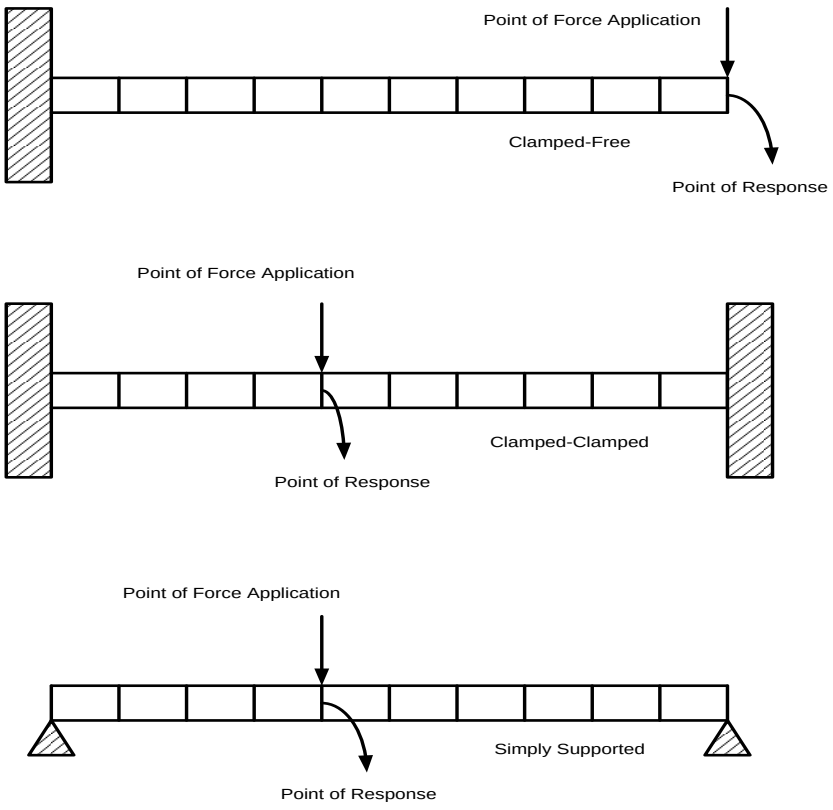

Figure 4.2: Points of force application and the corresponding response points of uniform laminated composite beams with clamped-free, clamped-clamped and simply supported boundary conditions

Exact natural frequencies of these uniform beams are obtained using equation (2.27) and are given as:

a) Simply supported beam:

Natural frequencies: 1^{st} NF= 1271 (rad/s), 2^{nd} NF= 5084 (rad/s), 3^{rd} NF= 11445 (rad/s)

b) Clamped-free beam:

Natural frequencies: 1^{st} NF= 452 (rad/s), 2^{nd} NF= 2837 (rad/s), 3^{rd} NF= 7947 (rad/s)

c) Clamped-clamped beam:

Natural frequencies: 1^{st} NF= 2881 (rad/s), 2^{nd} NF= 7944 (rad/s), 3^{rd} NF= 15585 (rad/s)

in which NF denotes natural frequency.

The forced vibration response of the beams are shown in Figure 4.3 for simply supported, clamped-free and clamped-clamped boundary conditions of uniform laminated composite beams using advanced and conventional finite element formulations, and Rayleigh-Ritz method.

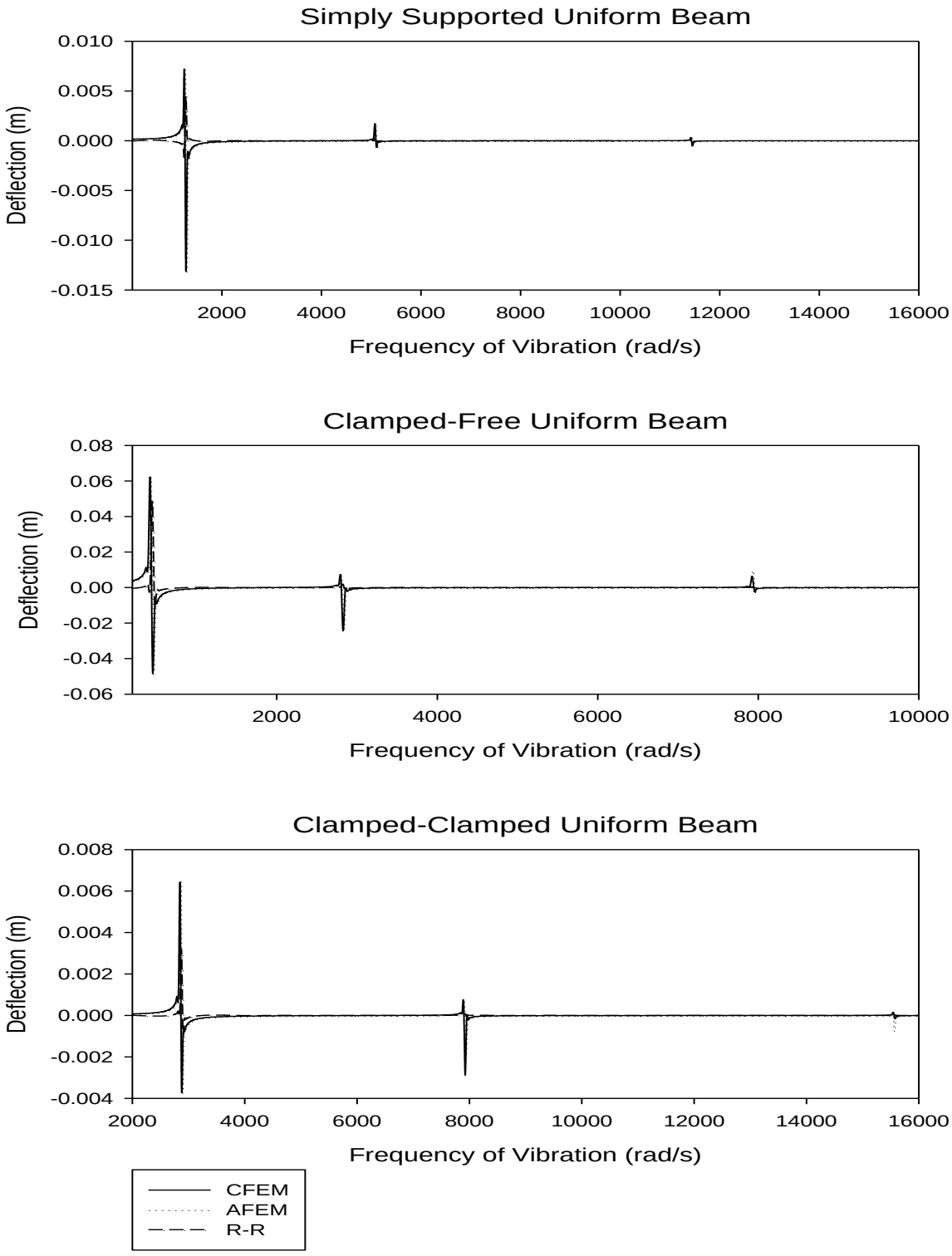

Figure 4.3: Forced vibration response of simply supported, clamped-free and clamped-clamped uniform laminated composite beams

In Figure 4.3, CFEM, AFEM and R-R denote Conventional Finite Element Method, Advanced Finite Element Method and Rayleigh-Ritz method respectively.

As illustrated in Figure 4.3, the forced vibration response of the simply supported, clamped-free and clamped-clamped uniform laminated composite beams were determined using conventional and advanced finite element formulations and have been compared with the existing results obtained using Rayleigh-Ritz method, and excellent agreement has been observed. It can be seen that the maximum deflections of each beam occur when the frequency of vibration is close to that beam's natural frequencies (resonances). As shown in this figure, the clamped-clamped beam has the lowest deflection while the clamped-free beam has the highest deflection.

In the second case uniform-thickness width-tapered laminated composite beams are considered with a) simply supported, b) clamped-free and c) clamped-clamped boundary conditions. Beams are made of 36 plies of NCT-301 graphite-epoxy prepreg. These beams are 25 cm long and have 1.66 cm width at the left end. The laminate configuration is $[0/90]_{9s}$. The width ratios (the ratio of the width of the beam at the left end to that of the beam at the right end) considered are 0.2, 0.4, 0.6 and 0.8.

The deflection of the response point versus frequency of vibration is to be found using conventional and advanced finite element methods. These results are compared with the existing results obtained using Rayleigh-Ritz method [45]. Sinusoidal force with the magnitude of 2 N is applied to the beams.

The results are shown in Figures 4.4, 4.5 and 4.6 for different boundary conditions. Each figure includes the forced vibration response for all the four width ratios for each boundary condition of the beams.

In the simply supported and clamped-clamped beams, force is applied at the middle of the beams while in the clamped-free beams the force is applied at the free end of the beams. The locations of the points of response are same as the locations of the points of force application.

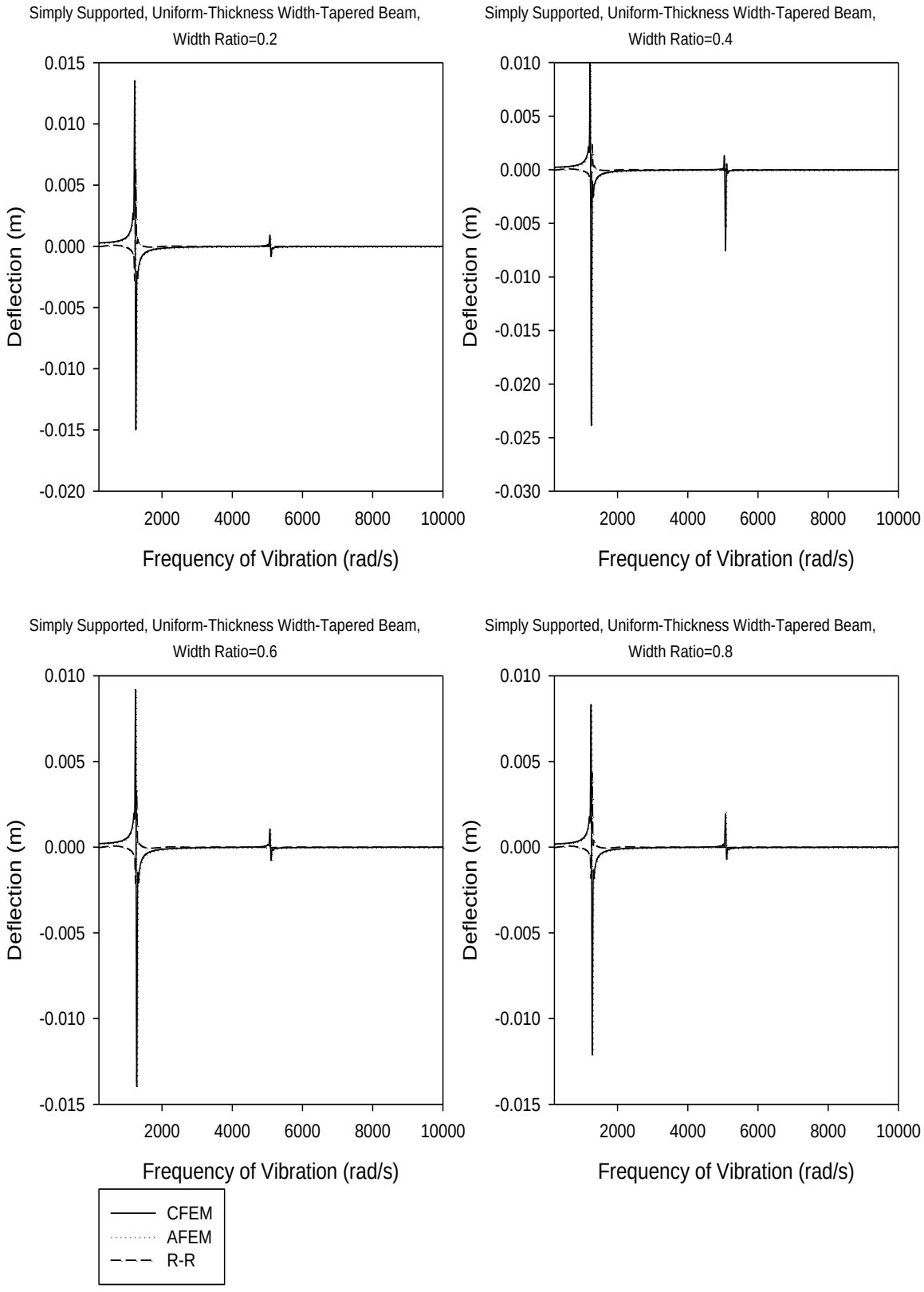

Figure 4.4: Forced vibration response of simply supported, uniform-thickness width-tapered laminated composite beams with different width ratios

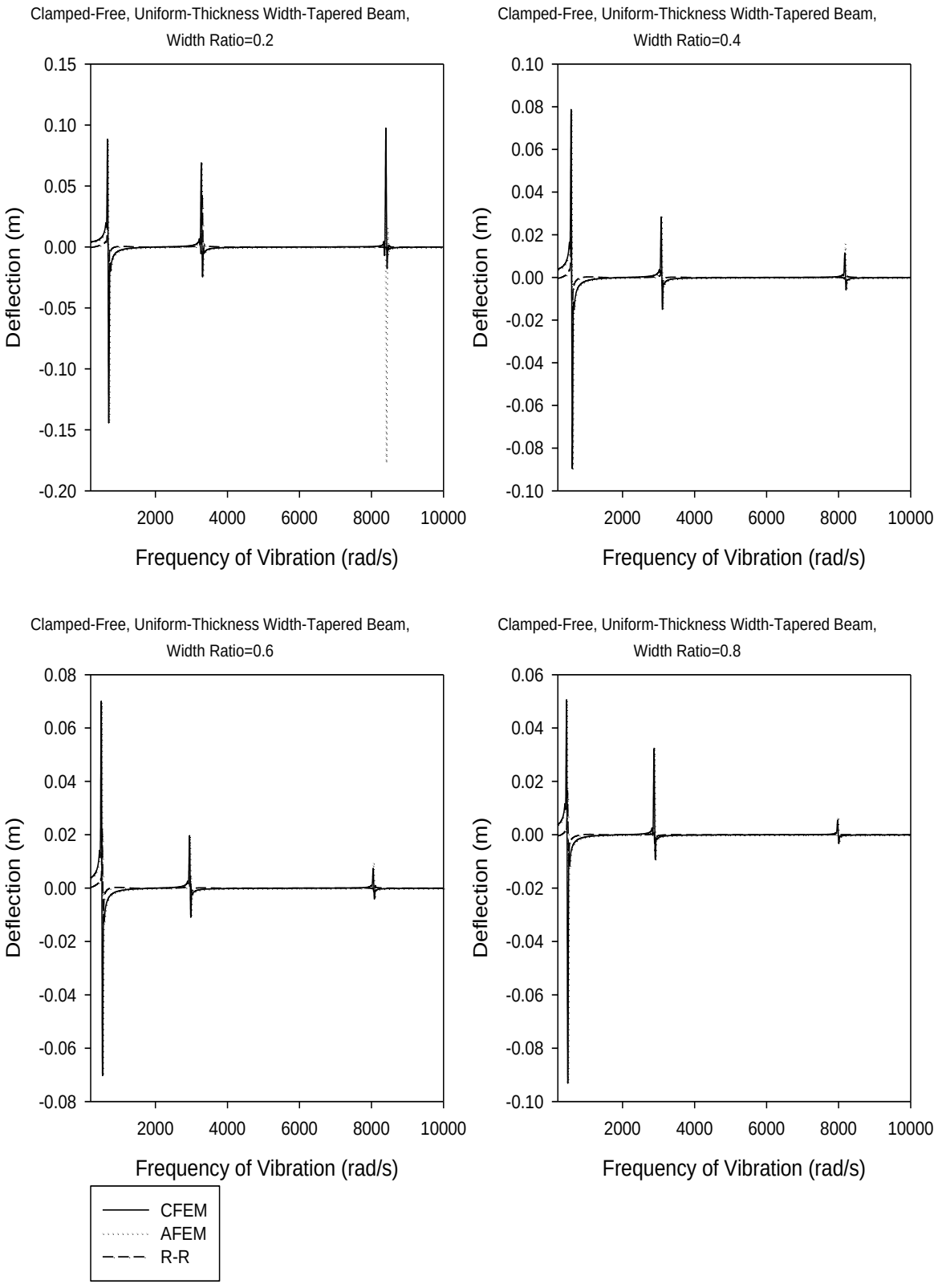

Figure 4.5: Forced vibration response of clamped-free, uniform-thickness width-tapered laminated composite beams with different width ratios

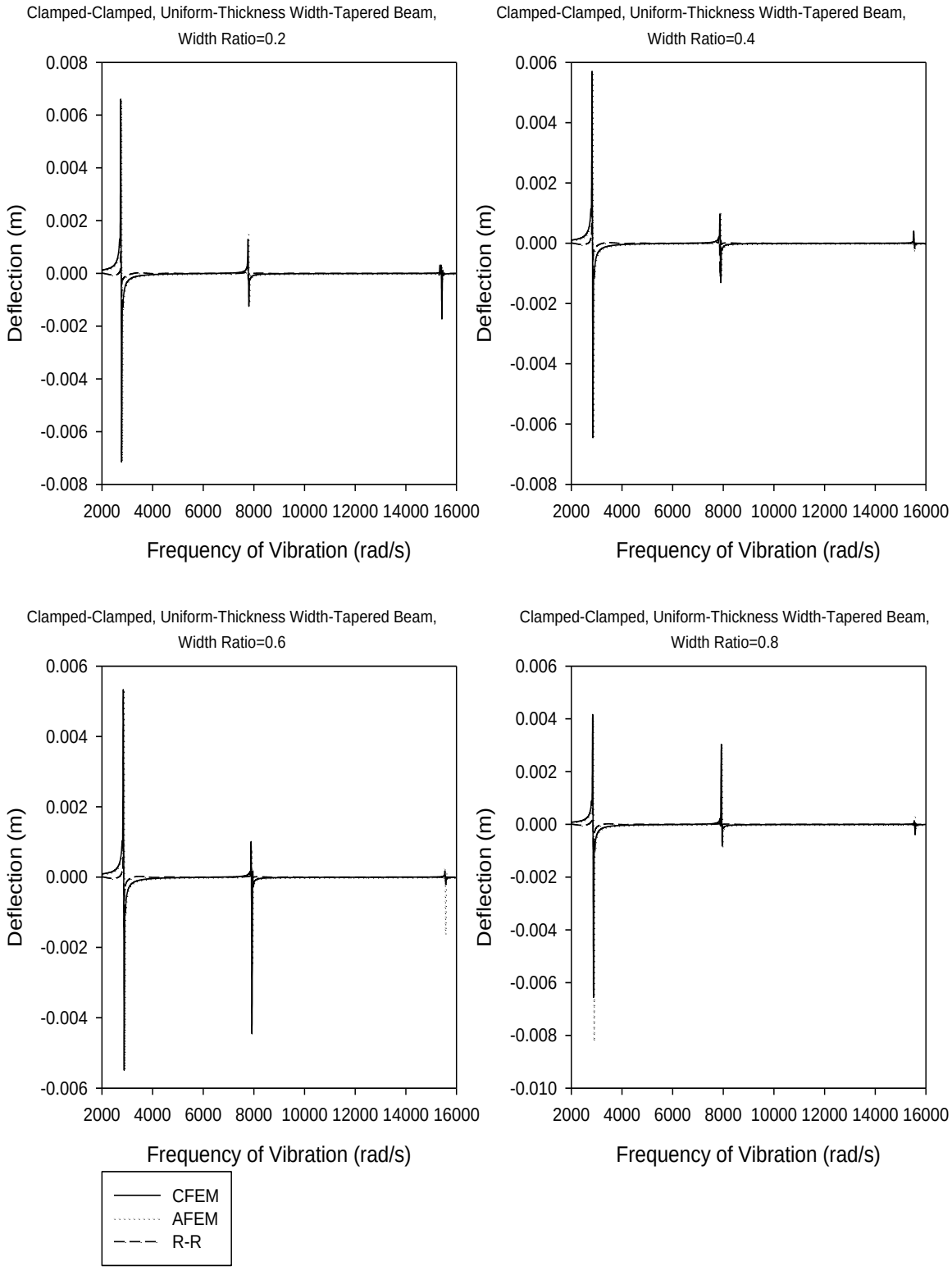

Figure 4.6: Forced vibration response of clamped-clamped, uniform-thickness width-tapered laminated composite beams with different width ratios

As illustrated in Figures 4.4, 4.5 and 4.6, the forced vibration response of the simply supported, clamped-free and clamped-clamped uniform-thickness width-tapered laminated composite beams were determined using conventional and advanced finite element formulations and have been compared with the existing results obtained using Rayleigh-Ritz method, and excellent agreement has been observed. It can be seen that in general, a clamped-clamped beam has the lowest amplitudes of deflection while a clamped-free beam has the highest amplitudes of deflection. As shown in these figures, as the width ratio of a beam increases, its amplitude of deflection will decrease.

In the third case thickness-tapered width-tapered beams are considered with a) simply supported, b) clamped-free and c) clamped-clamped boundary conditions. Beams are made of 36 plies at the thick section and 12 plies at the thin section and are made of NCT-301 graphite-epoxy prepreg. These beams are 25 cm long and have 1.66 cm width at the thick section. The laminate configuration is $[0/90]_{9s}$ at the thick section. The width ratio considered for these beams is 0.5.

The deflection of the response point versus frequency of vibration is to be determined using conventional and advanced finite element methods. These results are compared with the existing results obtained using Rayleigh-Ritz method [45]. Sinusoidal force with the magnitude of 2 N is applied to the beams. The results are shown in Figures 4.7, 4.8 and 4.9 for different boundary conditions. Each figure includes all the four configurations for each boundary condition considered. In the simply supported and clamped-clamped beams, forces are applied at the middle of the beams while in the clamped-free beams forces are applied at the free end. The locations of the points of response are same as the locations of the points of force application.

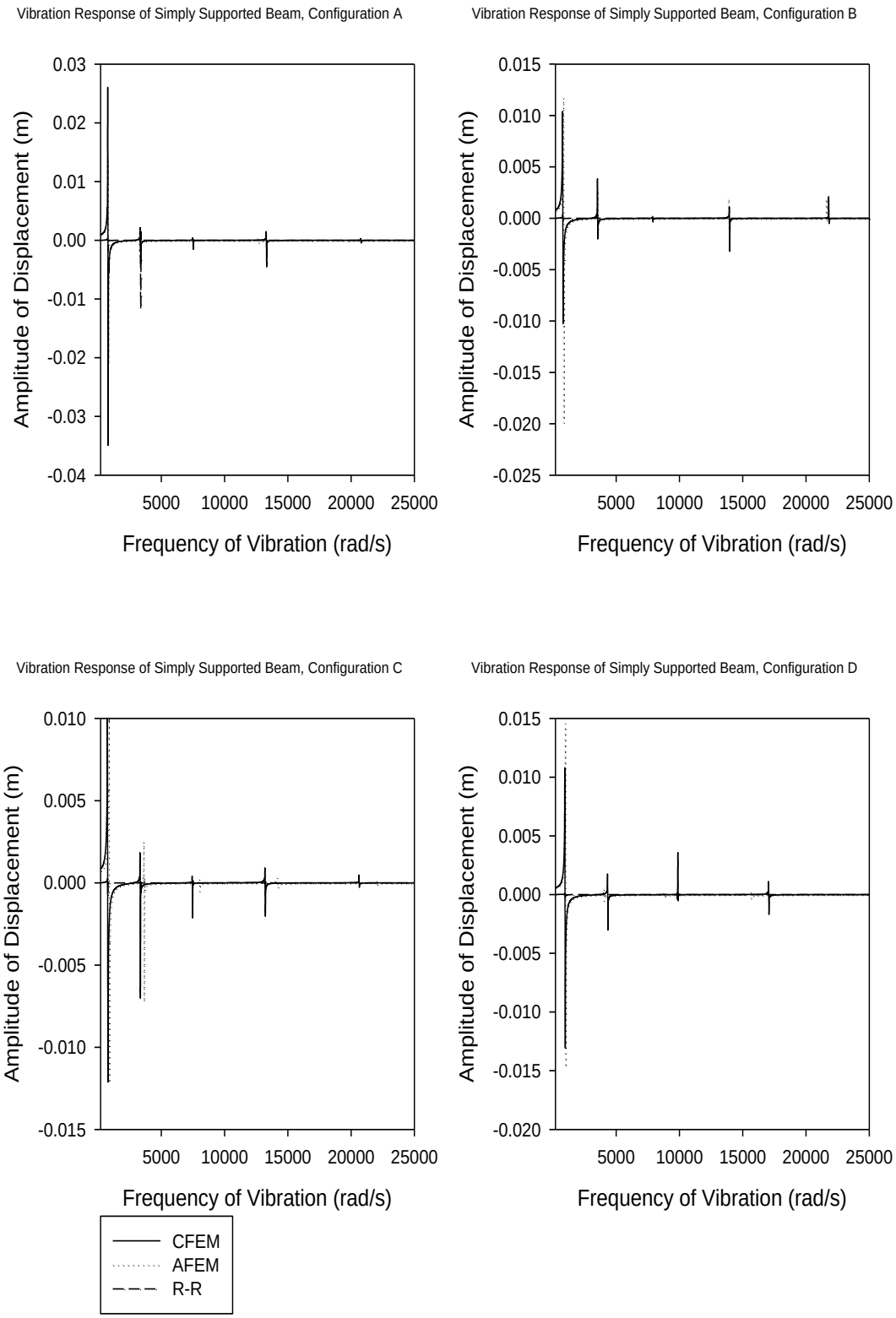

Figure 4.7: Forced vibration response of simply supported, thickness-tapered width-tapered laminated composite beams, configurations A, B, C and D

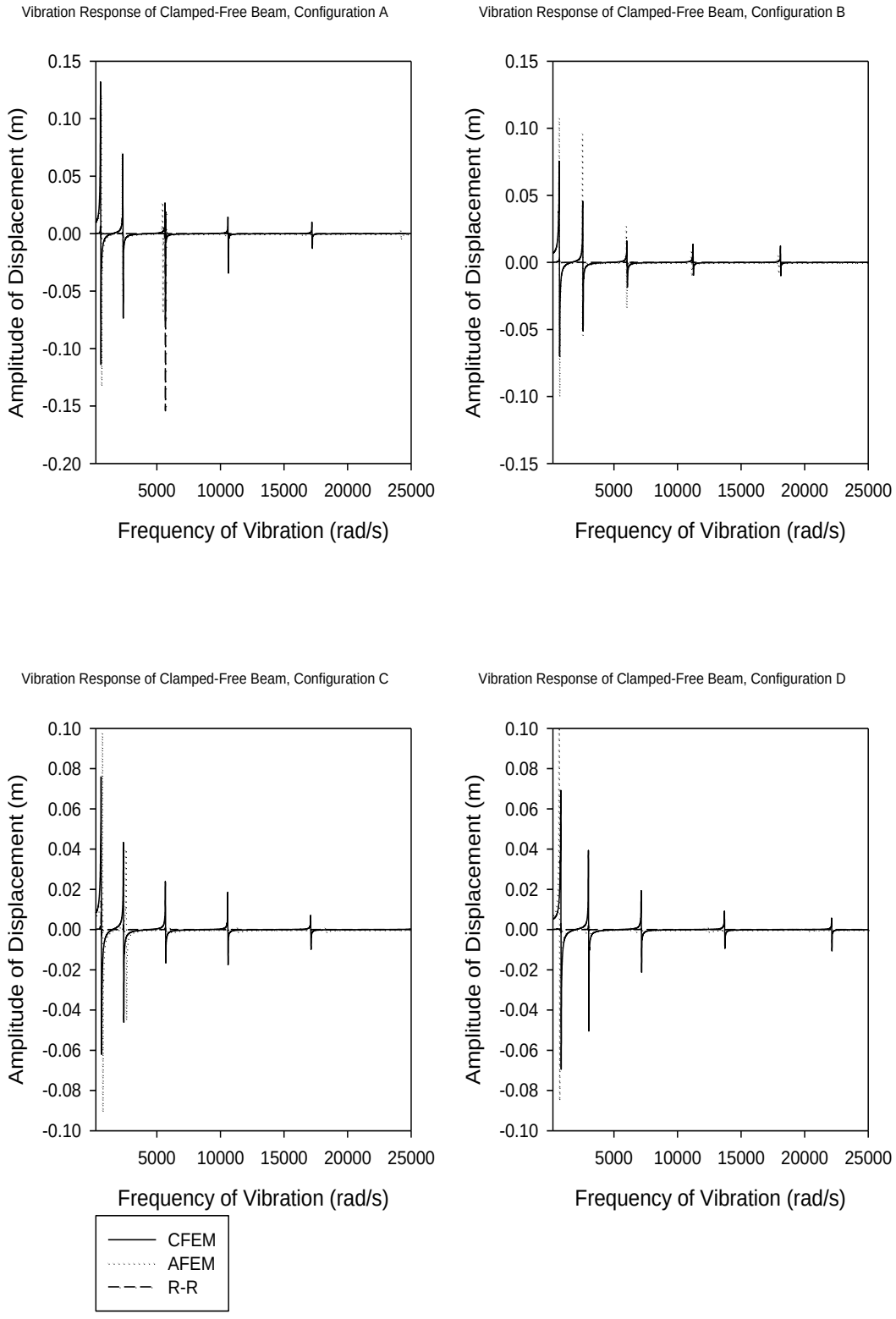

Figure 4.8: Forced vibration response of clamped-free, thickness-tapered width-tapered laminated composite beams, configurations A, B, C and D

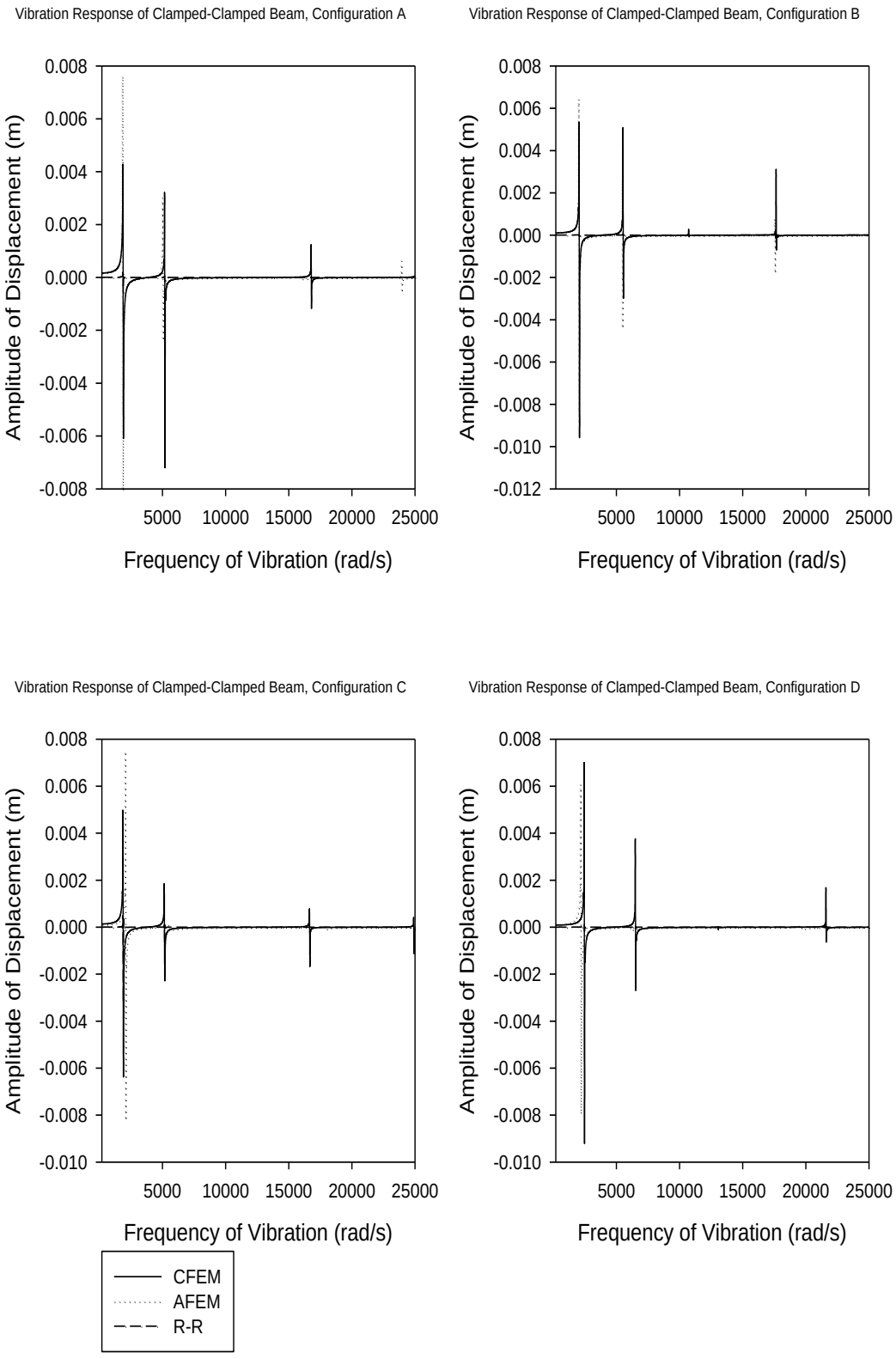

Figure 4.9: Forced vibration response of clamped-clamped, thickness-tapered width-tapered laminated composite beams, configurations A, B, C and D

As illustrated in Figures 4.7, 4.8 and 4.9, the forced vibration response of the simply supported, clamped-free and clamped-clamped thickness-tapered width-tapered laminated composite beams were determined using conventional and advanced finite element formulations and have been compared with the existing results obtained using Rayleigh-Ritz method, and excellent agreement has been observed. It can be seen that in general, the clamped-clamped beams have the lowest amplitudes of deflection while the clamped-free beams have the highest amplitudes of deflection. As shown in these figures, configuration A has the highest amplitudes of deflection, then configurations B and C have the second and the third highest amplitudes of deflection respectively and configuration D has the lowest amplitudes of deflection.

4.3. Damped forced vibration analysis

Considering the effect of damping in the forced vibration analysis of a beam has a large effect on reducing the deflection of the response point, especially when the frequency of vibration is close to the natural frequencies of the beam (near resonances). In order to take into account the effect of damping in the forced vibration analysis of the beams, Rayleigh damping method is used to model the viscous damping of the beams. Classical Rayleigh damping model uses a system damping matrix [C] defined as:

$$[C] = \alpha[M] + \beta[K] \tag{4.4}$$

in which α denotes the mass proportional Rayleigh damping constant and β is the stiffness proportional Rayleigh damping constant, and [M] and [K] are the mass and stiffness matrices respectively. The mass and stiffness proportional Rayleigh damping constants for NCT-301 carbon epoxy prepreg were obtained from experiment [45] on the beams and are equal to 2.14 and 2.76×10^{-5} respectively.

4.3.1. Formulation

The equation of motion for a damped linear system is given as:

$$[M]\{\ddot{w}\} + [C]\{\dot{w}\} + [K]\{w\} = \{F\} \tag{4.5}$$

in which the damping matrix is expressed as given by equation (4.4). Using the modal analysis and the eigenvalues and the orthonormal eigenvector matrix $[\tilde{S}]$ already obtained for the beam, the equation of motion can be decoupled for a damped system. One can decouple the equations of motion in a damped system, transforming the coordinates using orthonormal eigenvector matrix.

Substituting equation (4.2) and equation (4.4) into equation (4.5) and pre-multiplying by $[\tilde{S}]^T$ leads to:

$$[\tilde{S}]^T[M][\tilde{S}]\{\ddot{y}\} + \left(\alpha[\tilde{S}]^T[M][\tilde{S}] + \beta[\tilde{S}]^T[K][\tilde{S}]\right)\{\dot{y}\} + [\tilde{S}]^T[K][\tilde{S}]\{y\} = [\tilde{S}]^T\{F\} \tag{4.6}$$

Equation (4.6) is a decoupled equation of motion in the transformed system of coordinates {y}, which contains n (number of degrees of freedom of the beam) decoupled equations and can be solved using MATLAB® software. In the equation (4.6), $[\tilde{S}]^T[M][\tilde{S}]$ is an identity matrix and $[\tilde{S}]^T[K][\tilde{S}]$ is a diagonal matrix in which its diagonal coefficients represent the square of natural frequencies of the beams. These two facts can be used to check the system matrices prior to the forced vibration analysis of the beams. For the simplicity of the formulations it is considered that:

$$[\bar{M}] = [\tilde{S}]^T[M][\tilde{S}] \tag{4.7}$$

$$[\bar{K}] = [\tilde{S}]^T[K][\tilde{S}] \tag{4.8}$$

$$[\bar{F}] = [\tilde{S}]^T\{F\} \tag{4.9}$$

$$[\bar{C}] = \alpha[\bar{M}] + \beta[\bar{K}] \tag{4.10}$$

Inserting equations (4.7), (4.8), (4.9) and (4.10) into the equation (4.6), the equation of motion in the transformed coordinate system will be simplified as:

$$[\bar{M}]\{\ddot{y}\} + [\bar{C}]\{\dot{y}\} + [\bar{K}]\{y\} = [\bar{F}] \tag{4.11}$$

This equation can be solved in order to derive the amplitude of deflection for any degree of freedom of the beam using equation (4.12) [47]:

$$\bar{Y}_i = \frac{\bar{F}_i}{\sqrt{(\bar{K}(i,i) - \bar{M}(i,i)\omega^2)^2 + (\bar{C}(i,i)\omega)^2}} \tag{4.12}$$

in which i denotes the number of the specific degree of freedom the response of which needs to be derived, and $\bar{Y}_i$ represents the amplitude of deflection in the transformed coordinate system for that specific degree of freedom. $\bar{K}(i,i)$, $\bar{M}(i,i)$ and $\bar{C}(i,i)$ are coefficients on the diagonals of the decoupled stiffness, decoupled mass and decoupled damping matrices of the beam respectively in the transformed coordinate system. $\bar{F}_i$ denotes the i^{th} coefficient of the transformed force vector and ω is the frequency of vibration.

Using the orthonormal eigenvector matrix $[\tilde{S}]$ as in equation (4.2), one can derive the deflection in the original coordinate system, transforming the deflection in the transformed coordinate system.

In this study all the above steps are done using MATLAB® software. The material considered in this study is NCT-301 carbon epoxy prepreg [2]. The amplitude of deflection of the response point versus frequency of vibration is to be determined for the beams that are similar to those studied in the previous section for the undamped systems.

4.2.3. Validation

In order to validate the results, first the results obtained using conventional finite element method are compared with the existing results obtained using Rayleigh-Ritz method [45] for uniform-thickness width-tapered beams having simply supported, clamped-free and clamped-clamped boundary conditions.

Uniform-thickness width-tapered laminated composite beams are considered with a) simply supported, b) clamped-free and c) clamped-clamped boundary conditions. Width ratio considered is equal to 0.5. Beams are made of 36 plies of NCT-301 graphite epoxy prepreg. The laminate configuration is $[0/90]_{9s}$. Length of the beams is equal to 0.25 m and the width at the left section is 0.0166 m. The mass proportional damping constant is 2.14 and the stiffness proportional damping constant is 2.76×10^{-5}. Amplitude of deflection versus frequency of vibration of the response point is to be determined when applying sinusoidal force with the magnitude of 2N to the beams. The response point and the point of applied force are different for each boundary condition of the beam. Points of response and the points of force application for the three boundary conditions that are considered here are shown in Figure 4.2. The results are compared in Figure 4.10.

This comparison shows the maximum of 8 % and the average of 3.5 % of error between the results obtained using the conventional finite element formulation and the Rayleigh-Ritz method with respect to the results obtained using Rayleigh-Ritz method.

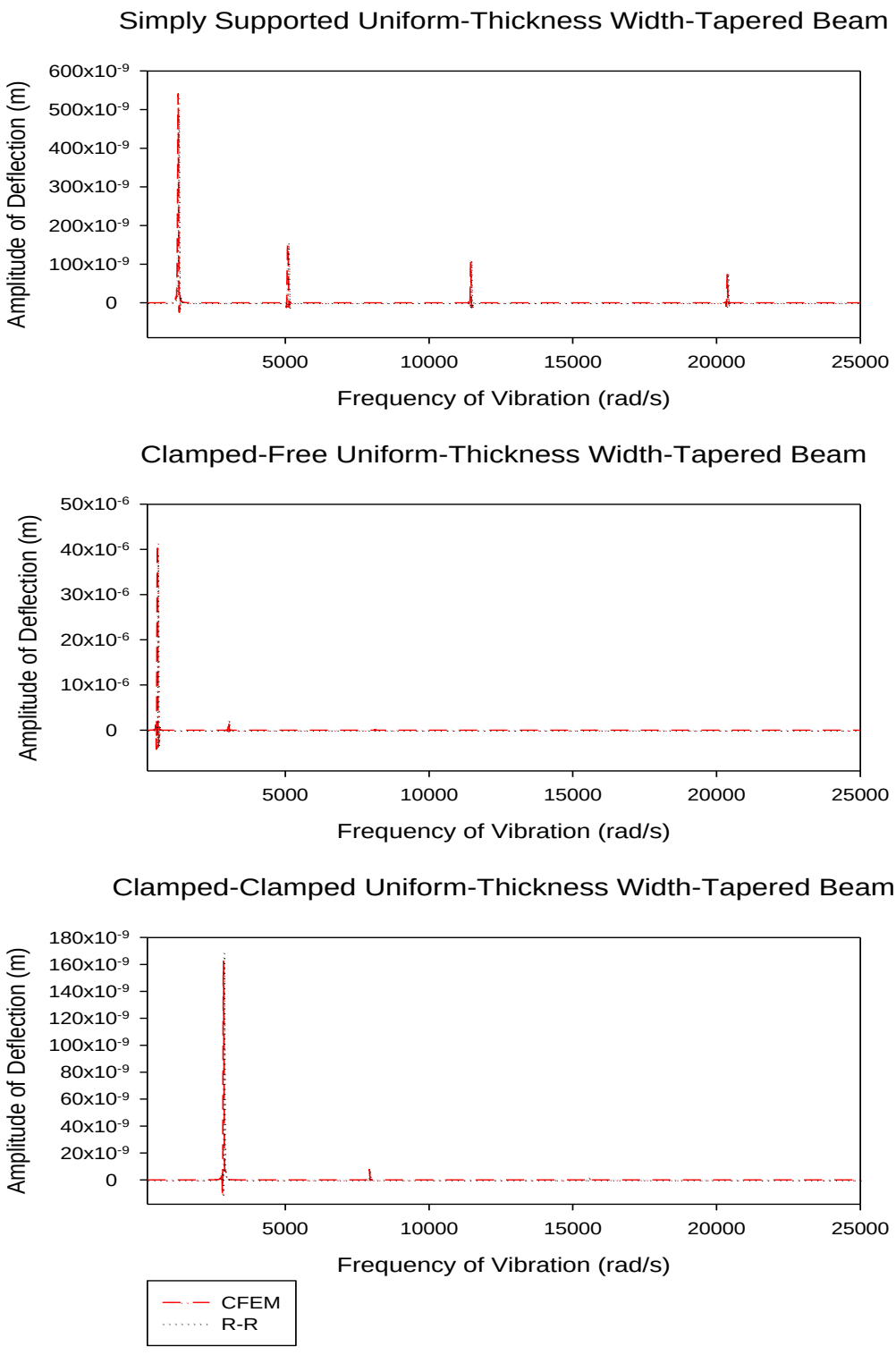

Figure 4.10: Amplitude of deflection versus frequency of vibration determined using conventional finite element and Rayleigh-Ritz methods for uniform-thickness width-tapered laminated composite beams with simply supported, clamped-free and clamped-clamped boundary conditions

As illustrated in Figure 4.10, the damped forced vibration response of the simply supported, clamped-free and clamped-clamped uniform-thickness width-tapered laminated composite beams were determined using conventional finite element formulation and has been compared with the existing results obtained using Rayleigh-Ritz method. Excellent agreement has been observed. It can be seen that in general, a clamped-clamped beam has the lowest amplitudes of deflection while a clamped-free beam has the highest amplitudes of deflection. As shown in this figure, damping has a large effect on reducing the deflection of the response point, especially when the frequency of vibration is close to the natural frequencies of the beam (near resonances).

Two more cases are provided to illustrate the effect of damping on the forced vibration response of laminated composite beams. The first case considers uniform laminated composite beams, while the second case considers thickness-tapered width-tapered laminated composite beams.

Uniform laminated composite beams are considered with a) simply supported, b) clamped-free and c) clamped-clamped boundary conditions. These beams are made of 36 plies of NCT-301 graphite epoxy prepreg. Length of the beams is equal to 0.25 m, width of the beams is equal to 0.0166 m and the laminate configuration considered is $[0/90]_{9s}$. The mass proportional damping constant is 2.14 and the stiffness proportional damping constant is 2.76×10^{-5}. Sinusoidal force with the magnitude of 2 N is applied to the beams. The response point and the point of applied force are different for each boundary condition of the beam. Points of response and the points of force application for the three boundary conditions that are considered here are shown in Figure 4.2. The amplitude of

deflection versus frequency of vibration for these three boundary conditions are shown in Figure 4.11.

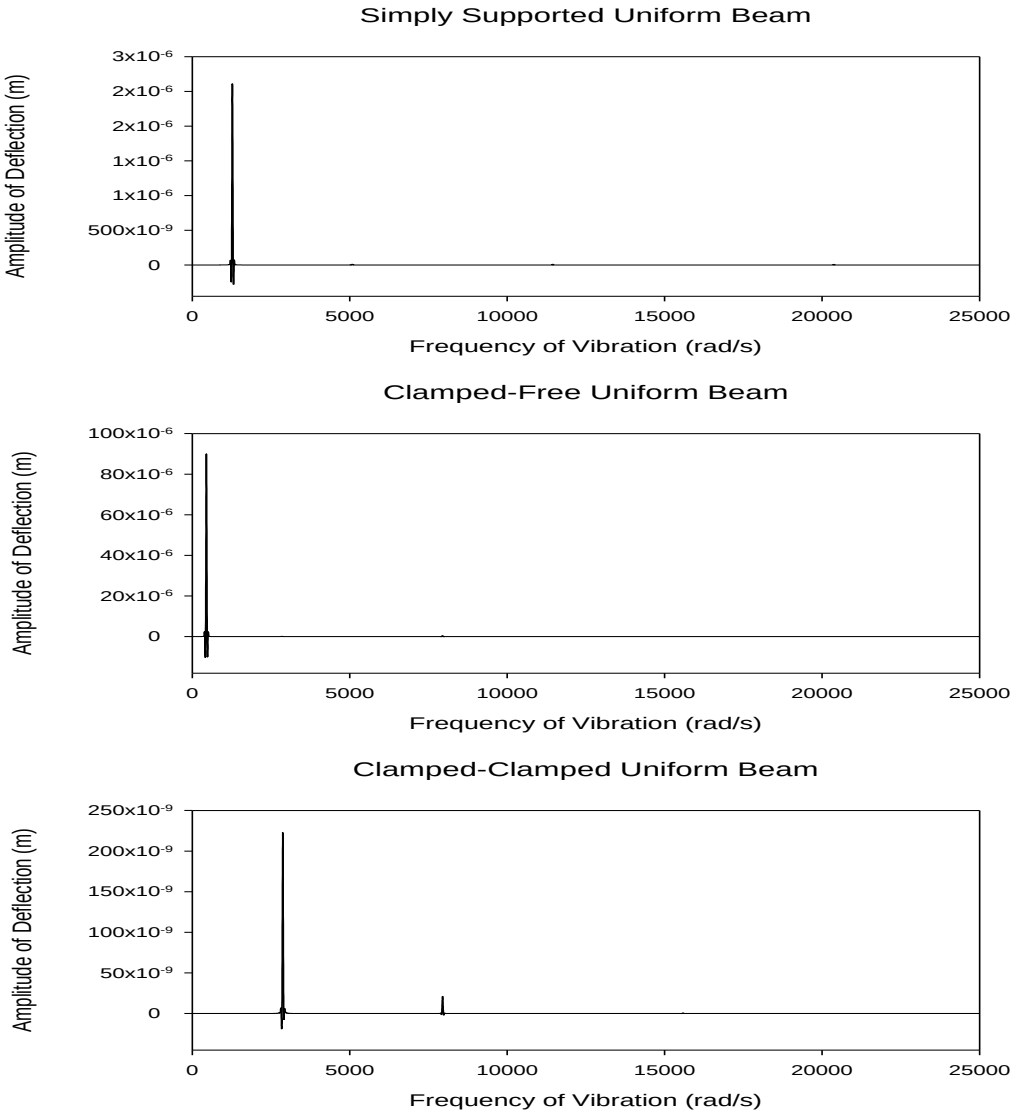

Figure 4.11: Amplitude of deflection versus frequency of vibration obtained using conventional finite element method for uniform laminated composite beams with simply supported, clamped free and clamped clamped boundary conditions

As illustrated in Figure 4.11, the damped forced vibration response of the simply supported, clamped-free and clamped-clamped uniform laminated composite beams were

determined using conventional finite element formulation. It can be seen that the maximum deflections of each beam happens when the frequency of vibration is close to that beam's natural frequencies (resonances). As shown in this figure, a clamped-clamped beam has the lowest deflection while a clamped-free beam has the highest deflection. Comparing the results represented in this figure and in Figure 4.3, it can be realized that damping has a large effect on reducing the deflection of the response point, especially near resonances.

Thickness-tapered width-tapered beams made of configurations A, B, C and D are considered for the damped forced vibration analysis. Simply supported, clamped-free and clamped-clamped boundary conditions are considered for these beams. These beams are made of 36 plies at the thick section and 12 plies at the thin section, and are made of NCT-301 graphite-epoxy prepreg. These beams are 0.25 m long and have 0.0166 m width at the thick section. The laminate configuration is $[0/90]_{9s}$ at the thick section. The width ratio considered is 0.5. The mass proportional damping constant is 2.14 and the stiffness proportional damping constant is 2.76×10^{-5}.

The deflection of the response point versus frequency of vibration is to be determined using conventional finite element method. A sinusoidal force with the magnitude of 2 N is applied to the beams. In the simply supported and clamped-clamped beams, force is applied at the middle of the beams while in the clamped-free beams the force is applied at the free end of the beams. The locations of the points of response are same as the locations of the points of force application.

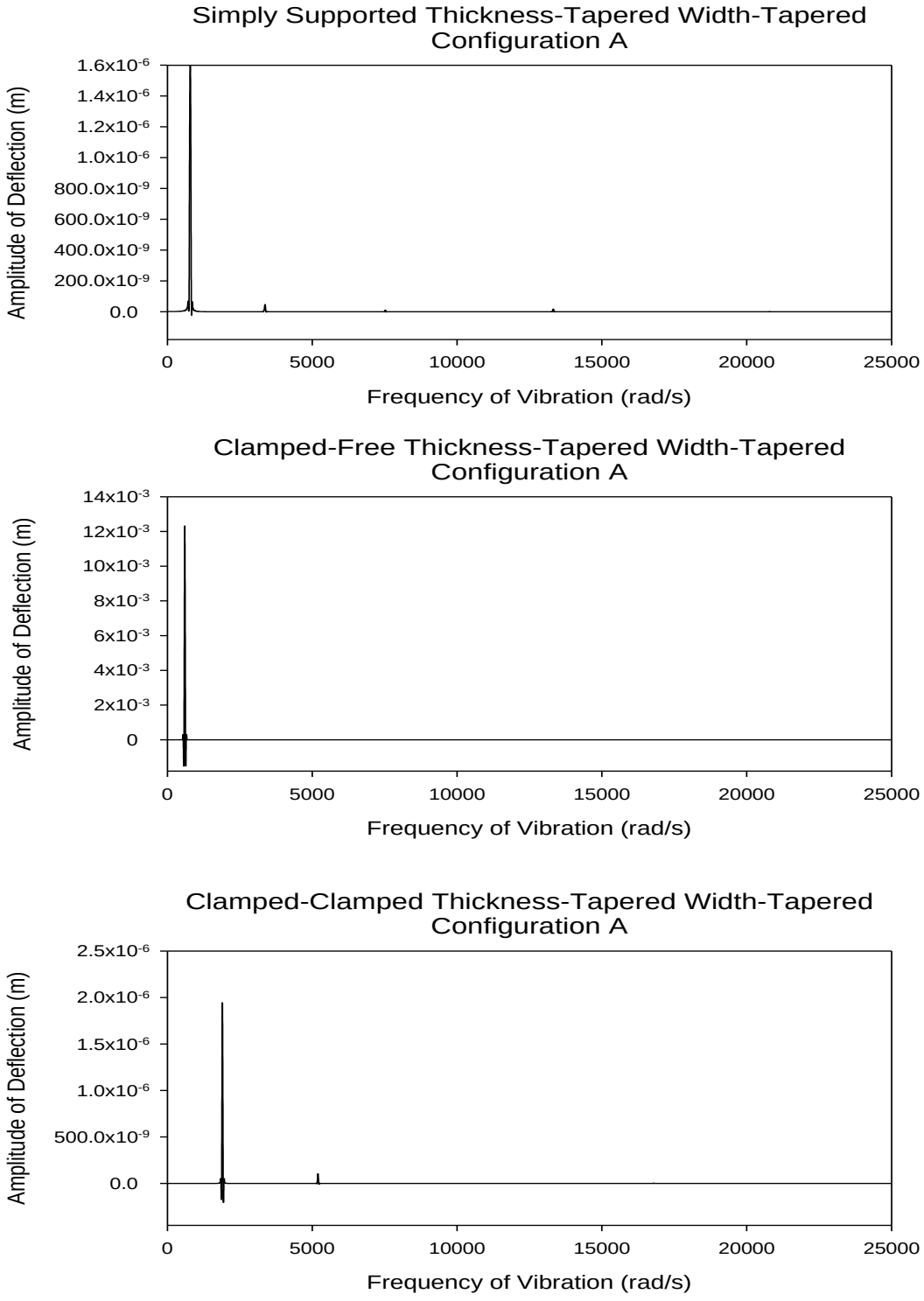

Figure 4.12: Amplitude of deflection versus frequency of vibration determined using conventional finite element method for simply supported, clamped-free and clamped-clamped thickness-tapered width-tapered laminated composite beams with Configuration A

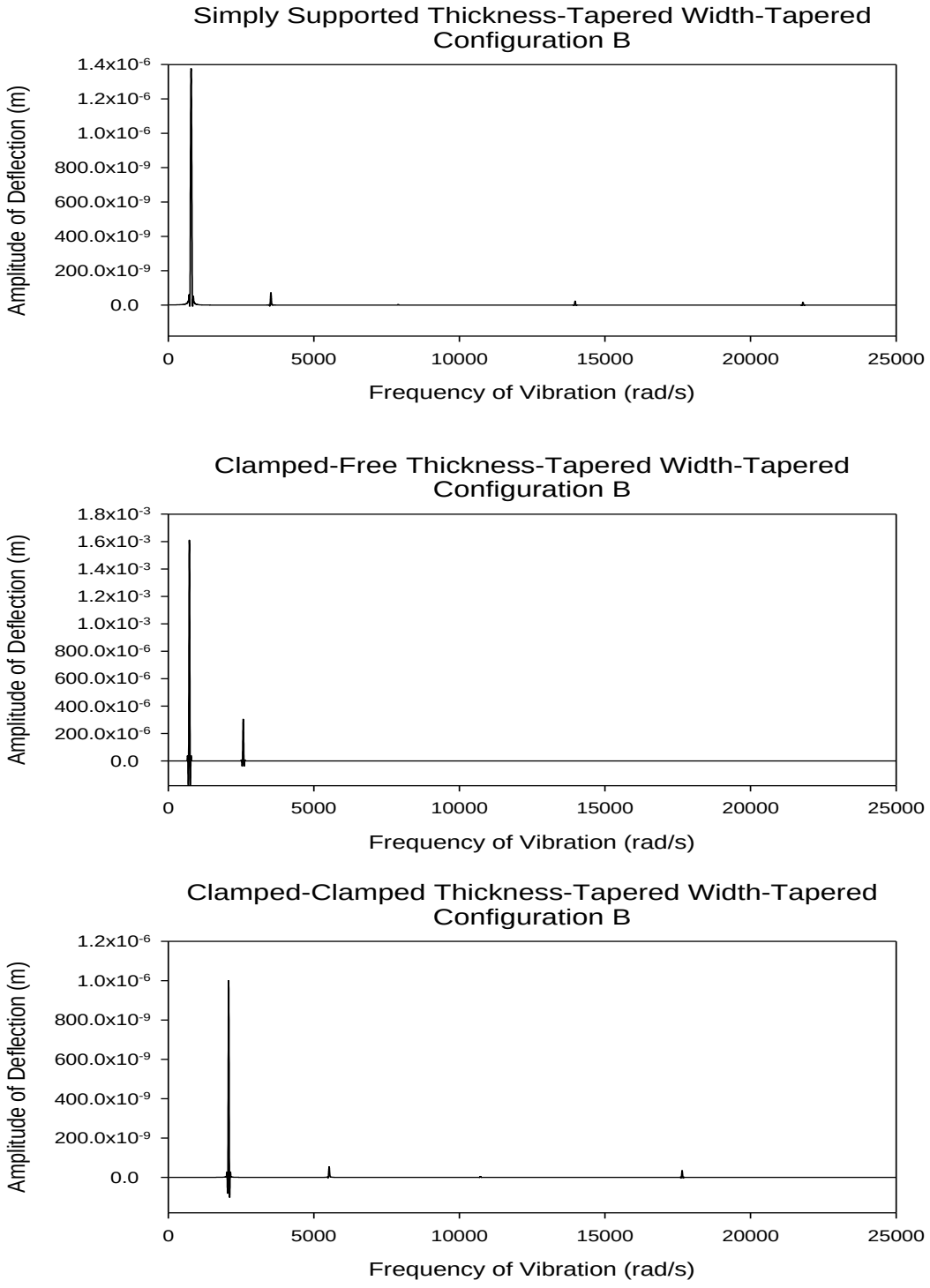

Figure 4.13: Amplitude of deflection versus frequency of vibration determined using conventional finite element method for simply supported, clamped-free and clamped-clamped thickness-tapered width-tapered laminated composite beams with Configuration B

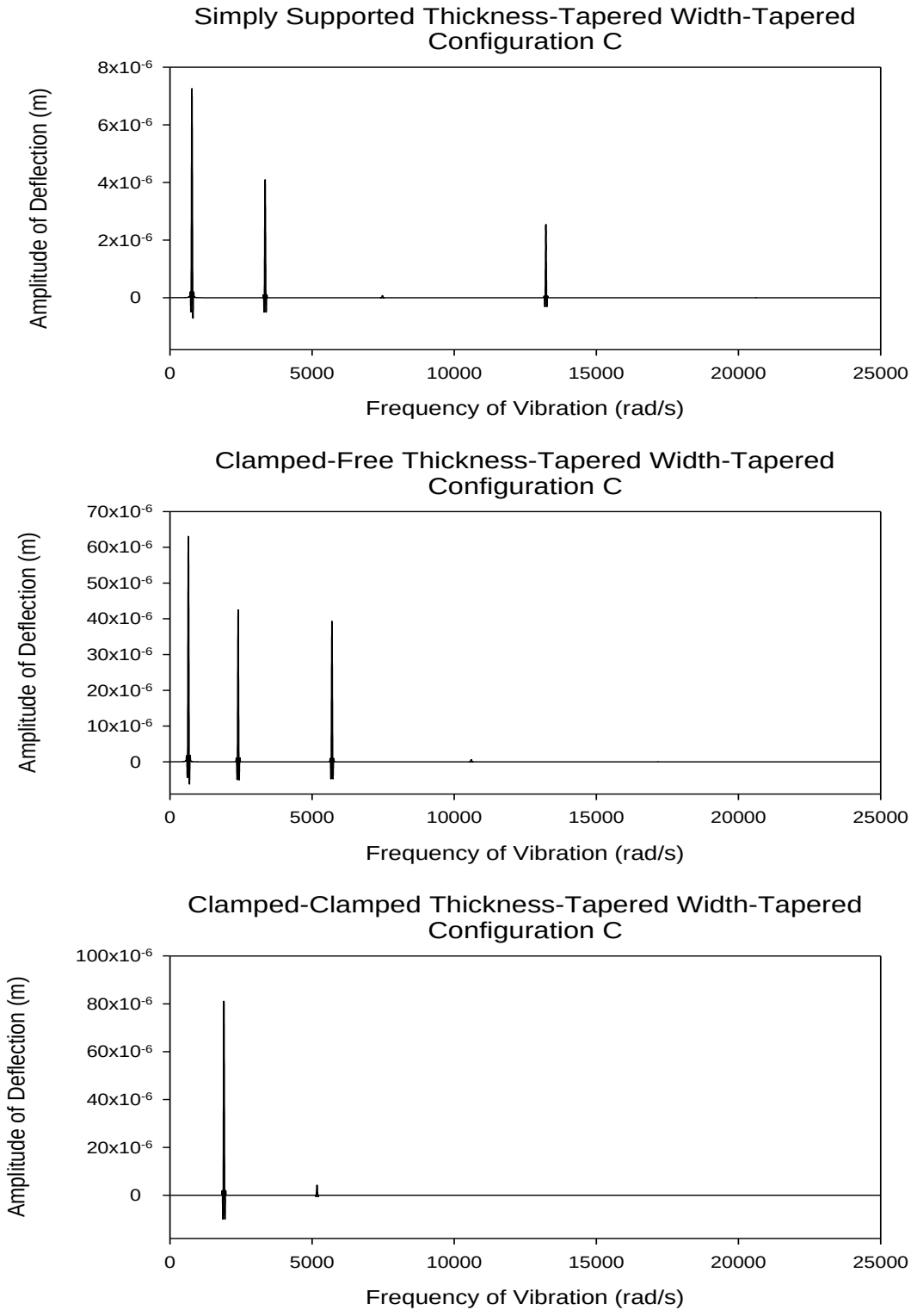

Figure 4.14: Amplitude of deflection versus frequency of vibration determined using conventional finite element method for simply supported, clamped-free and clamped-clamped thickness-tapered width-tapered laminated composite beams with Configuration C

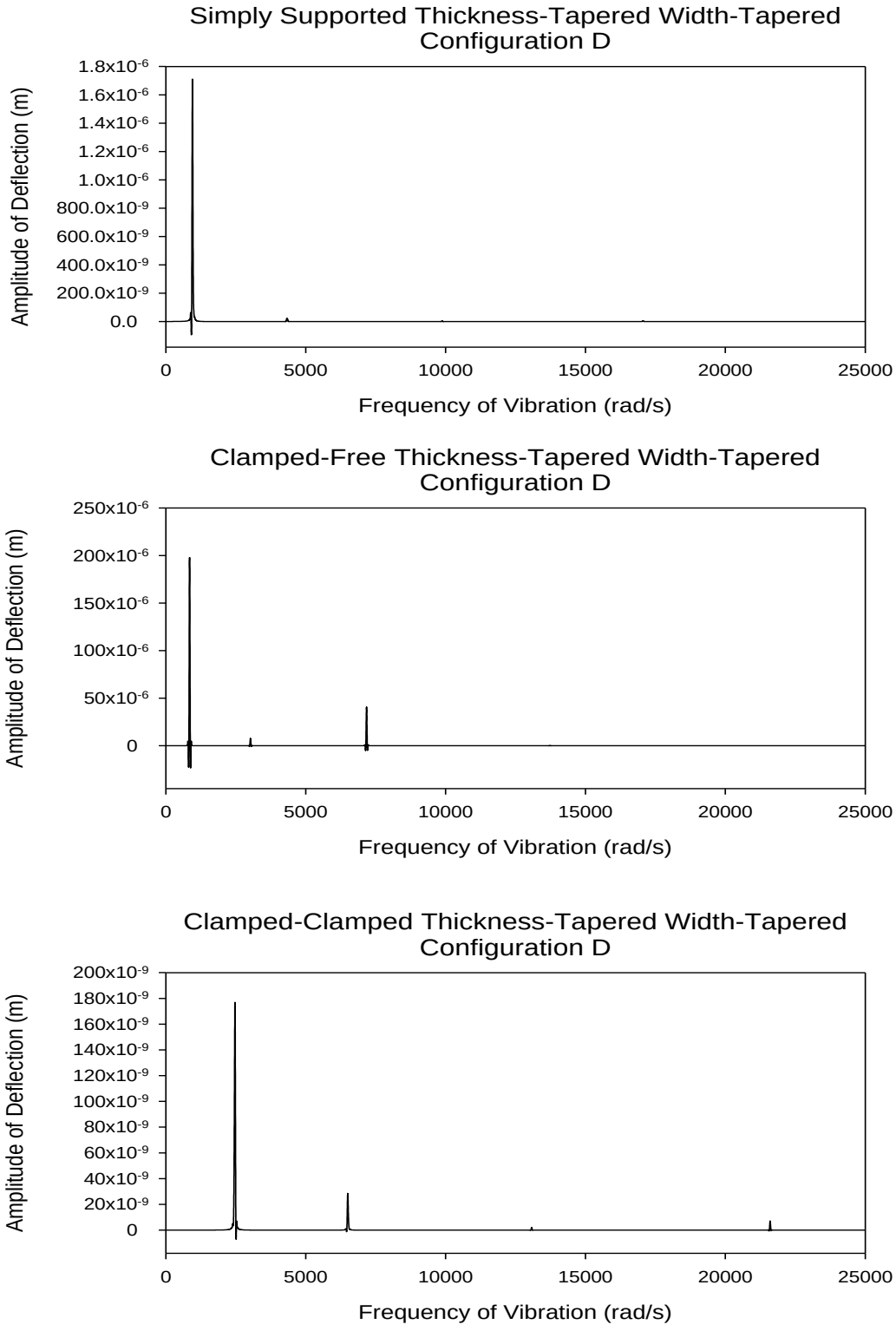

Figure 4.15: Amplitude of deflection versus frequency of vibration determined using conventional finite element method for simply supported, clamped-free and clamped-clamped thickness-tapered width-tapered laminated composite beams with Configuration D

As illustrated in Figures 4.12, 4.13, 4.14 and 4.15, the damped forced vibration response of the simply supported, clamped-free and clamped-clamped thickness-tapered width-tapered laminated composite beams were determined using conventional finite element formulation. It can be seen that in general, a clamped-clamped beam has the lowest amplitudes of deflection while a clamped-free beam has the highest amplitudes of deflection. As shown in these figures, configuration A has the highest amplitudes of deflection, then configurations B and C have the second and the third highest amplitudes of deflection respectively and configuration D has the lowest amplitudes of deflection. Comparing the results represented in these figures and in Figures 4.7, 4.8 and 4.9, it can be realized that damping has a large effect on reducing the deflection of the response point, especially near resonances.

4.4. Discussion and conclusion

In this chapter, forced vibration analysis of laminated composite beams has been carried out when applying a sinusoidal translational force to the beams. The analysis started with the undamped systems and the results were compared with the existing results obtained using the Rayleigh-Ritz method, excellent agreement have been observed. Then the forced vibration analysis of the damped systems has been carried out. In order to validate the results, the damped forced vibration results have been compared with the existing results obtained using Rayleigh-Ritz method, excellent agreement have been observed. Then more results were generated for different variable-thickness variable-width laminated composite beams.

Advanced and conventional finite element methods and modal analysis have been used in order to derive beam system matrices and to perform the forced vibration analysis.

It should be noted that although the comparison of the obtained results with the existing results shows excellent accuracy for both the undamped and the damped systems, the results determined for the damped systems provide slightly better accuracy, especially near resonances.

Numerous sets of plots were generated to display the amplitudes of deflection versus frequency of vibration for a variety of undamped and damped variable-thickness variable-width laminated composite beams having simply supported, clamped-free and clamped-clamped boundary conditions.

It can be concluded from the results presented in this chapter that in general: i) a clamped-clamped beam has the lowest amplitudes of deflection while a clamped-free beam has the highest amplitudes of deflection, ii) as the width ratio of a beam increases, its amplitude of deflection will decrease, iii) configuration A has the highest amplitudes of deflection, then configurations B and C have the second and the third highest amplitudes of deflection respectively and configuration D has the lowest amplitudes of deflection, and iv) comparing the results determined for the damped and undamped systems, it can be realized that damping has a large effect on reducing the deflection of the response point, especially near resonances.

Chapter-5

Vibration analysis of tapered laminated composite beams with elastic supports

5.1. Introduction

In the chapters 2 and 3 the free vibrations of variable-thickness variable-width laminated composite beams having simply supported, clamped-free and clamped-clamped boundary conditions have been studied. Conventional and advanced finite element formulations have been used in order to analyze the free vibrations of these beams. It is important to mention that most of the times in the practical situations, supports are not completely rigid. In this chapter, a simple approach is proposed that can be used to determine the natural frequencies of a beam having elastic supports made by any combination of translational and rotational springs. This approach may also be used in order to analyze the free vibration of beams having translational and rotational springs attached to them at any point through the length of the beams.

It is seen that, when an elastic support is stiff enough or is positioned properly, its effect on the vibration of the beam is similar to that of a rigid support. Formulations in this chapter can be used to assist in the practical design of a support.

Conventional and advanced finite element formulations are used in this chapter to analyze the free vibrations of variable-thickness variable-width laminated composite beams having different combinations of rigid and elastic supports.

5.2. Advanced and conventional finite element formulations

Four degrees of freedom per node (deflection w, rotation $-\frac{dw}{dx}$, curvature $-\frac{d^2w}{dx^2}$ and the gradient of curvature $\frac{d^3w}{dx^3}$) and two nodes per element are considered for the advanced finite element formulation and two degrees of freedom per node (deflection w and rotation $-\frac{dw}{dx}$) and two nodes per element are considered for the conventional finite element formulation. Similar formulations to those that were used in chapters 2 and 3, are used in this chapter to derive system's global stiffness and mass matrices based on advanced and conventional finite element formulations.

Suppose that there exist a translational spring and a rotational spring attached to a beam, in order to analyze the free vibration of this beam, first the global stiffness and the global mass matrices should be determined using the conventional or the advanced finite element formulation as have been studied in the chapter 2 and the chapter 3. Secondly, the effect of the translational and the rotational springs on free vibration of the beam is included simply by adding the stiffness of the springs to the corresponding coefficient of the global stiffness matrix. Having the new global stiffness matrix and the global mass matrix, the free vibration of the beam can be analyzed solving the similar eigenvalue problem to that considered in equation (2.26) using MATLAB® software.

The beams considered in this chapter may have any of the classical boundary conditions (simply supported, clamped-free and clamped-clamped) considered in the previous chapters and can have any combination of the translational and rotational springs attached to the beams.

5.3. Validation

5.3.1. Uniform beam

The natural frequencies of uniform beams were determined using conventional and advanced finite element formulations and have been validated in three cases: i) Uniform isotropic beam clamped at one end with a translational spring at the other end. ii) Uniform isotropic beams having three non-classical boundary conditions (free-translational spring, simply supported-translational spring and clamped-translational spring). iii) Uniform laminated composite beams having five non-classical boundary conditions (free-translational spring, simply supported-translational spring, clamped-translational spring, clamped-rotational spring and free-rotational spring).

A uniform isotropic beam is considered clamped at one end with a translational spring attached to the other end of the beam (clamped-translational spring) as shown in Figure 5.1.

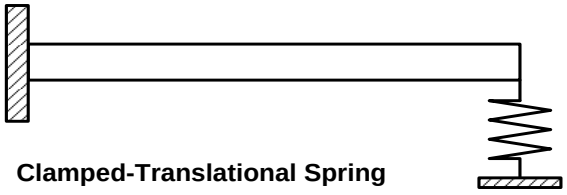

Figure 5.1: Uniform beam clamped at one end with a translational spring attached to the other end of the beam

This beam is made of aluminum alloy 7075 with the material properties shown in Table 5.1. This beam is 25 cm long, has the width of 1.5 cm and the thickness of 1.5 mm. Twenty different values are considered for the stiffness of the attached spring as shown in Table 5.2.

Table 5.1: Material properties of aluminum alloy 7075

Young's modulus (E)	70 GPa
In-plane shear modulus (G_{12})	35 GPa
Density	2700 kg/m^3
Poisson's ratio (ν_{12})	0.3

The first two natural frequencies of the beam versus stiffness of the translational spring are considered. The results determined using conventional and advanced finite element formulations are compared with the existing results [30] and shown in Table 5.2. Ten elements are used to determine the natural frequencies of these beams and the length of each element is equal to 2.5 cm.

In Table 5.2, the stiffness of the attached translational spring is represented by $\bar{k}$ which is defined as:

$$\bar{k} = \frac{k_t L^3}{EI} \tag{5.1}$$

in which k_t denotes the stiffness of the attached translational spring, L is the length of the beam and I represents the moment of inertia.

In Table 5.2, the natural frequencies of the beam are represented by λ_n which is defined as:

$$\omega_n = \frac{{\lambda_n}^2}{L^2}\sqrt{\frac{EI}{m}} \tag{5.2}$$

in which ω_n represents the natural frequency and m denotes the total mass of the beam.

Table 5.2: First two natural frequencies of a uniform isotropic clamped-translational spring beam determined using conventional and advanced finite element formulations and the comparison with the existing results

$\bar{k}$	λ_1 [30]	λ_1 CFEM	**Percentage Difference**	λ_1 AFEM	**Percentage Difference**	λ_2 [30]	λ_2 CFEM	**Percentage Difference**	λ_2 AFEM	**Percentage Difference**
2.5	2.169	2.168549	**0.02**	2.168547	**0.02**	4.718	4.718555	**0.01**	4.718475	**0.01**
5	2.367	2.366781	**0.01**	2.366778	**0.01**	4.743	4.743333	**0.01**	4.743251	**0.01**
7.5	2.517	2.517497	**0.02**	2.517493	**0.02**	4.768	4.768452	**0.01**	4.768368	**0.01**
10	2.639	2.638929	**0**	2.638925	**0**	4.794	4.793857	**0**	4.793771	**0**
15	2.827	2.826662	**0.01**	2.826656	**0.01**	4.845	4.845312	**0.01**	4.845221	**0**
20	2.968	2.967551	**0.02**	2.967543	**0.02**	4.897	4.897278	**0.01**	4.897182	**0**
25	3.078	3.078205	**0.01**	3.078196	**0.01**	4.949	4.949365	**0.01**	4.949264	**0.01**
30	3.168	3.167666	**0.01**	3.167655	**0.01**	5.001	5.001226	**0**	5.001119	**0**
40	3.303	3.30336	**0.01**	3.303346	**0.01**	5.103	5.10315	**0**	5.103032	**0**
50	3.401	3.400922	**0**	3.400907	**0**	5.201	5.201327	**0.01**	5.201197	**0**
60	3.474	3.473939	**0**	3.473922	**0**	5.295	5.294759	**0**	5.294617	**0.01**
70	3.53	3.530294	**0.01**	3.530275	**0.01**	5.383	5.382981	**0**	5.382826	**0**
80	3.575	3.574889	**0**	3.574869	**0**	5.466	5.465876	**0**	5.46571	**0.01**
100	3.541	3.640564	**2.81**	3.640542	**2.81**	5.616	5.616188	**0**	5.615996	**0**
125	3.696	3.695578	**0.01**	3.695554	**0.01**	5.777	5.777705	**0.01**	5.777484	**0.01**
150	3.733	3.733277	**0.01**	3.733252	**0.01**	5.914	5.914227	**0**	5.913978	**0**
200	3.781	3.781267	**0.01**	3.781241	**0.01**	6.128	6.128771	**0.01**	6.128473	**0.01**
300	3.83	3.829834	**0**	3.829806	**0.01**	6.404	6.404524	**0.01**	6.404152	**0**
400	3.854	3.85418	**0**	3.854151	**0**	6.566	6.566157	**0**	6.565736	**0**
500	3.869	3.868769	**0.01**	3.868739	**0.01**	6.668	6.668746	**0.01**	6.668291	**0**

In Table 5.2 CFEM and AFEM denote Conventional Finite Element Method and Advanced Finite Element Method respectively. In this table, the comparison of the natural frequencies obtained using advanced and conventional finite element methods is done with respect to the existing results [30]. Excellent agreement has been observed. As it can be seen, as the stiffness of the attached spring increases, the natural frequencies will increase.

Uniform isotropic beams are considered with a) free-translational spring, b) simply supported-translational spring and c) clamped-translational spring boundary conditions as shown in Figure 5.2.

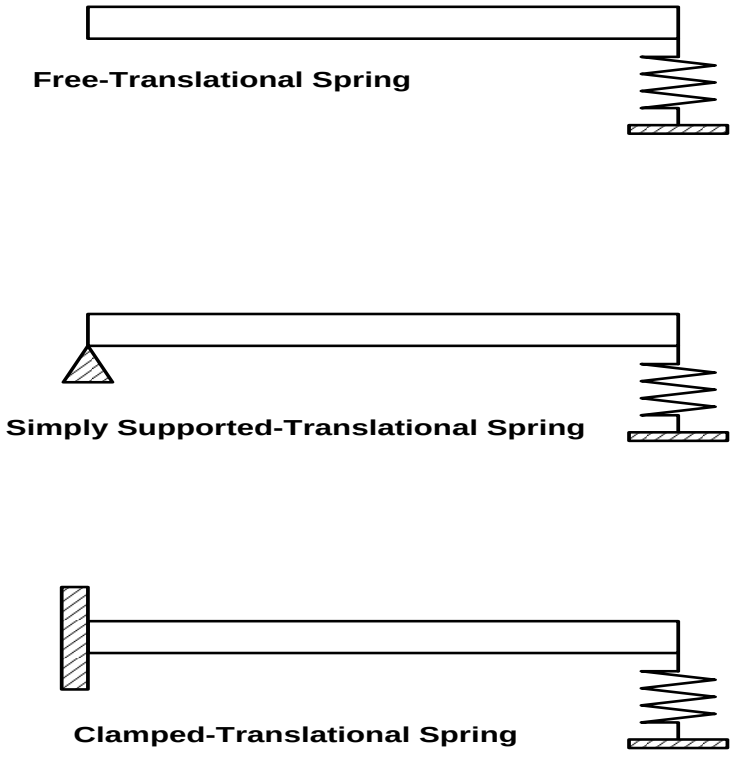

Figure 5.2: Uniform a) free-translational spring, b) simply supported-translational spring and c) clamped-translational spring beams

These beams are made of aluminum alloy 7075 with the material properties shown in Table 5.1. These beams are 25 cm long, have the width of 1.5 cm and the thickness of 1.5 mm. Spring's stiffness is equal to 47.24 N/m for all the beams. The first five natural frequencies of the beams are considered. The results determined using conventional and advanced finite element formulations are compared with the results obtained using Rayleigh-Ritz method [48] and shown in Table 5.3. Ten elements are used to determine the natural frequencies of these beams in both advanced and conventional finite element methods and the length of each element is equal to 2.5 cm.

Table 5.3: First five natural frequencies of uniform isotropic beams with free-translational spring, simply supported-translational spring and clamped-translational spring boundary conditions obtained using advanced and conventional finite element formulations and Rayleigh-Ritz method

Modes	**Free-TS**				
	AFEM	Percentage Difference	CFEM	Percentage Difference	R-R
1st	110.2	**0**	110.2	**0**	110.2
2nd	797.2	**0**	797.2	**0**	797.2
3rd	2178.5	**0**	2179	**0**	2178.5
4th	4266.5	**0**	4270.5	**0.1**	4266.5
5th	7051.3	**0**	7068.2	**0.2**	7051.3
Modes	**Simply Supported-TS**				
	AFEM	Percentage Difference	CFEM	Percentage Difference	R-R
1st	94.3	**0**	94.3	**0**	94.3
2nd	555.5	**0**	555.5	**0**	555.5
3rd	1766.1	**0**	1766.4	**0**	1766.1
4th	3679.2	**0**	3681.8	**0.1**	3679.2
5th	6289.8	**0**	6302.4	**0.2**	6289.8

Modes	Clamped-TS				
	AFEM	Percentage Difference	CFEM	Percentage Difference	R-R
1st	165.9	**0**	165.9	**0**	165.9
2nd	785.4	**0**	785.4	**0**	785.4
3rd	2179.3	**0**	2179.9	**0**	2179.3
4th	4266.5	**0**	4270.5	**0.1**	4266.5
5th	7051.3	**0**	7069	**0.3**	7051.3

In Table 5.3, CFEM and AFEM denote Conventional Finite Element Method and Advanced Finite Element Method respectively, R-R represents Rayleigh-Ritz method and TS denotes Translational Spring. In this table, the comparison of the natural frequencies obtained using advanced and conventional finite element formulations is done with respect to the results obtained using Rayleigh-Ritz method [48]. Excellent agreement has been observed. As it can be seen, the results determined using advanced finite element formulation are slightly more accurate than the results determined using conventional finite element formulation.

Uniform laminated composite beams are considered with a) free-translational spring, b) simply supported-translational spring, c) clamped-translational spring, d) clamped-rotational spring, and e) free-rotational spring boundary conditions as shown in Figure 5.3. These beams are made of 12 plies of NCT-301 graphite-epoxy prepreg and have 25 cm length and 1.5 cm width and the total thickness is 1.5 mm. The laminate

configuration is $[0/90]_{3s}$. The stiffness of the translational springs is equal to 47.24 N/m and the stiffness of the rotational springs is equal to 50 N.m/rad.

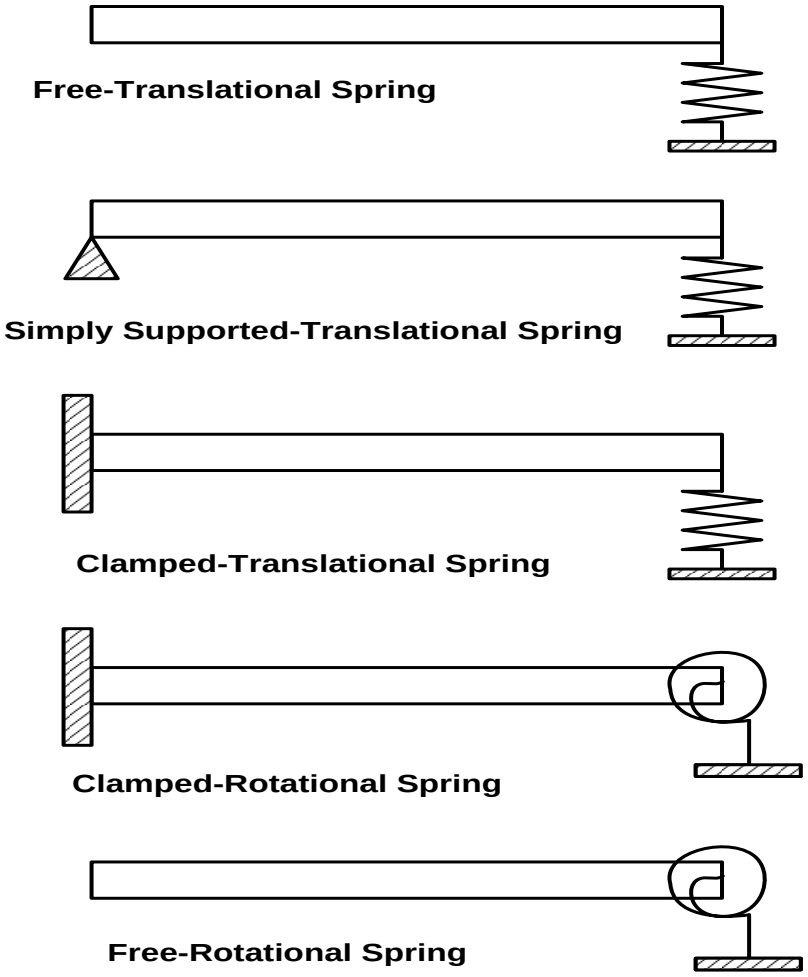

Figure 5.3: Uniform laminated composite beam with a) free-translational spring, b) simply supported-translational spring, c) clamped-translational spring, d) clamped-rotational spring, and e) free-rotational spring boundary conditions

The first four natural frequencies of the beams are considered. The results determined using conventional finite element formulation are compared with the results obtained using Rayleigh-Ritz method [48] and shown in Table 5.4.

Table 5.4: First four natural frequencies of uniform laminated composite beams with free-translational spring, simply supported-translational spring, clamped-translational spring, clamped-rotational spring and free-rotational spring boundary conditions obtained using conventional finite element formulation and Rayleigh-Ritz method

Modes	Free-TS		**Percentage Error**
	R-R	CFEM	
1^{st}	110.3	110.3	**0**
2^{nd}	822.6	822.6	**0**
3^{rd}	2248.9	2249.5	**0**
4^{th}	4404.8	4408.9	**0.1**
Modes	Simply Supported-TS		**Percentage Error**
	R-R	CFEM	
1^{st}	94.5	94.5	**0**
2^{nd}	572.8	572.8	**0**
3^{rd}	1823.2	1823.5	**0**
4^{th}	3798.4	3801.1	**0.1**
Modes	Clamped-TS		**Percentage Error**
	R-R	CFEM	
1^{st}	169	169	**0**
2^{nd}	810.3	810.4	**0**
3^{rd}	2249.8	2250.4	**0**
4^{th}	4404.7	4409	**0.1**
Modes	Clamped-RS		**Percentage Error**
	R-R	CFEM	
1^{st}	200.1	200.1	**0**
2^{nd}	1075.1	1075.1	**0**
3^{rd}	2657.8	2658.8	**0**
4^{th}	4946.2	4952.3	**0.1**
Modes	Free-RS		**Percentage Error**
	R-R	CFEM	
1^{st}	197.5	197.5	**0**
2^{nd}	1075.7	1075.8	**0**
3^{rd}	2657.8	2658.7	**0**
4^{th}	4946.3	4952.1	**0.1**

In the Table 5.4, RS denotes Rotational Spring. In this table, the comparison of the natural frequencies obtained using conventional finite element formulation is done with respect to the results obtained using Rayleigh-Ritz method [48]. Excellent agreement has been observed.

A uniform composite beam is considered clamped at one end with a translational spring at the other end as shown in Figure 5.1. This beam is made of 36 plies of NCT-301 graphite-epoxy prepreg and has the length of 25 cm, the width of 1.5 cm and the thickness of 4.5 mm. The laminate configuration is $[0/90]_{9s}$. The stiffness of the translational spring varies from zero to 400 KN/m which is considered to be a very stiff translational spring and is expected to behave similar to a simply supported boundary condition. First three natural frequencies of the beam are determined when the stiffness of the spring increases. It can be predicted that a natural frequency of a clamped-translational spring uniform beam lies between the natural frequencies of the same mode of a similar uniform beam with clamped-free and clamped-simply supported boundary conditions. These results are shown in Figure 5.4.

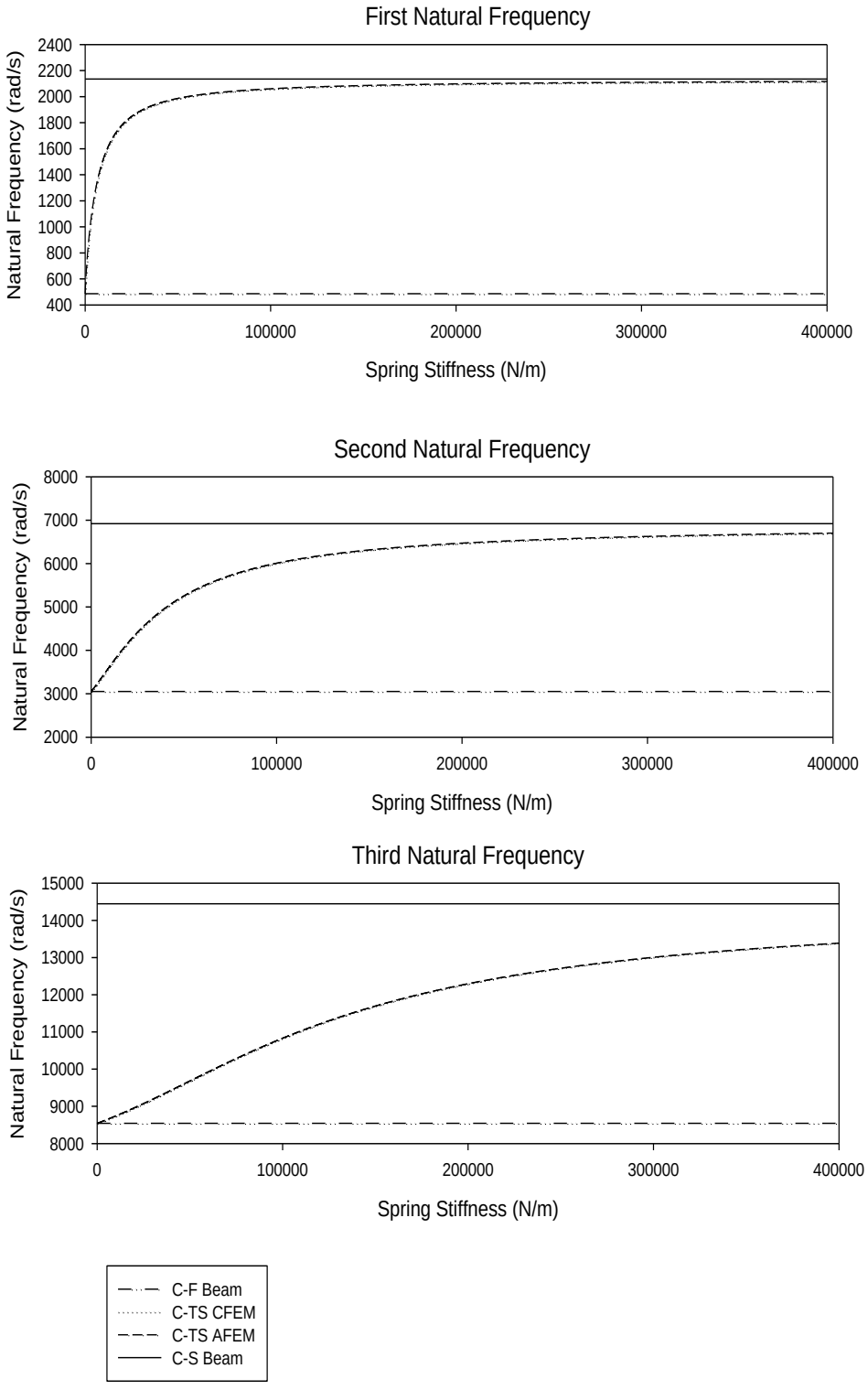

Figure 5.4: First three natural frequencies of a uniform clamped-free beam and a uniform clamped-simply supported beam and a uniform clamped-translational spring beam when the stiffness of the spring increases from zero to 400 KN/m

As it can be observed from Figure 5.4, the results determined using advanced and conventional finite element formulations match perfectly. It can also be concluded that as the stiffness of the translational spring increases, the beam will behave more likely as a clamped-simply supported beam.

A uniform clamped-simply supported composite beam is considered. A rotational spring is attached to the simply supported end of the beam as shown in Figure 5.5.

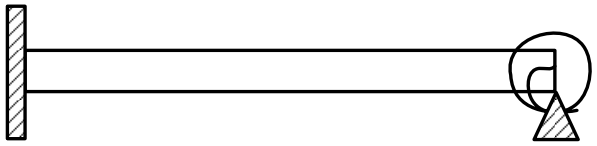

Figure 5.5: Clamped-simply supported uniform beam with a rotational spring attached to the simply supported end of the beam

This beam is made of 36 plies of NCT-301 graphite-epoxy prepreg and has the length of 25 cm, the width of 1.5 cm and the thickness of 4.5 mm. The laminate configuration is $[0/90]_{9s}$. The stiffness of the rotational spring varies from zero to 10 KN.m/rad which is a very stiff rotational spring and in this case is expected to behave similar to a clamped boundary condition. First three natural frequencies of the beam are determined when the stiffness of the spring increases. It can be predicted that a natural frequency of this uniform beam lies between the natural frequencies of the same mode of a similar uniform beam with clamped-simply supported and clamped-clamped boundary conditions. These results are shown in Figure 5.6.

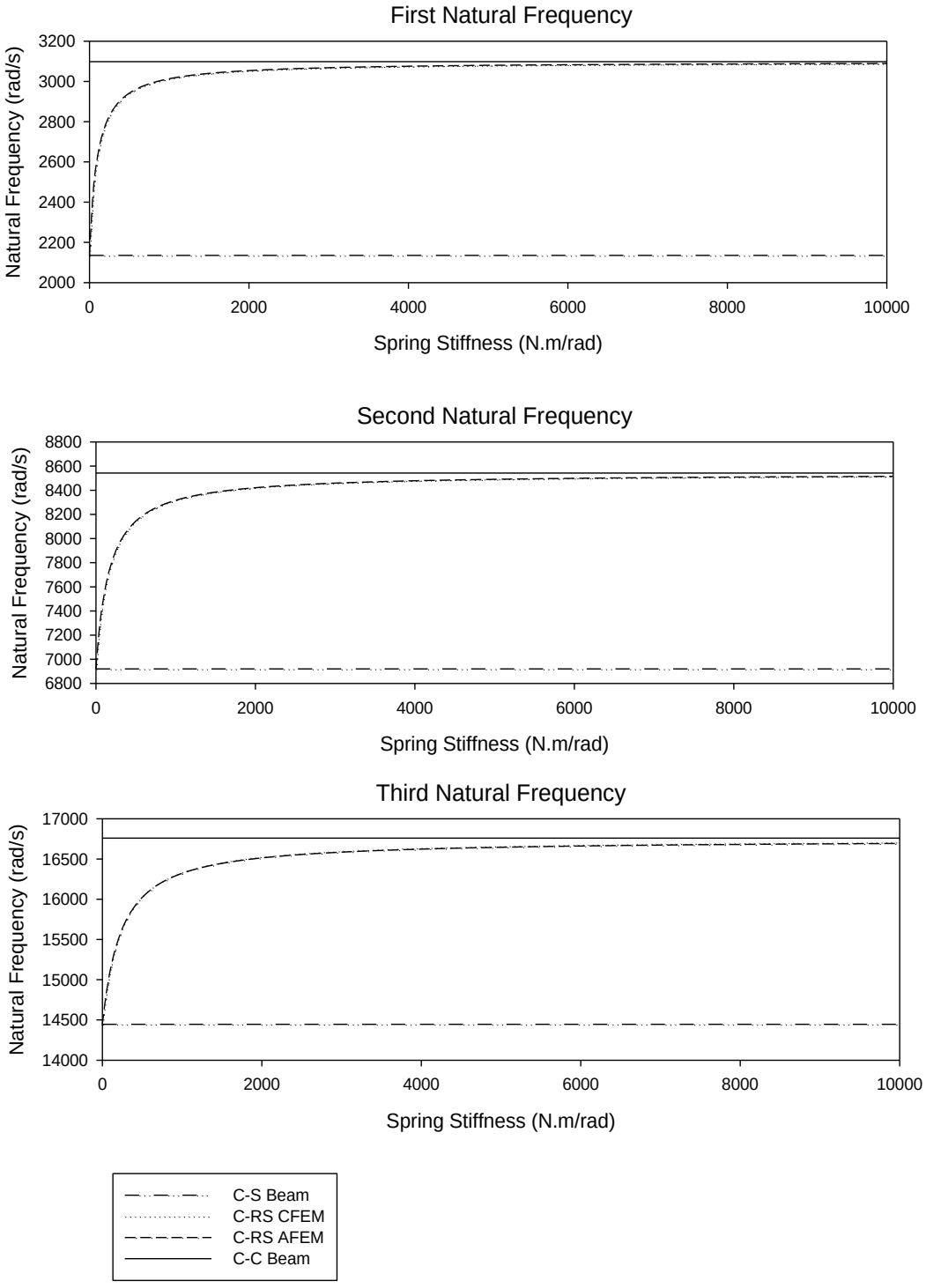

Figure 5.6: First three natural frequencies of a uniform clamped-simply supported beam and a uniform clamped-clamped beam and a uniform clamped-simply supported beam with a rotational spring attached to the simply supported end of the beam when the stiffness of the spring increases from zero to 10 KN.m/rad

As it can be observed from the Figure 5.6, the results determined using advanced and conventional finite element formulations match perfectly. It can also be concluded that as the stiffness of the rotational spring at the simply supported end of the beam increases, the beam will behave more likely as a clamped-clamped beam.

5.3.2. Thickness-tapered width-tapered composite beams

Natural frequency of a thickness-tapered width-tapered composite beam for each mode should be between the natural frequency of that mode of uniform-thickness width-tapered beams with number of plies equal to the number of plies at the thick section and at the thin section of the thickness-tapered beam. Uniform-thickness width-tapered beams considered here should have the similar material properties, boundary condition, length, width, width-ratio and ply orientations as those of the thickness-tapered width-tapered beam.

Thickness-tapered width-tapered beams are considered with a) clamped-translational spring and b) clamped-rotational spring boundary conditions. These beams are made of 20 plies at the thick section and 16 plies at the thin section and are made of NCT-301 graphite-epoxy prepreg as shown in Figure 5.7. Length of these beams is equal to 25 cm, their width is equal to 1.5 cm at the left end, their width-ratio is equal to 0.5 and the laminate configuration at the thick section is $[0/90]_{5s}$. The thickness of the beam is equal to 4.5 mm at the thick section and 1.5 mm at the thin section.

First three natural frequencies of the beams are considered. Obtained natural frequencies for each boundary condition of these thickness-tapered width-tapered beams should lie between the natural frequencies of a uniform-thickness width-tapered beam

with 20 plies and a uniform-thickness width-tapered beam with 16 plies with the same boundary condition as that of the considered thickness-tapered width-tapered beam.

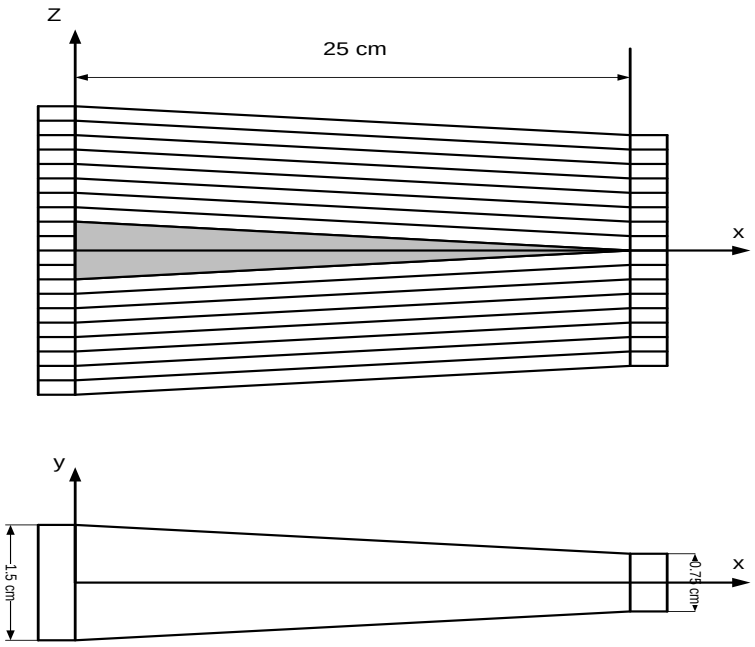

Figure 5.7: Thickness-tapered width-tapered beam, 20-16 plies

The first three natural frequencies of the clamped-translational spring beams are determined when the stiffness of the spring increases from 0 to 10 KN/m and are shown in Figure 5.8. The first three natural frequencies of the clamped-rotational spring beams are determined when the stiffness of the spring increases from 0 to 500 N.m/rad and are shown in Figure 5.9. These results are determined for a) a uniform-thickness width-tapered beam having 16 plies with $[0/90]_{4s}$ laminate configuration, b) a uniform-thickness width-tapered beam having 20 plies with $[0/90]_{5s}$ laminate configuration, and c) a thickness-tapered width-tapered beam made of 20 plies at the thick section and 16 plies at the thin section with $[0/90]_{5s}$ laminate configuration at the thick section.

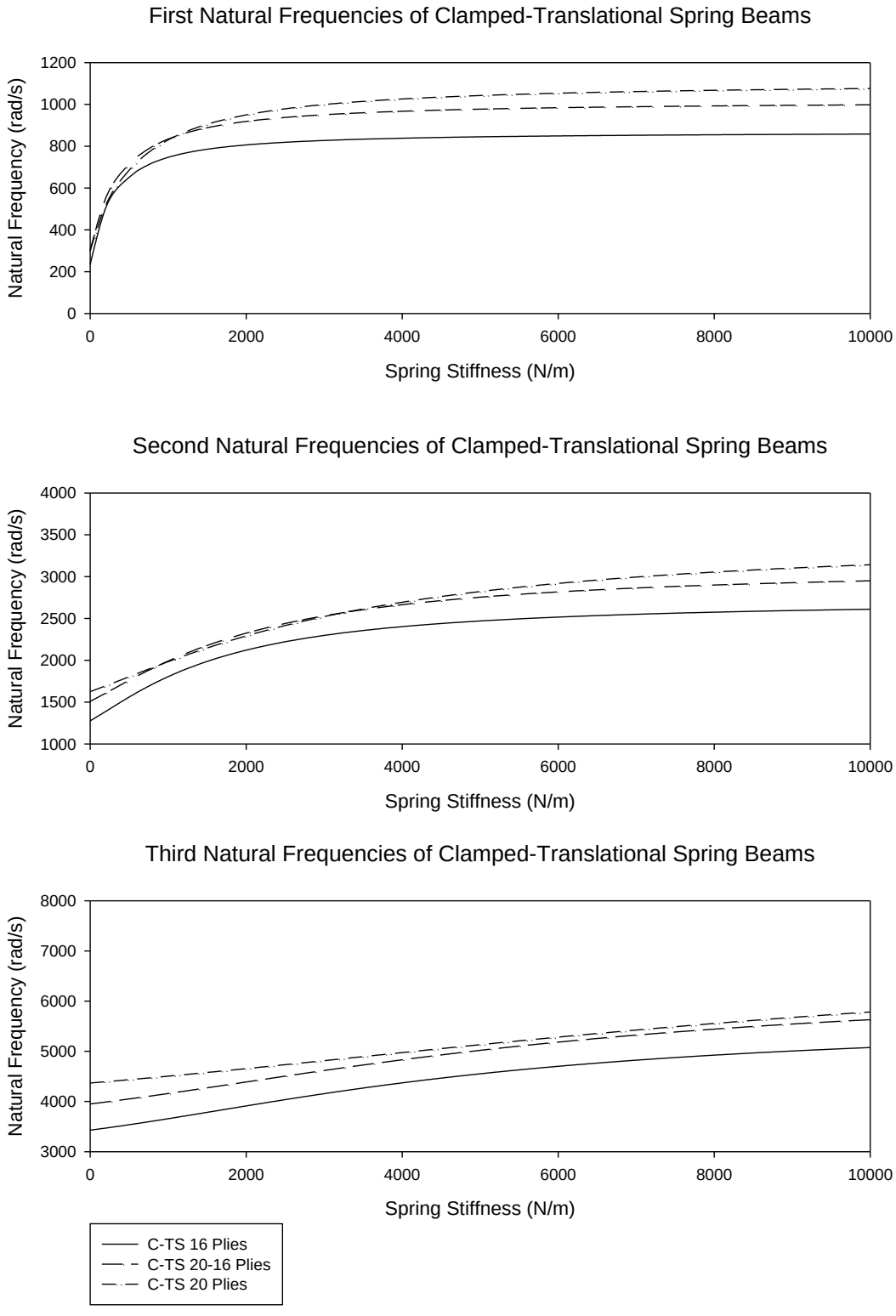

Figure 5.8: First three natural frequencies of uniform-thickness width-tapered beams with 16 and 20 plies and a 20-16 plies thickness-tapered width-tapered beam with clamped-translational spring boundary condition

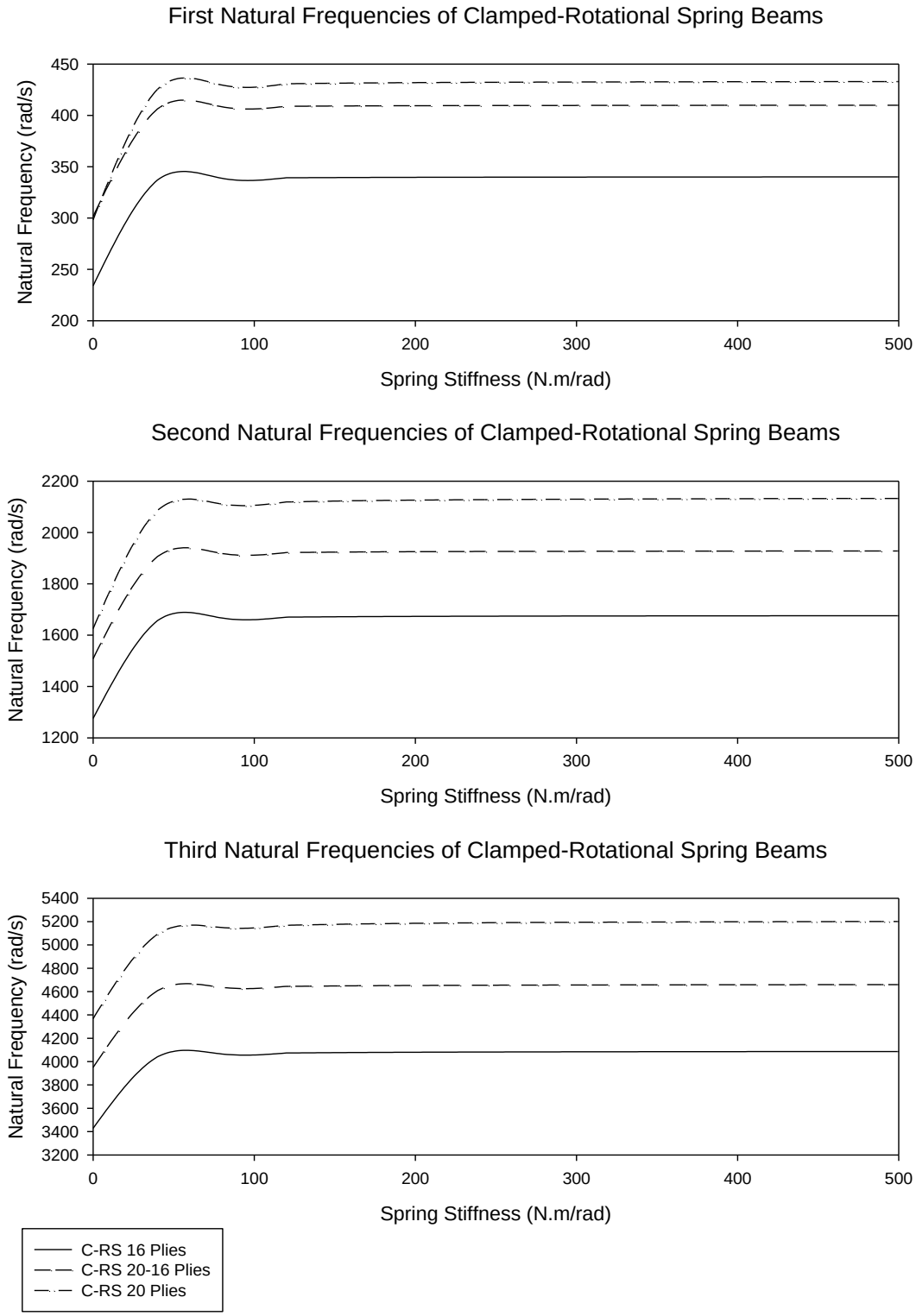

Figure 5.9: First three natural frequencies of uniform-thickness width-tapered beams with 16 and 20 plies and a 20-16 plies thickness-tapered width-tapered beam with clamped-rotational spring boundary condition

As expected and illustrated in Figures 5.8 and 5.9, the natural frequencies of the thickness-tapered width-tapered beam with clamped-translational spring and clamped-rotational spring boundary conditions lie between the natural frequencies of uniform-thickness width-tapered beams with 16 plies and 20 plies having similar boundary conditions. Except in the case of fundamental natural frequencies of the beams with clamped-translational spring boundary condition, in which, when the stiffness of the translational spring is low, the decrease in weight at the right end of the thickness-tapered width-tapered beam will cause it to have higher fundamental natural frequency than the uniform-thickness width-tapered beam with 20 plies. These results are determined using conventional finite element formulation. Ten elements are used to determine the natural frequencies of these beams and the length of each element is equal to 2.5 cm.

Thickness-tapered width-tapered beams are considered with clamped-translational spring boundary condition. Width-ratio of these beams is equal to 0.5 and their length is equal to 25 cm. The beams are made of configurations A, B, C and D. These beams are made of 36 plies at the thick section and 12 plies at the thin section and are made of NCT-301 graphite-epoxy prepreg as shown in Figure 2.13. The laminate configuration at the thick section is $[0/90]_{9s}$. Width is equal to 1.5 cm at the left end and 0.75 cm at the right end**.** The first three natural frequencies of the beams are to be determined when the stiffness of the spring increases from 0 to 50 KN/m. It can be predicted that a natural frequency of a clamped-translational spring beam lies between the natural frequencies of the same mode of a similar beam with clamped-free and clamped-simply supported boundary conditions. These results are shown in Figures 5.10 and 5.11.

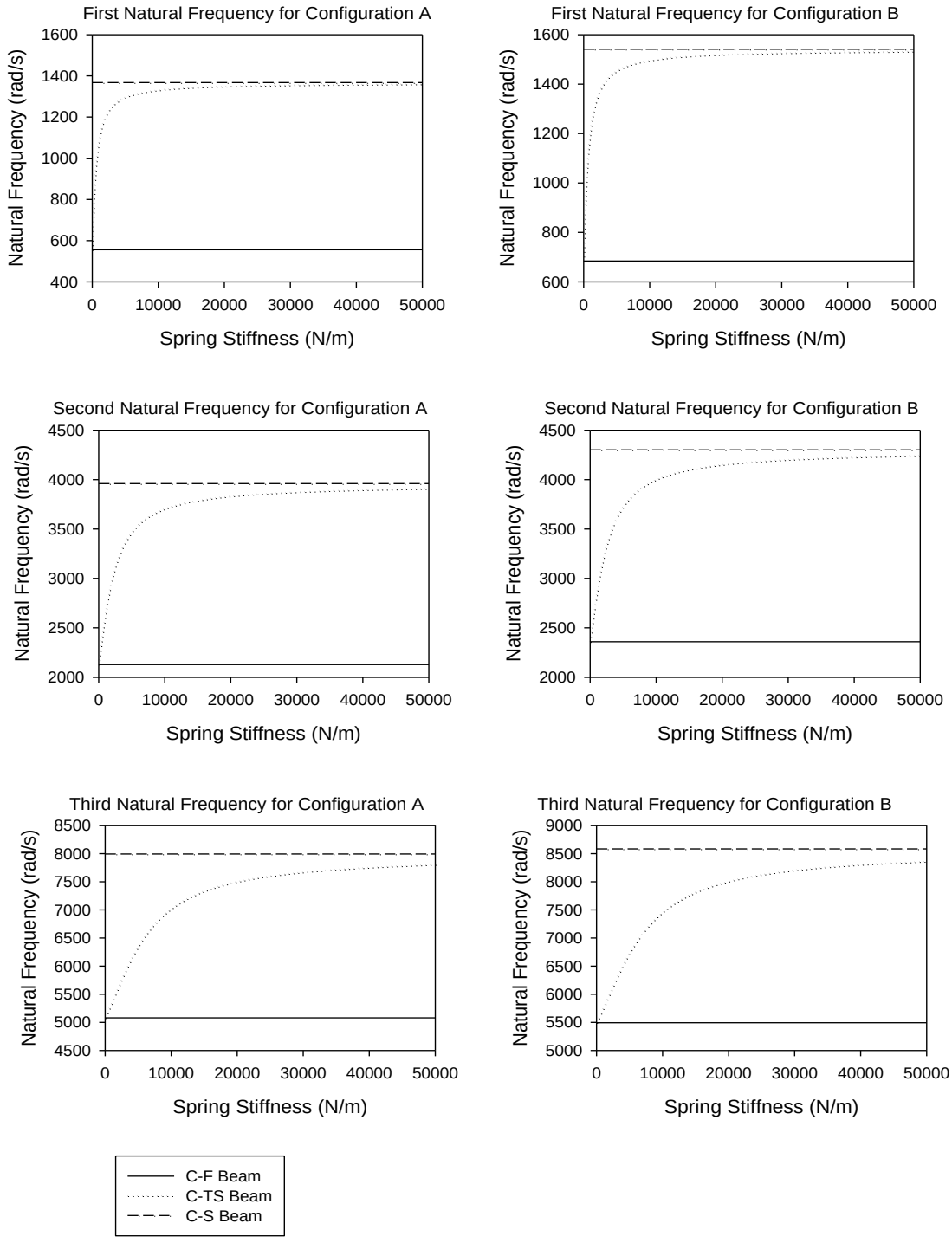

Figure 5.10: First three natural frequencies of thickness-tapered width-tapered laminated composite beams with clamped-free, clamped-simply supported and clamped-translational spring boundary conditions made of configurations A and B

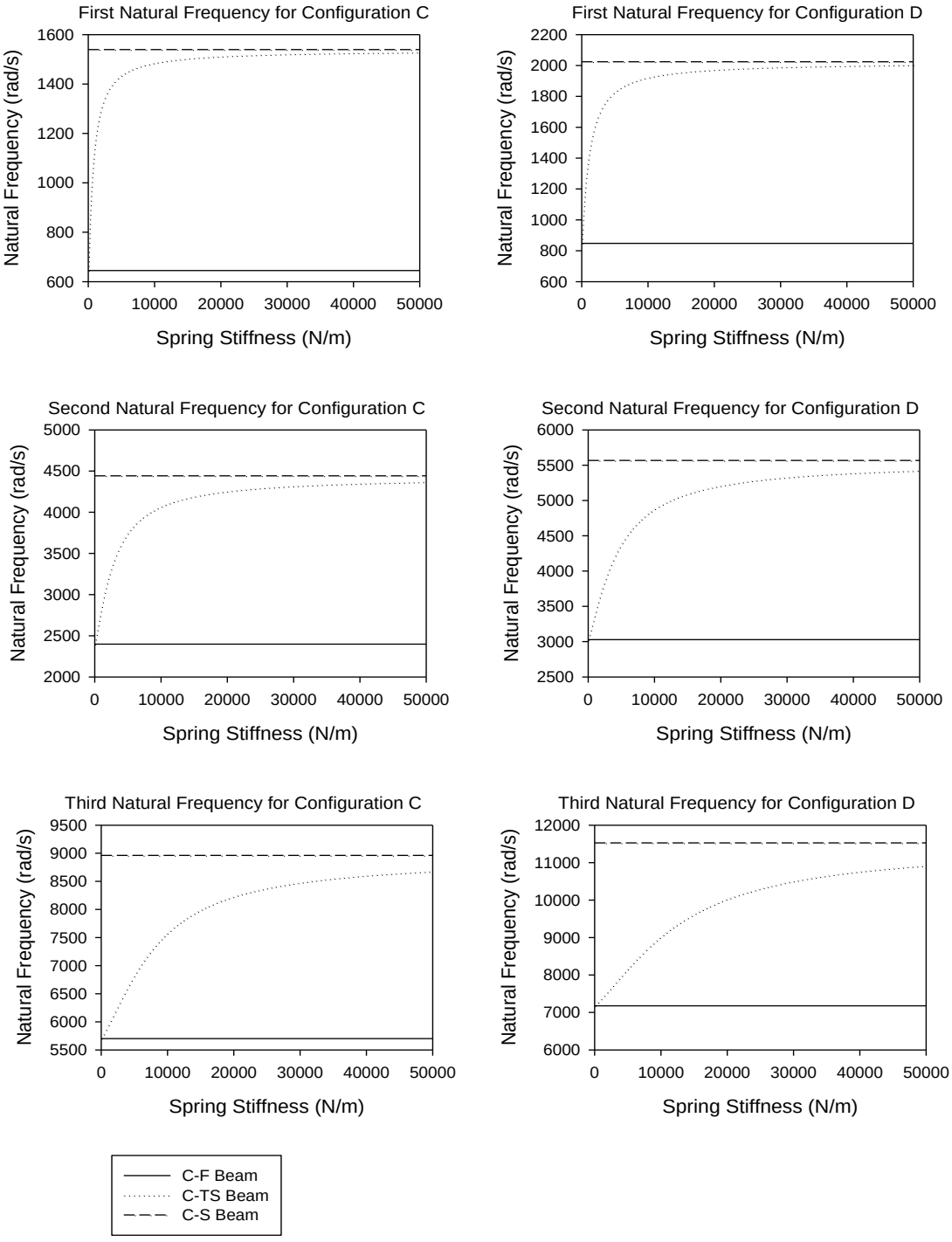

Figure 5.11: First three natural frequencies of thickness-tapered width-tapered laminated composite beams with clamped-free, clamped-simply supported and clamped-translational spring boundary conditions made of configurations C and D

As illustrated in Figures 5.10 and 5.11, for all the thickness-tapered configurations the natural frequencies of a clamped-translational spring beam lies between the natural frequencies of the similar beams with clamped-free and clamped-simply supported boundary conditions.

Thickness-tapered width-tapered beams are considered which are clamped at the left end and are supported with a translational spring and a rotational spring at the other end. Width ratio of these beams is equal to 0.5 and their length is equal to 25 cm. The beams are made of configurations A, B, C and D. These beams are made of 36 plies at the thick section and 12 plies at the thin section and are made of NCT-301 graphite-epoxy prepreg as shown in Figure 2.13. The laminate configuration at the thick section is $[0/90]_{9s}$. Width is equal to 1.5 cm at the left end and 0.75 cm at the right end**.** The first three natural frequencies of these beams are to be determined. The translational spring is 200 KN/m stiff while the stiffness of the rotational spring increases from 0 to 500 N.m/rad. It can be predicted that a natural frequency of any of these beams lies between the natural frequencies of the same mode of a similar beam with clamped-simply supported and clamped-clamped boundary conditions since the translational spring is stiff enough to behave like a simply supported boundary condition. These results are shown in Figures 5.12 and 5.13.

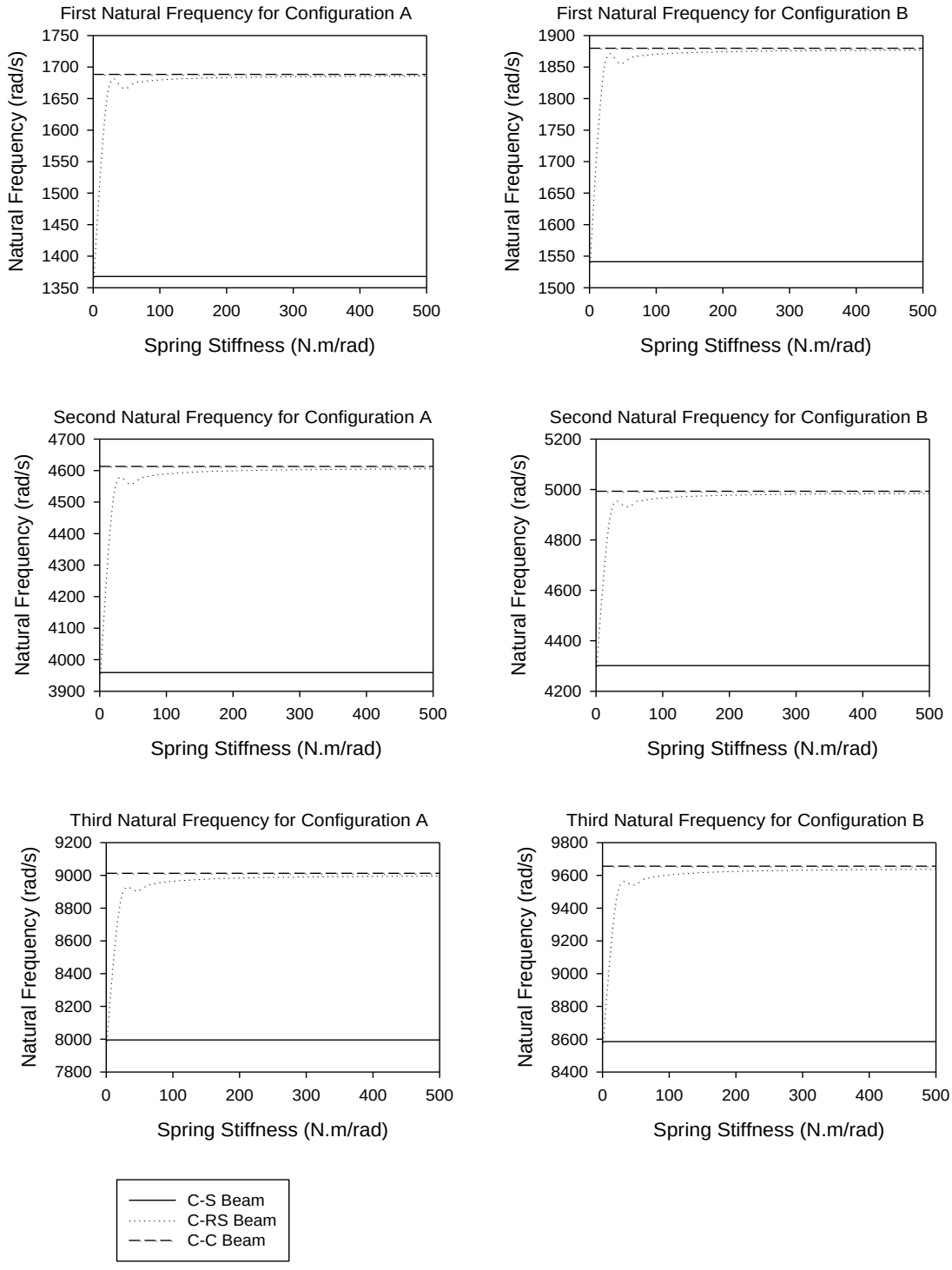

Figure 5.12: First three natural frequencies of thickness-tapered width-tapered laminated composite beams with clamped-simply supported, clamped-clamped and clamped-translational and rotational springs boundary conditions made of configurations A and B

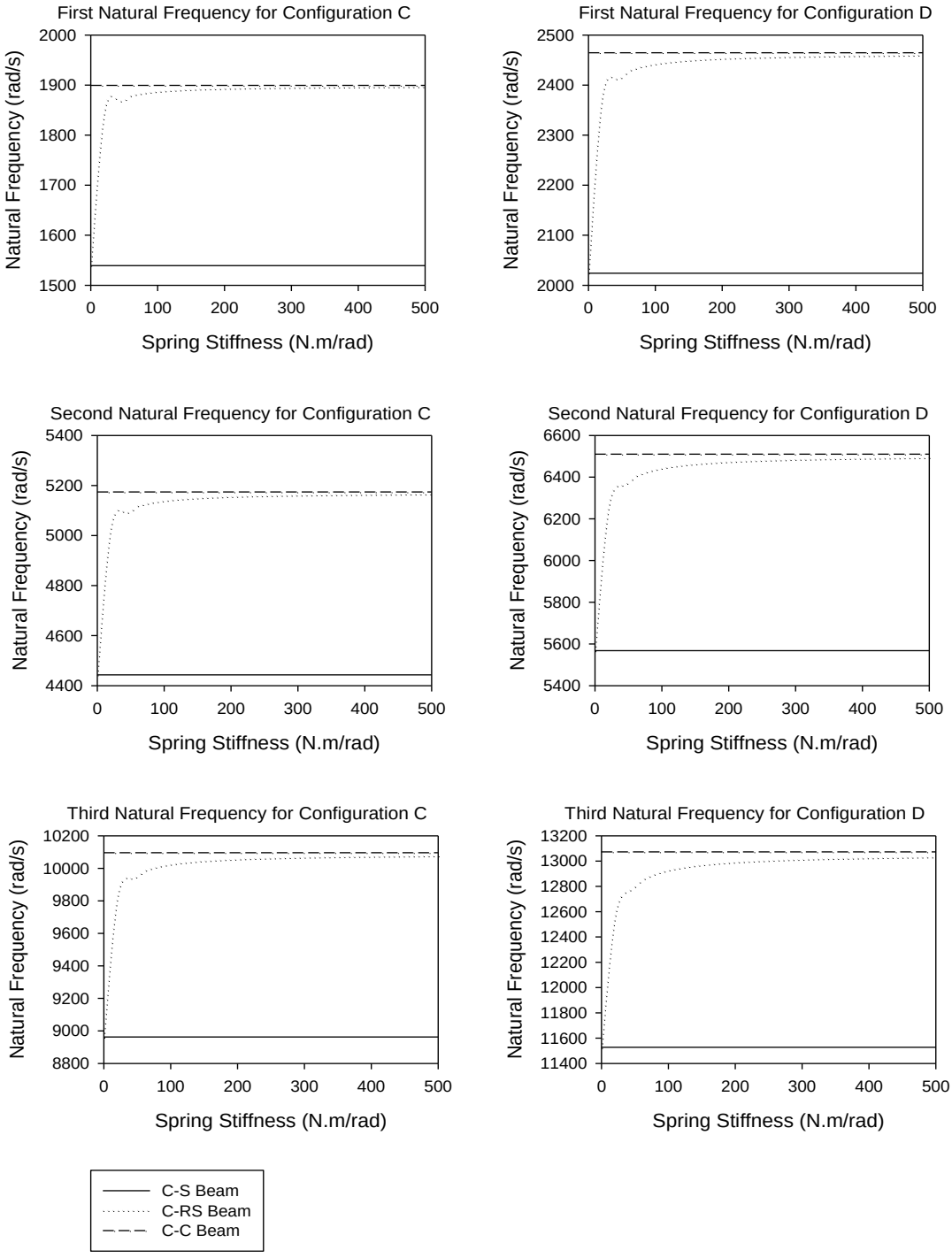

Figure 5.13: First three natural frequencies of thickness-tapered width-tapered laminated composite beams with clamped-simply supported, clamped-clamped and clamped-translational and rotational springs boundary conditions made of configurations C and D

As illustrated in Figures 5.12 and 5.13, for all the thickness-tapered configurations the natural frequencies of a clamped-translational and rotational springs beam when the stiffness of the translational spring is high enough to behave like a simply supported boundary condition, lies between the natural frequencies of the similar beams with clamped-simply supported and clamped-clamped boundary conditions.

Thickness-tapered width-tapered beams are considered with clamped-free and clamped-translational spring boundary conditions. Three width-ratios are considered for these beams (0.2, 0.5 and 0.8) and their length is equal to 25 cm. The beams are made of configurations A, B, C and D. These beams are made of 36 plies at the thick section and 12 plies at the thin section and are made of NCT-301 graphite-epoxy prepreg as shown in Figure 2.13. The laminate configuration at the thick section is $[0/90]_{9s}$. Width is equal to 1.5 cm at the left end**.** The fundamental natural frequency of the beams is to be determined. Clamped-free, clamped-translational spring with 5 KN/m stiffness and clamped-translational spring with 15 KN/m stiffness beams are considered. The results are given in Table 5.5.

Table 5.5: Natural frequencies of clamped-free and clamped-translational spring thickness-tapered width-tapered beams

Clamped-Translational Spring	Configuration A			Configuration B			Configuration C			Configuration D		
Width-Ratio	0.2	0.5	0.8	0.2	0.5	0.8	0.2	0.5	0.8	0.2	0.5	0.8
Spring-Stiffness (KN/m)=0	683	556	491	836	684	609	789	645	571	1037	848	752
Spring-Stiffness (KN/m)=5	1374	1296	1231	1561	1453	1368	1534	1435	1353	1990	1829	1698
Natural Frequency Ratio	**2.01**	**2.33**	**2.51**	**1.87**	**2.12**	**2.25**	**1.94**	**2.23**	**2.37**	**1.92**	**2.16**	**2.26**
Spring-Stiffness (KN/m)=15	1402	1343	1295	1594	1511	1446	1574	1503	1444	2067	1955	1864
Natural Frequency Ratio	**2.05**	**2.42**	**2.64**	**1.91**	**2.21**	**2.38**	**2.00**	**2.33**	**2.53**	**1.99**	**2.31**	**2.48**

In Table 5.5 the Natural Frequency Ratio denotes the ratio of the fundamental natural frequency of the specific clamped-translational spring beam to that of the clamped-free beam.

As it can be observed from Table 5.5, as the width-ratio of a beam increases, its fundamental natural frequency will decrease due to the weight increase at the free end of the beam which is a common fact for the beams with both the clamped-free and the clamped-translational spring boundary conditions. It can also be concluded that when the stiffness of the spring is equal to 5 KN/m, the fundamental natural frequency approximately doubles up, while when the stiffness of the spring is increased to 15 KN/m although the fundamental natural frequency of the beam increases, the change in the fundamental natural frequency is not very significant. It can also be concluded from the natural frequency ratios of the beams with different width-ratios that as the width-ratio of a beam increases, the natural frequency ratio of the beam increases and consequently the beam becomes more sensitive in terms of the natural frequency to the attached spring, this fact is more significant as the stiffness of the spring increases.

Thickness-tapered width-tapered beams are considered with clamped-free and clamped-rotational spring boundary conditions. Three width-ratios are considered for these beams (0.2, 0.5 and 0.8) and their length is equal to 25 cm. The beams are made of configurations A, B, C and D. These beams are made of 36 plies at the thick section and 12 plies at the thin section and are made of NCT-301 graphite-epoxy prepreg as shown in Figure 2.13. The laminate configuration at the thick section is $[0/90]_{9s}$. Width is equal to 1.5 cm at the left end**.** The fundamental natural frequency of the beams is to be

determined. Clamped-free, clamped-rotational spring with 10 N.m/rad stiffness and clamped-rotational spring with 30 N.m/rad stiffness beams are considered.

Table 5.6: Natural frequencies of clamped-free and clamped-rotational spring thickness-tapered width-tapered beams

Clamped-Rotational Spring	Configuration A			Configuration B			Configuration C			Configuration D		
Width-Ratio	0.2	0.5	0.8	0.2	0.5	0.8	0.2	0.5	0.8	0.2	0.5	0.8
Spring-Stiffness (N.m/rad)=0	683	556	491	836	684	609	789	645	571	1037	848	752
Spring-Stiffness (N.m/rad)=10	743	627	563	905	764	688	858	726	653	1132	954	855
Natural Frequency Ratio	**1.09**	**1.13**	**1.15**	**1.08**	**1.12**	**1.13**	**1.09**	**1.13**	**1.14**	**1.09**	**1.13**	**1.14**
Spring-Stiffness (N.m/rad)=30	745	632	571	907	769	696	862	735	664	1140	970	877
Natural Frequency Ratio	**1.09**	**1.14**	**1.16**	**1.09**	**1.12**	**1.14**	**1.09**	**1.14**	**1.16**	**1.10**	**1.14**	**1.17**

In Table 5.6 the Natural Frequency Ratio denotes the ratio of the fundamental natural frequency of the specific clamped-rotational spring beam to that of the clamped-free beam.

As it can be observed from Table 5.6, as the width-ratio of a beam increases, its fundamental natural frequency will decrease due to the weight increase at the free end of the beam which is a common fact for the beams with both the clamped-free and the clamped-rotational spring boundary conditions. It can also be concluded that when the stiffness of the spring is equal to 10 N.m/rad, the fundamental natural frequency increases approximately by 10 percent, while when the stiffness of the spring is increased to 30 N.m/rad although the fundamental natural frequency of the beam increases, the change in the fundamental natural frequency is not significant. It can also be concluded from the natural frequency ratios of the beams with different width-ratios that as the width-ratio of

a beam increases, the natural frequency ratio of the beam increases and consequently the beam becomes more sensitive in terms of the natural frequency to the attached spring, this fact is slightly more significant as the stiffness of the spring increases.

Thickness-tapered width-tapered beams are considered with clamped-translational spring and clamped-translational and rotational springs boundary conditions. Three width-ratios are considered for these beams (0.2, 0.5 and 0.8) and their length is equal to 25 cm. The beams are made of configurations A, B, C and D. These beams are made of 36 plies at the thick section and 12 plies at the thin section and are made of NCT-301 graphite-epoxy prepreg as shown in Figure 2.13. The laminate configuration at the thick section is $[0/90]_{9s}$. Width is equal to 1.5 cm at the left end**.** The fundamental natural frequency of the beams is to be determined. The stiffness of the translational spring is constant for all the boundary conditions considered here and is equal to 50 KN/m and it is attached to the free end of all the beams while in the first considered boundary condition the beam doesn't have any rotational spring attached to it and in the second considered boundary condition, in addition to the translational spring, the beam has a rotational spring attached to its free end with the stiffness of 10 N.m/rad and in the third considered boundary condition, in addition to the translational spring, the beam has a rotational spring attached to its free end with the stiffness of 30 N.m/rad.

Table 5.7: Natural frequencies of clamped-translational spring and clamped-translational and rotational spring thickness-tapered width-tapered beams

Clamped-Translational (50 KN/m) and Rotational Springs	Configuration A			Configuration B			Configuration C			Configuration D		
Width-Ratio	0.2	0.5	0.8	0.2	0.5	0.8	0.2	0.5	0.8	0.2	0.5	0.8
Spring-Stiffness (N.m/rad)=0	1411	1360	1318	1606	1532	1476	1589	1528	1479	2095	2003	1929
Spring-Stiffness (N.m/rad)=10	1653	1611	1559	1860	1792	1723	1843	1781	1713	2382	2270	2164
Natural Frequency Ratio	**1.17**	**1.18**	**1.18**	**1.16**	**1.17**	**1.17**	**1.16**	**1.17**	**1.16**	**1.14**	**1.13**	**1.12**
Spring-Stiffness (N.m/rad)=30	1671	1647	1608	1879	1831	1776	1871	1834	1783	2428	2350	2262
Natural Frequency Ratio	**1.18**	**1.21**	**1.22**	**1.17**	**1.20**	**1.20**	**1.18**	**1.20**	**1.21**	**1.16**	**1.17**	**1.17**

In Table 5.7 the Natural Frequency Ratio denotes the ratio of the fundamental natural frequency of the specific clamped-translational and rotational springs beam to that of the clamped-translational spring beam.

As it can be observed from Table 5.7, as the width-ratio of a beam increases, its fundamental natural frequency will decrease due to the weight increase at the free end of the beam which is a common fact for the beams with both the clamped-translational spring and the clamped-translational and rotational springs boundary conditions. It can also be concluded that when the stiffness of the rotational spring is equal to 10 N.m/rad, the fundamental natural frequency increases approximately by 17 percent, while when the stiffness of the rotational spring is increased to 30 N.m/rad although the fundamental natural frequency of the beam increases, the change in the fundamental natural frequency is not significant. It can also be concluded from the natural frequency ratios of the beams with different width-ratios that as the width-ratio of a beam increases, the natural frequency ratio of the beam increases and consequently the beam becomes more sensitive

in terms of the natural frequency to the attached springs, this fact is more significant as the stiffness of the rotational spring increases. Comparing the natural frequency ratios represented in Tables 5.6 and 5.7, it can be concluded that if in addition to the rotational spring, there is a translational spring attached to the free end of a beam, the change in the natural frequency ratio of the beam as its width-ratio increases becomes less significant.

Thickness-tapered width-tapered beams are considered with clamped-rotational spring and clamped-translational and rotational springs boundary conditions. Three width-ratios are considered for these beams (0.2, 0.5 and 0.8) and their length is equal to 25 cm. The beams are made of configurations A, B, C and D. These beams are made of 36 plies at the thick section and 12 plies at the thin section and are made of NCT-301 graphite-epoxy prepreg as shown in Figure 2.13. The laminate configuration at the thick section is $[0/90]_{9s}$. Width is equal to 1.5 cm at the left end**.** The fundamental natural frequency of the beams is to be determined. The stiffness of the rotational spring is constant for all the boundary conditions considered here and is equal to 100 N.m/rad and it is attached to the free end of all the beams while in the first considered boundary condition the beam doesn't have any translational spring attached to it and in the second considered boundary condition, in addition to the rotational spring, the beam has a translational spring attached to its free end with the stiffness of 5 KN/m and in the third considered boundary condition, in addition to the rotational spring, the beam has a translational spring attached to its free end with the stiffness of 15 KN/m.

Table 5.8: Natural frequencies of clamped-rotational spring and clamped-translational and rotational spring thickness-tapered width-tapered beams

Clamped-Translational and Rotational (100 N.m/rad) Springs	Configuration A			Configuration B			Configuration C			Configuration D		
Width-Ratio	0.2	0.5	0.8	0.2	0.5	0.8	0.2	0.5	0.8	0.2	0.5	0.8
Spring-Stiffness (KN/m)=0	746	634	574	908	772	699	864	738	669	1143	977	887
Spring-Stiffness (KN/m)=5	1587	1501	1411	1776	1651	1535	1746	1625	1508	2208	1993	1813
Natural Frequency Ratio	**2.13**	**2.37**	**2.46**	**1.96**	**2.14**	**2.20**	**2.02**	**2.20**	**2.25**	**1.93**	**2.04**	**2.04**
Spring-Stiffness (KN/m)=15	1653	1618	1569	1857	1793	1724	1844	1791	1725	2380	2272	2157
Natural Frequency Ratio	**2.22**	**2.55**	**2.73**	**2.04**	**2.32**	**2.47**	**2.14**	**2.43**	**2.58**	**2.08**	**2.32**	**2.43**

In Table 5.8 the Natural Frequency Ratio denotes the ratio of the fundamental natural frequency of the specific clamped-translational and rotational springs beam to that of the clamped-rotational spring beam.

As it can be observed from Table 5.8, as the width-ratio of a beam increases, its fundamental natural frequency will decrease due to the weight increase at the free end of the beam which is a common fact for the beams with both the clamped-rotational spring and the clamped-translational and rotational springs boundary conditions. It can also be concluded that when the stiffness of the translational spring is equal to 5 KN/m, the fundamental natural frequency increases approximately by 110 percent, while when the stiffness of the translational spring is increased to 15 KN/m although the fundamental natural frequency of the beam increases, the change in the fundamental natural frequency is not as significant. It can also be concluded from the natural frequency ratios of the beams with different width-ratios that as the width-ratio of a beam increases, the natural frequency ratio of the beam increases and consequently the beam becomes more sensitive

in terms of the natural frequency to the attached springs, this fact is more significant as the stiffness of the translational spring increases. Comparing the natural frequency ratios represented in Tables 5.5 and 5.8, it can be concluded that if in addition to the translational spring, there is a rotational spring attached to the free end of a beam, the change in the natural frequency ratio of the beam as its width-ratio increases is almost equally significant.

5.4. Discussion and conclusion

In this chapter, free vibration analysis of variable-thickness variable-width laminated composite beams with elastic supports has been carried out. Translational and rotational springs were used to model elastic supports. The analysis started with uniform isotropic beams having a combination of elastic and rigid supports, the results were obtained using conventional and advanced finite element formulations and were compared and validated with the existing results. Then the free vibration of uniform laminated composite beams with different combinations of elastic and rigid supports were studied and the results were compared and validated with the results obtained using Rayleigh-Ritz method. Then the free vibration of variable-thickness variable-width laminated composite beams with elastic supports were studied. It is illustrated that the natural frequencies of a thickness-tapered width-tapered beam with an elastic boundary condition lies between the natural frequencies of uniform-thickness width-tapered beams with number of plies equal to the number of plies at the thick section and at the thin section of the thickness-tapered width-tapered beam having similar boundary conditions.

Natural frequencies of different beams with clamped-translational spring boundary condition were determined when the stiffness of the spring changes from zero

(clamped-free beam) to considerably very high value. It is shown that a highly stiff translational spring attached to the free end of the beam behaves almost as a simply supported boundary condition with respect to the free vibration of the beams. Then the natural frequencies of different beams with clamped-translational and rotational springs boundary condition were determined when the stiffness of the rotational spring changes from zero to a very high value and the stiffness of the translational spring is very high. It is shown that a support made of highly stiff translational and rotational springs behaves almost as a clamped boundary condition with respect to the free vibration of the beams.

Chapter-6

Conclusions and recommendations

6.1. Major contributions

In the present thesis, free and forced vibration analysis of symmetric variable-thickness variable-width laminated composite beams has been carried out using advanced and conventional finite element formulations. These formulations have been developed based on Kirchhoff one dimensional laminated beam theory. The free and forced vibrations of i) uniform, ii) uniform-thickness width-tapered, iii) uniform-width thickness-tapered and iv) thickness-tapered width-tapered laminated composite beams have been studied. Four degrees of freedom per node (deflection, rotation, curvature and the gradient of curvature) and two nodes per element are considered for the advanced finite element formulation and two degrees of freedom per node (deflection and rotation) and two nodes per element are considered for the conventional finite element formulation. Numerical and symbolic computations have been performed using MATLAB® software. The efficiency and the accuracy of the formulations used are established very systematically. A comprehensive parametric study is conducted in order to study the effects of various material, geometric and structural properties on the free and the forced vibrations of the beams. Four different thickness-tapering configurations (configurations A, B, C and D) and numerous values for the width-ratio of the beams were considered in the analysis. Different boundary conditions modeled by rigid and elastic supports were considered in the free vibration analysis of the beams. Undamped

and damped forced vibration response of the beams have been determined. In order to take into account the effect of damping in the forced vibration analysis of the beams, Rayleigh damping method is used to model the viscous damping of the beams. The material chosen in this study is NCT-301 graphite-epoxy prepreg which is available in the laboratory of Concordia Centre for Composites (CONCOM).

6.2. Conclusions

The most important and principal conclusions of this study are given in the following:

a) In the second and the third chapters of the present thesis, free vibrations of the composite beams were studied using conventional and advanced finite element formulations. It was shown that in order to obtain accurate results using conventional finite element method compared to advanced finite element method, large number of elements is required. The effects of the number of elements on the accuracy of the results, the thickness-tapering configurations on the free vibration, the ply orientations on the natural frequencies and the thickness-tapering angle and the width-ratio on the natural frequencies of the simply supported, clamped-free and clamped-clamped variable-thickness variable-width laminated composite beams were studied. Comparing the results obtained using conventional and advanced finite element formulations, it can be concluded that the accuracy can be obtained more efficiently and rapidly by increasing the number of degrees of freedom in the element rather than increasing the number of elements.

b) In the fourth chapter of this thesis, forced vibration response of the variable-thickness variable-width laminated composite beams was studied using modal analysis.

Undamped and damped systems were considered. The effects of the thickness-tapering configurations, the thickness-tapering angle and the width-ratio on the forced vibration response of the simply supported, clamped-free and clamped-clamped undamped and damped variable-thickness variable-width laminated composite beams were studied in this chapter. It can be concluded that, considering the effect of damping in the forced vibration analysis of a beam has a large effect on reducing the deflection of the response point, especially when the frequency of vibration is close to the natural frequencies of the beam (near resonances). The determined results were compared and validated with the existing results obtained using Rayleigh-Ritz method. It can be seen that although the comparison of the obtained results with the existing results shows excellent accuracy for both the undamped and the damped systems, the results determined for the damped systems provide slightly better accuracy, especially near resonances.

c) In the fifth chapter, free vibrations of variable-thickness variable-width laminated composite beams with elastic supports were studied using advanced and conventional finite element formulations. Elastic supports were modeled using translational and rotational springs. Various combinations of rigid and elastic supports were considered. The effects of the stiffness of the translational and rotational springs on the free vibrations of different variable-thickness variable-width laminated composite beams were studied. It can be observed from the free vibration analysis of the beams with rigid boundary conditions that, beams with clamped-clamped boundary condition have the highest natural frequencies and are the stiffest beams, beams with simply supported boundary conditions have the second highest natural frequencies and clamped-free beams are the least stiff beams among all the considered rigid boundary conditions. It can be

illustrated from the results obtained for the beams with elastic boundary conditions that a support made of a highly stiff translational spring behaves almost as a simply supported boundary condition and a support made of highly stiff translational and rotational springs behaves almost as a clamped boundary condition with respect to the free vibration of the beams.

d) Based on the results obtained, configuration D has the highest natural frequencies and is the most stiff configuration, configuration C and configuration B have the second highest and the third highest natural frequencies respectively. Configuration A has the lowest natural frequencies and is the least stiff configuration among all the considered configurations.

e) It can be illustrated that as the width-ratio of the beam increases, the natural frequencies of the simply supported and the clamped-clamped beams will increase while the natural frequencies of the clamped-free beams will decrease which is due to the increase in the weight of the beam at its free end.

f) As it can be understood from the forced vibration response of the simply supported, clamped-free and clamped-clamped variable-thickness variable-width laminated composite beams: i) a clamped-clamped beam has the lowest amplitudes of deflection while a clamped-free beam has the highest amplitudes of deflection, ii) as the width-ratio of a beam increases, its amplitude of deflection will decrease, except in the case of a clamped-free beam in which as the width-ratio increases, the weight at the free end of the beam will increase and will cause higher amplitude of deflection and iii) configuration A has the highest amplitudes of deflection, then configurations B and C

have the second and the third highest amplitudes of deflection respectively and configuration D has the lowest amplitudes of deflection.

g) It is shown that configuration D is the stiffest configuration considered in this study. The size and the location of resin pockets and how they are separated have a large effect on the stiffness of the beams. In configuration D, large resin pockets are separated with a bended continues composite ply which increases the stiffness of this configuration whereas in the other configurations composite plies are dropped somehow that there does not exist any continues ply between the resin pockets.

BIBLIOGRAHY

[1] O. Ochoa and J.N. Reddy, Finite Element Analysis of Composite Laminates, Boston: Kluwer Academic Publishers, 1992.

[2] N. R. C. Committee on High-Performance Structural Fibers for Advanced Polymer Matrix Composites, High-Performance Structural Fibers for Advanced Polymer Matrix Composites, Washington, D.C.: The National Academic Press, 2005.

[3] Bhese, "Strategy Composite Materials & Structures," [Online].

[4] H. Eftakher, "Free and Forced Vibrations of Tapered Composite Beams Including the Effects of Axial Force and Damping," Montreal, 2008.

[5] J. Reddy, An Introduction to the Finite Element Method, 3rd ed., McGraw-Hill Education, 2005.

[6] R. B. Abararcar and P. F. Cunniff, "The Vibration of Cantilever Beams of Fiber Reinforced Materials," *Journal of Composite Materials,* vol. 6, pp. 504-516, 1972.

[7] A. K. Miller and D. F. Adams, "An Analytic Means of Determining the Flexural and Torsional Resoant Frequencies of Generally Orthotropic Beams," *Journal of Sound and Vibration,* vol. 41, pp. 443-449, 1975.

[8] A. T. Chen and T. Y. Yang, "Static and Dynamic Formulation of a Symmetrically Laminated Beam Finite Element for a Microcomputer," *Journal of Composite Materials*, vol. 19, pp. 459-475, 1985.

[9] K. Chandrashekhara, K. Krishnamurthy and S. Roy, "Free Vibration of Composite Beams Including Rotary Inertia and Shear Deformation," *Journal of Composite Structures*, vol. 14, pp. 269-279, 1990.

[10] D. Hodges, A. R. Atilgan, M. V. Fulton and L. W. Rehfield, "Free-Vibration Analysis of Composite Beams," *Journal of the American Helicopter Society*, vol. 36, pp. 36-47, 1991.

[11] S. Krishnaswamy, K. Chandrashekhara and W. Z. B. Wu, "Analytical Solutions to Vibration of Generally Layered Composite Beams," *Journal of Sound and Vibration*, vol. 159, pp. 85-99, 1992.

[12] A. A. Khedeir and J. N. Reddy, "Free Vibration of Cross-Ply Laminated Beams with Arbitrary Boundary Conditions," *International Journal of Engineering*, vol. 32, pp. 1971-1980, 1994.

[13] J. R. Vinson and R. L. Sierakowski, The Behavior of Structures Composed of Composite Materials, 2nd ed., Kluwer Academic Publishers, 2002.

[14] A. Abramovich, "Shear Deformation and Rotary Inertia Effects of Vibrating Composite Beams," *Journal of Composite Structures*, vol. 20, pp. 165-173, 1992.

[15] J. N. Reddy, Mechanics of Laminated Composite Plates and Shells: Theory and Analysis, CRC Press, 2003.

[16] J. M. Bertholet, Composite Materials: Mechanical Behaviour and Stractural Analysis, New York: Springer, 1999.

[17] J. M. Whitney, Structural Analysis of Laminated Anisotropic Plates, Lancaster: Technomic Publishing Company, 1987.

[18] R. M. Jones, Mechanics of Composite Materials, Washington: Scripta Book Co., 1975.

[19] H. Abramovich and A. Livishits, "Feee Vibration of Non-Symmetric Cross-Ply Laminated Composite Beams," *Journal of Sound and Vibration,* vol. 176, pp. 596-612, 1994.

[20] H. Matsunaga, "Vibration and Buckling of Multilayered Composite Beams According to Higher Order Deformation Theories," *Journal of Sound and Vibration,* vol. 246, pp. 47-62, 2001.

[21] R. S. Rao and N. Ganesan, "Dynamic Response of Non-Uniform Composite Beams," *Journal of Sounds and Vibration,* vol. 200, pp. 563-577, 1997.

[22] S. H. Farghaly and R. M. Gadelrab, "Free Vibration of a Stepped Composite Timoshenko Cantilever Beam," *Journal of Sound and Vibration,* vol. 187, pp. 886-

896, 1995.

[23] K. He, S. V. Hoa and R. Ganesan, "The Study of Tapered Laminated Composite Structures: A Review," *Composites Science and Technology,* vol. 60, pp. 2643-2657, 2000.

[24] M. P. Singh and A. S. Abdelnassar, "Random Response of Symmetric Cross-ply Composite Beams with Arbitrary Boundary Conditions," *AIAA Journal,* vol. 30, pp. 1081-1088, 1992.

[25] K. Chandrashenkhara and K. M. Bangera, "Free Vibration of Composite Beams Using a Refined Shear Flexible Beam Element," *Journal of Computers and Structures,* vol. 43, pp. 719-727, 1992.

[26] N. Asghar, K. K. Rakesh and J. N. Reddy, "Forced Vibration of Low-Velocity Impact of Laminated Composite Plates," *Journal of Computational Mechanics,* vol. 13, pp. 360-379, 1994.

[27] M. H. Kadivar and S. R. Bohebpour, "Forced Vibration of Unsymmetrical Laminated Composite Beams Under the Action of Moving Loads," *Journal of Composites Science and Technology,* vol. 58, pp. 1675-1684, 1998.

[28] F. C. Faruk, "Free and Forced Vibrations of Non-Uniform Composite Beams," *Journal of Composite Structures,* vol. 88, pp. 413-420, 2008.

[29] O. Hasan and M. Sabuncu, "Stability Analysis of a Cantilever Composite Beam on

Elastic Supports," *Journal of Composites Science and Technology,* vol. 65, pp. 1982-1995, 2005.

[30] K. Karnovsky and O. Lebed, Formulas for Structural Dynamics: Tables, Graphs and Solutions, McGraw-Hill Professional, 2000.

[31] S. R. Marur and T. Kant, "Free Vibration Analysis of Fiber Reinforced Composite Beams Using Higher Order Theories and Finite Element Modeling," *Journal of Sounds and Vibration,* vol. 194, pp. 337-351, 1996.

[32] G. Shi and K. Y. Lam, "Finite Element Vibration Analysis of Composite Beams Based on Higher-Order Beam Theories," *Journal of Sound and Vibration,* vol. 219, pp. 707-721, 1999.

[33] M. Ganapathi, B. P. Patel and M. Touratier, "Influence of Amplitude of Vibration on Loss Factors of Laminated Composite Beams and Plates," *Journal of Sound and Vibration,* vol. 1999, pp. 730-738, 1999.

[34] M. A. Abd El-Maksoud, "Dynamic Analysis and Buckling of Variable-Thickness Laminated Composite Beams Using Conventional and Advanced Finite Element Formulations," 2000.

[35] O. C. Zienkiewics, The Finite Element Method, New York: McGraw-Hill, 1979.

[36] R. D. Cook, D. S. Malkus and M. E. Plesha, Concepts and Applications of Finite Element Analysis, New York: Wiley Publishing Company, 1989.

[37] C. W. S. To, "Higher Order Tapered Beam Finite Elements for Vibration Analysis," *Journal of Sound and Vibration,* vol. 63, pp. 33-50, 1979.

[38] R. S. Gupta and S. S. Rao, "Finite Element Eigenvalue Analysis of Tapered and Twisted Timoshenko Beams," *Journal of Sound and Vibration,* vol. 56, pp. 187-200, 1978.

[39] P. R. Heyliger and J. N. Reddy, "A Higher Order Beam Finite Element for Bending and Vibration Problems," *Journal of Sound and Vibration,* vol. 126, pp. 309-326, 1988.

[40] A. Zabihollah, "Vibration and Buckling Analysis of Tapered Composite Beams Using Conventional and Advanced Finite Element Formulations," Montreal, 2003.

[41] R. Ganesan and A. Zabihollah, "Vibration Analysis of Tapered Composite Beams Using a Higher-order Finite Element; Part I: Formulation," *Journal of Composite Structures,* vol. 77, pp. 300-318, 2007.

[42] R. Ganesan and A. Zabihollah, "Vibration Analysis of Tapered Composite Beams Using a Higher-order Finite Element; Part II: Parametric Study," *Journal of Composite Structures,* vol. 77, pp. 319-330, 2007.

[43] M. S. Nabi and N. Ganesan, "A Generalized Element for the Free Vibration Analysis of Composite Beams," *Journal of Computers and Structures,* vol. 51, pp. 607-610,

1994.

[44] L. Chen, "Free Vibration Analysis of tapered Composite Beams Using Hierarchical Finite Element Method," Montreal, 2004.

[45] K. B. Vijay, "Dynamic Response of Width- and Thickness-tapered Composite Beams Using Rayleigh-Ritz Method and Modal Testing," Montreal, 2012.

[46] "http://www.newportad.com/pdf/PL-NB-301.pdf," [Online].

[47] W. T. Thomson, Theory of Vibrations with Applications, 5th ed., Prentice Hall, 1997.

[48] N. Mantha, "Private Comunications".

APPENDIX

I- Coefficients of the stiffness matrix for width-tapered thickness-tapered laminated composite beams using advanced finite element formulation

$$k_{11} = \sum_{k=1}^{n} 70Hb_e(\bar{Q}_{11})_k t'_k \frac{48H^2m^2l^2 + 156H^2mcl + 156H^2c^2 + 13{t'_k}^2}{429l^3}$$

$$k_{12} = \sum_{k=1}^{n} -5Hb_e(\bar{Q}_{11})_k t'_k \frac{258H^2m^2l^2 + 936H^2mcl + 1092H^2c^2 + 91{t'_k}^2}{429l^2}$$

$$k_{13} = \sum_{k=1}^{n} H(\bar{Q}_{11})_k t'_k \frac{68H^2m^2l^2 + 208H^2mcl + 156H^2c^2 + 13{t'_k}^2}{3432(D_{11})_1}$$

$$k_{14} = \sum_{k=1}^{n} -H(\bar{Q}_{11})_k t'_k \frac{501H^2m^2l^2 + 1677H^2mcl + 1560H^2c^2 + 130{t'_k}^2}{1287l(D_{11})_1}$$

$$k_{15} = \sum_{k=1}^{n} -70Hb_e(\bar{Q}_{11})_k t_k' \frac{48H^2m^2l^2 + 156H^2mcl + 156H^2c^2 + 13{t_k'}^2}{429l^3}$$

$$k_{16} = \sum_{k=1}^{n} -5Hb_e(\bar{Q}_{11})_k t_k' \frac{414H^2m^2l^2 + 1248H^2mcl + 1092H^2c^2 + 91{t_k'}^2}{429l^2}$$

$$k_{17} = \sum_{k=1}^{n} H(\bar{Q}_{11})_k t_k' \frac{16H^2m^2l^2 + 104H^2mcl + 156H^2c^2 + 13{t_k'}^2}{3432(D_{11})_2}$$

$$k_{18} = \sum_{k=1}^{n} H(\bar{Q}_{11})_k t_k' \frac{384H^2m^2l^2 + 1443H^2mcl + 1560H^2c^2 + 130{t_k'}^2}{1287l(D_{11})_2}$$

$$k_{22} = \sum_{k=1}^{n} 10Hb_e(\bar{Q}_{11})_k t_k' \frac{144H^2m^2l^2 + 598H^2mcl + 780H^2c^2 + 65{t_k'}^2}{1001l}$$

$$k_{23} = \sum_{k=1}^{n} -Hl(\bar{Q}_{11})_k t_k' \frac{99H^2m^2l^2 + 351H^2mcl + 312H^2c^2 + 26{t_k'}^2}{9009(D_{11})_1}$$

$$k_{24} = \sum_{k=1}^{n} H(\bar{Q}_{11})_k t_k' \frac{14652H^2m^2l^2 + 56160H^2mcl + 59124H^2c^2 + 4927{t_k'}^2}{72072(D_{11})_1}$$

$$k_{25} = \sum_{k=1}^{n} 5Hb_e(\bar{Q}_{11})_k t_k' \frac{258H^2m^2l^2 + 936H^2mcl + 1092H^2c^2 + 91{t_k'}^2}{429l^2}$$

$$k_{26} = \sum_{k=1}^{n} 5Hb_e(\bar{Q}_{11})_k t_k' \frac{942H^2m^2l^2 + 2964H^2mcl + 2964H^2c^2 + 247{t_k'}^2}{3003l}$$

$$k_{27} = \sum_{k=1}^{n} -Hl(\bar{Q}_{11})_k t_k' \frac{-144H^2m^2l^2 + 780H^2c^2 + 65{t_k'}^2}{72072(D_{11})_2}$$

$$k_{28} = \sum_{k=1}^{n} -H(\bar{Q}_{11})_k t_k' \frac{3888H^2m^2l^2 + 18720H^2mcl + 28236H^2c^2 + 2353{t_k'}^2}{72072(D_{11})_2}$$

$$k_{33} = \sum_{k=1}^{n} Hl^3(\bar{Q}_{11})_k t_k' \frac{30H^2m^2l^2 + 117H^2mcl + 156H^2c^2 + 13{t_k'}^2}{270270b_e{(D_{11})_1}^2}$$

$$k_{34} = \sum_{k=1}^{n} -Hl^2(\bar{Q}_{11})_k t_k' \frac{993H^2m^2l^2 + 3900H^2mcl + 5460H^2c^2 + 455{t_k'}^2}{540540{b_e(D_{11})_1}^2}$$

$$k_{35} = \sum_{k=1}^{n} -H(\bar{Q}_{11})_k t_k' \frac{68H^2m^2l^2 + 208H^2mcl + 156H^2c^2 + 13{t_k'}^2}{3432(D_{11})_1}$$

$$k_{36} = \sum_{k=1}^{n} -Hl(\bar{Q}_{11})_k t_k' \frac{636H^2m^2l^2 + 1560H^2mcl + 780H^2c^2 + 65{t_k'}^2}{72072(D_{11})_1}$$

$$k_{37} = \sum_{k=1}^{n} -Hl^3(\bar{Q}_{11})_k t_k' \frac{50H^2m^2l^2 + 156H^2mcl + 156H^2c^2 + 13{t_k'}^2}{720720b_e(D_{11})_1(D_{11})_2}$$

$$k_{38} = \sum_{k=1}^{n} -Hl^2(\bar{Q}_{11})_k t_k' \frac{942H^2m^2l^2 + 3120H^2mcl + 3900H^2c^2 + 325{t_k'}^2}{2162160b_e(D_{11})_1(D_{11})_2}$$

$$k_{44} = \sum_{k=1}^{n} Hl(\bar{Q}_{11})_k t_k' \frac{574H^2m^2l^2 + 2340H^2mcl + 3900H^2c^2 + 325{t_k'}^2}{18018{b_e(D_{11})_1}^2}$$

$$k_{45} = \sum_{k=1}^{n} H(\bar{Q}_{11})_k t_k' \frac{501H^2m^2l^2 + 1677H^2mcl + 1560H^2c^2 + 130{t_k'}^2}{1287l(D_{11})_1}$$

$$k_{46} = \sum_{k=1}^{n} H(\bar{Q}_{11})_k t_k' \frac{13404H^2m^2l^2 + 37752H^2mcl + 28236H^2c^2 + 2353{t_k'}^2}{72072(D_{11})_1}$$

$$k_{47} = \sum_{k=1}^{n} Hl^2(\bar{Q}_{11})_k t_k' \frac{1722H^2m^2l^2 + 4680H^2mcl + 3900H^2c^2 + 325{t_k'}^2}{2162160b_e(D_{11})_1(D_{11})_2}$$

$$k_{48} = \sum_{k=1}^{n} -Hl(\bar{Q}_{11})_k t_k' \frac{-44H^2m^2l^2 + 156H^2mcl + 156H^2c^2 + 13{t_k'}^2}{72072b_e(D_{11})_1(D_{11})_2}$$

$$k_{55} = \sum_{k=1}^{n} 70Hb_e(\bar{Q}_{11})_k t_k' \frac{48H^2m^2l^2 + 156H^2mcl + 156H^2c^2 + 13{t_k'}^2}{429l^3}$$

$$k_{56} = \sum_{k=1}^{n} 5Hb_e(\bar{Q}_{11})_k t_k' \frac{414H^2m^2l^2 + 1248H^2mcl + 1092H^2c^2 + 91{t_k'}^2}{429l^2}$$

$$k_{57} = \sum_{k=1}^{n} -H(\bar{Q}_{11})_k t'_k \frac{16H^2m^2l^2 + 104H^2mcl + 156H^2c^2 + 13{t'_k}^2}{3432(D_{11})_2}$$

$$k_{58} = \sum_{k=1}^{n} -H(\bar{Q}_{11})_k t'_k \frac{384H^2m^2l^2 + 1443H^2mcl + 1560H^2c^2 + 130{t'_k}^2}{1287l(D_{11})_2}$$

$$k_{66} = \sum_{k=1}^{n} 10Hb_e(\bar{Q}_{11})_k t'_k \frac{326H^2m^2l^2 + 962H^2mcl + 780H^2c^2 + 65{t'_k}^2}{1001l}$$

$$k_{67} = \sum_{k=1}^{n} -Hlb_e(\bar{Q}_{11})_k t'_k \frac{60H^2m^2l^2 + 273H^2mcl + 312H^2c^2 + 26{t'_k}^2}{9009(D_{11})_2}$$

$$k_{68} = \sum_{k=1}^{n} -H(\bar{Q}_{11})_k t'_k \frac{17616H^2m^2l^2 + 62088H^2mcl + 59124H^2c^2 + 4927{t'_k}^2}{72072(D_{11})_2}$$

$$k_{77} = \sum_{k=1}^{n} Hl^3(\bar{Q}_{11})_k t'_k \frac{69H^2m^2l^2 + 195H^2mcl + 156H^2c^2 + 13{t'_k}^2}{270270b_e{(D_{11})_2}^2}$$

$$k_{78} = \sum_{k=1}^{n} Hl^2(\bar{Q}_{11})_k t'_k \frac{2553H^2m^2l^2 + 7020H^2mcl + 5460H^2c^2 + 455{t'_k}^2}{540540b_e{(D_{11})_2}^2}$$

$$k_{88} = \sum_{k=1}^{n} Hl(\bar{Q}_{11})_k t'_k \frac{2134H^2m^2l^2 + 5460H^2mcl + 3900H^2c^2 + 325{t'_k}^2}{18018b_e{(D_{11})_2}^2}$$

II- Coefficients of the mass matrix for width-tapered thickness-tapered laminated composite beams using advanced finite element formulation

$$m_{11} = \frac{lb_e\rho(1042c + 235ml)}{2574}$$

$$m_{12} = \frac{-l^2b_e\rho(453c + 139ml)}{6006}$$

$$m_{13} = \frac{-l^4\rho(383c + 143ml)}{1081080(D_{11})_1}$$

$$m_{14} = \frac{-l^3\rho(548c + 191ml)}{72072(D_{11})_1}$$

$$m_{15} = \frac{245lb_e\rho(2c + ml)}{5148}$$

$$m_{16} = \frac{l^2b_e\rho(1143c + 547ml)}{36036}$$

$$m_{17} = \frac{-l^4\rho(521c + 235ml)}{2162160(D_{11})_2}$$

$$m_{18} = \frac{-l^3\rho(620c + 287ml)}{144144(D_{11})_2}$$

$$m_{22} = \frac{lb_e\rho(1042c + 235ml)}{2574}$$

$$m_{23} = \frac{-l^5\rho(72c + 29ml)}{720720(D_{11})_1}$$

$$m_{24} = \frac{l^4\rho(245c + 94ml)}{120120(D_{11})_1}$$

$$m_{25} = \frac{-l^2b_e\rho(1143c + 596ml)}{36036}$$

$$m_{26} = \frac{-373l^3b_e\rho(2c + ml)}{72072}$$

$$m_{27} = \frac{l^5\rho(55c + 26ml)}{720720(D_{11})_2}$$

$$m_{28} = \frac{l^4\rho(995c + 482ml)}{720720(D_{11})_2}$$

$$m_{33} = \frac{l^7\rho(16c + 7ml)}{25945920b_e(D_{11})_1{}^2}$$

$$m_{34} = \frac{-l^6\rho(26c + 11ml)}{2162160b_e(D_{11})_1{}^2}$$

$$m_{35} = \frac{l^4\rho(521c + 286ml)}{2162160(D_{11})_1}$$

$$m_{36} = \frac{l^5\rho(55 + 29ml)}{720720(D_{11})_1}$$

$$m_{37} = \frac{-l^7\rho(2c + ml)}{3706560b_e(D_{11})_1(D_{11})_2}$$

$$m_{38} = \frac{-l^6\rho(43c + 22ml)}{4324320b_e(D_{11})_1(D_{11})_2}$$

$$m_{44} = \frac{l^5\rho(86c + 35ml)}{360360b_e(D_{11})_1{}^2}$$

$$m_{45} = \frac{-l^3\rho(620c + 333ml)}{144144(D_{11})_1}$$

$$m_{46} = \frac{-l^4\rho(995c + 513ml)}{720720(D_{11})_1}$$

$$m_{47} = \frac{l^6\rho(43c + 21ml)}{4324320b_e(D_{11})_1(D_{11})_2}$$

$$m_{48} = \frac{131l^5\rho(2c + ml)}{1441440b_e(D_{11})_1(D_{11})_2}$$

$$m_{55} = \frac{b(x)l\rho(1042c + 807ml)}{2574}$$

$$m_{56} = \frac{b_e l^2\rho(453c + 314ml)}{6006}$$

$$m_{57} = \frac{-l^4\rho(383c + 240ml)}{1081080(D_{11})_2}$$

$$m_{58} = \frac{-l^3\rho(548c + 357ml)}{72072(D_{11})_2}$$

$$m_{66} = \frac{b_e l^3\rho(110c + 71ml)}{6006}$$

$$m_{67} = \frac{-l^5\rho(72c + 43ml)}{720720(D_{11})_2}$$

$$m_{68} = \frac{-l^4\rho(245c + 151ml)}{120120(D_{11})_2}$$

$$m_{77} = \frac{l^7\rho(16c + 9ml)}{25945920b_e{(D_{11})_2}^2}$$

$$m_{78} = \frac{l^6\rho(26c + 15ml)}{2162160b_e{(D_{11})_2}^2}$$

$$m_{88} = \frac{l^5\rho(86c + 51ml)}{360360b_e{(D_{11})_2}^2}$$

III- Coefficients of the stiffness matrix for thickness-tapered laminated composite beams using conventional finite element formulation

$$k_{11}^e = \sum_{k=1}^{n} b(\bar{Q}_{11})_k t_k \frac{24m^2l^2 + 60clm + 60c^2 + {t_k'}^2}{5l^3}$$

$$k_{12}^e = \sum_{k=1}^{n} b(\bar{Q}_{11})_k t_k (-\frac{1}{10}) \frac{14m^2l^2 + 40clm + 60c^2 + 5{t_k'}^2}{l^2}$$

$$k_{13}^e = \sum_{k=1}^{n} b(\bar{Q}_{11})_k t_k (-\frac{1}{5}) \frac{14m^2l^2 + 40clm + 60c^2 + 5{t_k'}^2}{l^2}$$

$$k_{14}^e = \sum_{k=1}^{n} b(\bar{Q}_{11})_k t_k (-\frac{1}{10}) \frac{34m^2l^2 + 80clm + 60c^2 + 5{t_k'}^2}{l^2}$$

$$k_{22}^e = \sum_{k=1}^{n} b(\bar{Q}_{11})_k t_k \frac{8m^2l^2 + 30clm + 60c^2 + 5{t_k'}^2}{15l}$$

$$k_{23}^e = \sum_{k=1}^{n} b(\bar{Q}_{11})_k t_k \left(\frac{1}{10}\right) \frac{14m^2l^2 + 40clm + 60c^2 + 5{t_k'}^2}{l^2}$$

$$k_{24}^{e} = \sum_{k=1}^{n} b(\bar{Q}_{11})_k t_k \frac{26m^2l^2 + 60clm + 60c^2 + 5t_k'^2}{30l}$$

$$k_{33}^{e} = \sum_{k=1}^{n} b(\bar{Q}_{11})_k t_k \frac{24m^2l^2 + 60clm + 60c^2 + 5t_k'^2}{5l^3}$$

$$k_{34}^{e} = \sum_{k=1}^{n} b(\bar{Q}_{11})_k t_k \left(\frac{1}{10}\right) \frac{34m^2l^2 + 80clm + 60c^2 + 5t_k'^2}{l^2}$$

$$k_{44}^{e} = \sum_{k=1}^{n} b(\bar{Q}_{11})_k t_k \frac{38m^2l^2 + 90clm + 60c^2 + 5t_k'^2}{15l}$$